REFINEMENT METHOD FOR WEIGHTING SCHEME OF FULLY SPATIAL BEAMFORMER

Chayanit Bunsanit

A Thesis Submitted in Partial Fulfillment of the Requirements for the Degree of Doctor of Philosophy in Telecommunication Engineering

Suranaree University of Technology

Academic Year 2012

วิธีการปรับแต่งสำหรับแผนการถ่วงน้ำหนักของตัวก่อรูปลำคลื่น เชิงตำแหน่งเพียงอย่างเดียว

นางสาวชยานิษฐ์ บุญสนิท

วิทยานิพนธ์นี้เป็นส่วนหนึ่งของการศึกษาตามหลักสูตรปริญญาวิศวกรรมศาสตรดุษฎีบัณฑิต
สาขาวิชาวิศวกรรมโทรคมนาคม
มหาวิทยาลัยเทคโนโลยีสุรนารี
ปีการศึกษา 2555

REFINEMENT METHOD FOR WEIGHTING SCHEME OF FULLY SPATIAL BEAMFORMER

Suranaree University of Technology has approved this thesis submitted in partial fulfillment of the requirements for the Degree of Doctor of Philosophy.

Thesis Examining Committee

_____
(Asst. Prof. Dr. Peerapong Uthansakul)
Chairperson

_____
(Asst. Prof. Dr. Monthippa Uthansakul)
Member (Thesis Advisor)

_____
(Asst. Prof. Dr. Piyaporn Krachodnok)
Member

_____
(Asst. Prof. Dr. Chanchai Thaijiam)
Member

_____
(Dr. Dheerasak Anantakul)
Member

(Prof. Dr. Sukit Limpijumnong)	(Assoc. Prof. Flt. Lt. Dr. Kontorn Chamniprasart)
Vice Rector for Academic Affairs	Dean of Institute of Engineering

ชยานิษฐ์ บุญสนิท : วิธีการปรับแต่งสำหรับแผนการถ่วงน้ำหนักของตัวก่อรูปลำคลื่นเชิงตำแหน่งเพียงอย่างเดียว (REFINEMENT METHOD FOR WEIGHTING SCHEME OF FULLY SPATIAL BEAMFORMER) อาจารย์ที่ปรึกษา : ผู้ช่วยศาสตราจารย์ ดร.มนต์ทิพย์ภา อุฑารสกุล, 127 หน้า.

ในปัจจุบันการติดต่อสื่อสารแบบไร้สายได้เข้ามามีบทบาทสำคัญในชีวิตประจำวันเพิ่มมากขึ้น ซึ่งจะเห็นได้จากความต้องการในการใช้งานโทรศัพท์เคลื่อนที่ที่มีปริมาณเพิ่มขึ้นอย่างรวดเร็วโดยเฉพาะความต้องการอัตราความเร็วในการส่งข้อมูลที่สูงเพื่อรองรับการใช้บริการในด้านต่าง ๆการเพิ่มประสิทธิภาพของระบบสื่อสารไร้สาย และการจัดสรรการใช้ทรัพยากรความถี่ให้มีประสิทธิภาพเพียงพอต่อความต้องการของผู้ใช้งานจึงมีความจำเป็นอย่างยิ่ง ระบบสายอากาศเก่งเป็นระบบหนึ่งที่ตอบสนองความต้องการเหล่านี้ได้ เนื่องจากสามารถเพิ่มคุณภาพของสัญญาณได้ โดยระบบสายอากาศเก่งสามารถหันพูคลื่นหลัก ไปยังทิศทางของสัญญาณที่ต้องการ ในขณะเดียวกันก็สามารถหันจุดศูนย์หรือพูข้างไปยังทิศทางของสัญญาณแทรกสอด สายอากาศเก่งจะประกอบด้วย 2 ส่วน คือ ส่วนของสายอากาศแถวลำดับ และส่วนของตัวประมวลผลสัญญาณ ซึ่งส่วนหลังนี้เองที่จะเป็นตัวควบคุมการก่อรูปลำคลื่นของสายอากาศเก่งไปยังทิศทางที่ต้องการ โดยการควบคุมนั้นจะอาศัยวิธีการประมวลผลทางสัญญาณเพื่อหาค่าสัมประสิทธิ์การถ่วงน้ำหนักเพื่อไปถ่วงสัญญาณที่สายอากาศแถวลำดับแต่ละตัวให้ก่อรูปลำคลื่นไปในทิศทางที่ต้องการ โดยระบบสายอากาศเก่งนั้นมักใช้กับสัญญาณที่มีแถบความถี่แคบ แต่ในปัจจุบันความต้องการของผู้ใช้บริการที่มีสูงมาก การส่งสัญญาณจะต้องอาศัยแถบความถี่ที่กว้าง การที่จะนำเอาระบบสายอากาศเก่งแบบเดิมที่ทำงานได้ดีกับสัญญาณที่มีแถบความถี่แคบมาใช้กับสัญญาณที่มีแถบความถี่กว้างนั้น ระบบจะไม่สามารถลดผลกระทบของสัญญาณแทรกสอดได้ดีเหมือนเดิม ดังนั้นในวิทยานิพนธ์นี้จะนำเสนอวิธีการประมวลผลสัญญาณสำหรับสัญญาณในแถบความถี่กว้างที่เรียกว่าการประมวลผลสัญญาณเชิงตำแหน่งเพียงอย่างเดียว โดยการประมวลผลแบบนี้จะใช้หลักการของการแปลงฟูเรียร์ผกผันของสัญญาณเวลาดิสครีต (Inverse Discrete Fourier Transform : IDFT) และจะให้ค่าสัมประสิทธิ์การถ่วงน้ำหนักที่เป็นค่าจริงเพียงอย่างเดียว ซึ่งในทางปฏิบัติสามารถใช้ตัวลดทอน หรือตัวขยายสัญญาณในการถ่วงน้ำหนัก แต่อย่างไรก็ตามช่วงความต่างของค่าสัมประสิทธิ์การถ่วงน้ำหนักที่ได้มีช่วงการทำงานที่กว้างมาก ซึ่งในความเป็นจริงเป็นการยากที่จะสามารถหาตัวลดทอนสัญญาณ หรือตัวขยายสัญญาณที่มีช่วงการทำงานที่กว้างมากเช่นนั้น วิทยานิพนธ์ฉบับนี้จึงนำเสนอวิธีการปรับแต่งค่าสัมประสิทธิ์การถ่วงน้ำหนักที่ได้จากการประมวลผลสัญญาณ

เชิงตำแหน่งเพียงอย่างเดียวของระบบสายอากาศเก่งที่ใช้งานในแถบความถี่กว้างด้วยการจำลองในคอมพิวเตอร์ เพื่อให้ช่วงการทำงานของค่าการถ่วงน้ำหนักแคบลง นอกจากนี้วิทยานิพนธ์ฉบับนี้ยังได้นำเสนอการออกแบบและสร้างระบบสายอากาศเก่งต้นแบบเพื่อให้สามารถก่อรูปลำคลื่นไปในทิศทางที่ต้องการ โดยอาศัยค่าถ่วงน้ำหนักที่ได้จากวิธีการปรับแต่ง แล้วจึงนำไปทดสอบ และเปรียบเทียบกับการคำนวณที่ได้จาการจำลองด้วยคอมพิวเตอร์ จากการทดสอบระบบสายอากาศเก่งต้นแบบพบว่า ระบบสายอากาศเก่งที่ออกแบบจะให้แบบรูปการแผ่พลังงานที่มีการชี้ทิศทางของพูคลื่นหลัก ความกว้างของลำคลื่นหลัก และค่าเฉลี่ยของพูคลื่นเล็กใกล้เคียงกับค่าที่ได้จากการคำนวณโดยการจำลองในคอมพิวเตอร์

สาขาวิชาวิศวกรรมโทรคมนาคม ลายมือชื่อนักศึกษา _____

ปีการศึกษา 2555 ลายมือชื่ออาจารย์ที่ปรึกษา _____

CHAYANIT BUNSANIT : REFINEMENT METHOD FOR WEIGHTING SCHEME OF FULLY SPATIAL BEAMFORMER. THESIS ADVISOR : ASST. PROF. MONTHIPPA UTHANSAKUL, Ph.D., 127 PP.

ANTENNA ARRAY/FULLY SPATIAL SIGNAL PROCESSING/ WIDEBAND SMART ANTENNAS

Smart antenna systems are one of the best solution for increasing the system capacity and performance in wireless communication systems. This is because the systems can form main beam towards a desired direction and create nulls or sidelobes towards interference directions. As a result, a great improve in system performance and also saving energy can be obtained. The smart antenna systems usually consist of antenna array and a suitable signal processing unit adjusting the weighting coefficients at individual antenna elements to ease the effect of interference signal. The signal processing works according to the utilized algorithms. However, in the future communication systems, wideband signal will be utilized to fulfill the requirement of higher data rate transmission. One interesting algorithm of signal processing operating in wide frequency band is fully spatial signal processing, so called wideband spatial beamformer. In the part of signal processing, weighting coefficients are so far calculated using two-dimensional Inverse Discrete Fourier Transform (IDFT) technique applied to the required radiation pattern. The obtained weighting coefficients become real-values which can be simply realized by attenuators or amplifiers. However, the range between maximum and minimum values of weighting coefficients is relatively wide. This is considerably not practical. Therefore, this thesis presents the refinement method for fully spatial beamformer. The aim of the proposed

method is to reduce the range of overall weighting coefficients, so called dynamic range of weights. Furthermore, the full prototype of wideband spatial beamformer are designed and constructed in order to validate the proposed refinement method. The results in the term of radiation pattern from simulation and measurement are in good agreement.

School of Telecommunication Engineering Student's Signature _____

Academic Year 2012 Advisor's Signature _____

ACKNOWLEDGEMENTS

The author wishes to acknowledge the funding support from Suranaree University of Technology (SUT).

The grateful thanks and appreciation are given to the thesis advisor, Asst. Prof. Dr. Monthippa Uthansakul for her consistent supervision and thoughtfully comment on several drafts and advice towards the completion of this study.

My thanks go to Asst. Prof. Dr. Peerapong Uthansakul, Asst. Prof. Dr. Piyaporn Krachodnok, Asst. Prof. Dr. Chanchai Thaijiam and Dr. Dheerasak Anantakul for their valuable suggestion and guidance given as examination committees.

The author is also grateful to all faculty and staff members of the School of Telecommunication Engineering and colleagues for their help and assistance throughout the period of this work.

Finally, I would also like to express my deep sense of gratitude to my parents for their support and encouragement me thoughout the course of this study at the Suranaree University of Technology.

Chayanit Bunsanit

.

TABLE OF CONTENTS

Page

ABSTRACT (THAI) I

ABSTRACT (ENGLISH) III

ACKNOWLEDGMENTS V

TABLE OF CONTENTS VI

LIST OF TABLES IX

LIST OF FIGURES XI

CHAPTER

I INTRODUCTION 1

1.1 Background of Problems 1

1.2 Research Objectives 3

1.3 Scope of and limitation of the Study 4

1.4 Contributions 4

1.5 Thesis Organization 4

II LITERATURE REVIEW 6

2.1 Introduction 6

2.2 Smart Antenna Systems 6

2.2.1 Switched-Beam Antennas 7

2.2.2 Adaptive array Antennas 10

2.3 Impact of Wideband Signals on Smart antenna Systems 13

TABLE OF CONTENTS (Continued)

Page

2.4 Wideband Smart Antennas 15

2.4.1 Space-Time Signal Processing 16

2.4.2 Space-Frequency Signal Processing 17

2.4.3 Fully Spatial Signal Processing 18

2.5 Chapter Summary 19

III BACKGROUND THEORY 21

3.1 Introduction 21

3.2 Wideband Fully Spatial Beamformer 21

3.3 Design for Low Sidelobe Level 30

3.4 Multi-Beam Formation 33

3.5 Chapter Summary 35

IV REFINEMENT ALGORITHM FOR WIDEBAND FULLY SPATIAL BEAMFORMER 37

4.1 Introduction 37

4.2 Refinement Algorithm 37

4.3 Performance Evaluation of Refinement Algorithm 40

4.4 Chapter Summary 51

V PROTOTYPE OF WIDEBAND FULLY SPATIAL BEAMFORMER 52

5.1 Introduction 52

5.2 Antennas 53

TABLE OF CONTENTS (Continued)

Page

5.2.1 Design of Antenna Element 53
5.2.2 Practical Realization 57
5.3 Weighting Networks 60
5.3.1 Weighting Systems 61
5.3.2 Control Devices 70
5.4 Prototype of Fully Spatial Beamformer 71
5.5 Chapter Summary 72
VI EXPERIMENTAL RESULTS 73
6.1 Introduction 73
6.2 Experimental Setup 73
6.3 Experimental Result and Discussion 76
6.4 Error in Average Minor Lobe Level 81
6.5 Chapter Summary 82
VII CONCLUSIONS 83
7.1 Conclusion 83
REFERENCES 86
APPENDICES
APPENDIX A. ANTENNA DESIGN 95
APPENDIX B. TECHNICAL PUBLICATION 103
BIOGRAPHY 127

LIST OF TABLES

Table **Page**

2.1 Element of phasing, beam direction, and inter-element phasing for the Butler matrix (Liberti and Rappaport, 1999) 9

3.1 Weighting Coefficients for 4×4 beamformer when desired direction is 45° 29

4.1 Parameter given in simulation for refinement algorithm 41

4.2 The attenuations and parameters of refinement algorithm from simulation when desired direction is 35° 42

4.3 The Comparative value of attention factors using IDFT method and refinement method 46

4.4 The weighting coefficients for refinement algorithm 48

5.1 64 possible combinations of C0.5-C16 for digital step attenuator 62

5.2 The RF control bits select the desired switch state 66

5.3 Summary of specification of Arduino Duemilanove 71

6.1 Weighting Coefficients (dB) from IDFT method of 4×4 beamformer in 6 directions 74

6.2 Weighting coefficients (dB) from proposed refinement algorithm of 4×4 beamformer in 6 directions 75

6.3 The parameters of refinement method for each desired directions 76

LIST OF TABLES (Continued)

Table **Page**

A.1 Measured impedance bandwidth for the square element beveled on one side of the planar element, showing an increase in upper edge frequency with increase of angle (Ammann, 2001). 99

A.1 Measured impedance bandwidth for the square element beveled on twi side of the planar element, showing an increase in upper edge frequency with increase of angle (Ammann, 2001). 100

LIST OF FIGURES

Figure **Page**

2.1 Smart antenna system 7

2.2 Structure of switched-beam antenna 8

2.3 Configuration of Butler matrix 9

2.4 Four beam-patterns produced using Butler matrix 10

2.5 Block diagram of adaptive antenna system 11

2.6 Radiation pattern of smart antennas associated with narrowband 14

2.7 Radiation pattern of smart antennas associated with narrowband weighting scheme in presence of wideband incoming signal having bandwidth 500 MHz (Uthansakul and Bialkowski, 2004) 15

2.8 Configuration of space-time signal processor 17

2.9 Space-frequency signal processor for wideband smart antennas 18

2.10 Space-time signal processor for wideband smart antennas 19

3.1 Layout of array configuration for fully spatial beamformer 22

3.2 Location of desired points on the intersection of the constant angle and constant frequency loci 27

3.3 Plot of objective function using Sinc created on $u_1 - u_2$ plane for frequencies from 1.9 to 2.4 GHz 29

LIST OF FIGURES (Continued)

Figure **Page**

3.4 Simulation radiation pattern of 4×4 beamformer represented by Sinc plotted for frequencies from 1.9 to 2.4 GHz. When the desired main-beam direction is 45° 30

3.5 Radiation pattern of 4×4 beamformer using Chebyshev polynomial plotted for frequencies from 1.9 to 2.4 GHz. When the desired main-beam direction is 45° 32

3.6 Plot of $H(u_2,u_2)$ when desired beam angle are $-65°$ and $65°$ 34

3.7 Radiation pattern of 8x8 beamformer for desired direction of $-65°$ and $65°$ plotting for frequencied from 1.9 to 2.4 GHz 35

4.1 Relative between ratio of weighting coefficient and deviation of main beam direction 44

4.2 Relative between ratio of weighting coefficient and deviation of average minor lobe level 44

4.3 Relative between ratio of weighting coefficient and deviation of first null beamwidth 45

4.4 The comparison of radiation performance using IDFT method and Refinement method at 2.15 GHz when the main beam is pointed to 45° 47

4.5 Radiation pattern using IDFT method from frequencies 1.9 to 2.4 GHz when main-beam is pointed to 45° 47

LIST OF FIGURES (Continued)

Figure **Page**

4.6 Radiation pattern using proposed refinement method from Frequencies 1.9 to 2.4 GHz when main-beam is pointed to 45° 48

5.1 Prototype diagram of wideband spatial beamformer 53

5.2 Planar monopole antenna structure at (a) front view (b) back view 54

5.3 Geometry of a planar antenna structure and its coordinate system 55

5.4 Simulated return loss of the designed antenna shown in Figure 5.2 55

5.5 Simulation of E-plane pattern (a) y-z plane (b) x-y plane 56

5.6 Simulation H-plane (x-z plane) pattern 56

5.7 Photograph of fabricated wideband planar monopole antenna 57

5.8 Measured return loss of the design antenna Figure 5.7 58

5.9 Measured E-plane pattern (a) y-z plane (b) x-y plane 59

5.10 Measured for H-plane (x-z plane) pattern 59

5.11 Photograph of fabricated 4×4 antenna 60

5.12 Photograph of digital step attenuator 61

5.13 Simplified schematic of digital step attenuator 61

5.14 Set up for digital attenuator testing 64

5.15 Measured attenuation factor of digital step attenuator 64

5.16 Photograph of digital switch 65

5.17 Functional diagram of the RF switch 65

5.18 Diagram of Phase Shifter 67

LIST OF FIGURES (Continued)

Figure **Page**

5.19 Photograph of Phase shifter 67

5.20 Measured return loss (S_{11}) of phase shifter 67

5.21 Measured return loss of (S_{22}) of phase shifter 68

5.22 Measured insertion loss (S_{21}) of phase shifter 68

5.23 Phase difference between input and output signal of phase shifter 69

5.24 Photograph of 2:1 power combiner 69

5.25 Photograph of 16:1 power combiner 70

5.26 Photograph of ATMEGA 328 microprocessor 71

5.27 Photograph of full prototype of wideband fully spatial beamformer 72

6.1 Assembly of beamformer prototype tested in anechoic chamber 74

6.2 Simulated radiation pattern using refinement method for frequencies frequency 2.15 GHz when the main beam direction is (a) 7° (Case A) and (b) 34° (Case C) 77

6.3 (a) Simulated and (b) measured radiation pattern using refinement method for frequencies from 1.9 to 2.4 GHz when the main beam direction is 7° (Case A) 78

6.4 (a) Simulated and (b) measured radiation pattern using refinement method for frequencies from 1.9 to 2.4 GHz when the main beam direction is -17° (Case B) 78

LIST OF FIGURES (Continued)

Figure **Page**

6.5 (a) Simulated and (b) measured radiation pattern using refinement method for frequencies from 1.9 to 2.4 GHz when the main beam direction is 34° (Case C) 79

6.6 (a) Simulated and (b) measured radiation pattern using refinement method for frequencies from 1.9 to 2.4 GHz when the main beam direction is -34° (Case D) 79

6.7 (a) Simulated and (b) measured radiation pattern using refinement method for frequencies from 1.9 to 2.4 GHz when the main beam direction is 57° (Case E) 80

6.8 (a) Simulated and (b) measured radiation pattern using refinement method for frequencies from 1.9 to 2.4 GHz when the main beam direction is 75° (Case F) 80

6.9 Radiation pattern for frequency at 2.15 GHz when the main beam direction is 2°. 82

A.1 Some examples of 'fat monopole' antenna (Huang, Y and Boyle, K, 2008). 96

A.2 Symmetry pentagonal planar monopole with monopole with bevel illustrated (Ammann, 2001) 97

A.3 Simple square geometry with one and two sides beveled, forming asymmetrical and symmetrical pentagon (Ammann, 2001) 98

LIST OF FIGURES (Continued)

Figure **Page**

A.4 Measured return loss for the simple square geometry (dashed), with a single 10 (Solid), $20°$ (dot-dash), $30°$ (dash-dash) (Ammann, 2001) 98

A.5 (a) Normalized *H*-plane pattern $E_\theta(\phi, \theta = 90°)$ for the symmetrically beveled square monopole on a 150 mm. square ground plane. (b) Normalized *E*-plane pattern $E_\theta(\theta, \phi = 90°)$ for the symmetrically beveled square monopole on a 150 mm. square ground plane. (c) Normalized *E*-plane pattern $E_\theta(\theta, \phi = 0°)$ for the symmetrically beveled square monopole on a 150 mm. square ground plane (Ammann, 2001) 100

A.6 a) Antenna structure illustrated in literature of Al-Husseini, El-Hajj and Kabalan. (2008) (b) Antenna structure designed for this thesis 102

CHAPTER I

INTRODUCTION

1.1 Background of problems

So far, wireless communication systems have grown rapidly and the new services are driven by user's demand requiring a high data rate. Wireless communication systems have to support not only speech but also internet, multimedia communications and contained several technologies operating in different frequency band e.g. WiFi, WiMAX, Bluetooth and broadband WLAN. This is leading to the huge expansion of wireless communication systems. As a result, this implies a tremendous increase in system capacity and also the systems are demanded for better coverage, wider frequency range, higher quality of service and more capacity. One way of achieving this increase in capacity is to introduce smart antennas (Jana, 2000). Smart antenna systems can form main beam towards a desired direction and create nulls or side-lobes towards interference directions. As a result, the greatly improving system performance and also saving energy can be obtained (Stine, 2006). In general, smart antennas are an array antennas connected to signal processing unit adjusting the weighting coefficients at individual antenna elements to ease the effect of interference signal. The signal processing works according to the utilized algorithms. So far, the beamforming algorithms for smart antennas in wireless communications have concerned only narrowband operation and cannot be directly extended to wideband signal. This is because such adverse effects as main-beam squinting and null shifting

are occurred (Uthansakul and Bialkowski, 2004; Hefnawi and Delisle, 2000). However, in order to support high-data rate transmission, new efforts are currently required to deal with smart antennas capable of operating in wide frequency range (Hefnawi and Delisle, 2001). From literatures of Rivas, Shuguo, and Donglin (2010); Rui, Yuchun, and Xiaowei, (2007); Uthansakul and Bialkowski, (2004) are presented smart antenna systems can be divided into three categories. The first category utilizes space-time signal processing, so call spatio-temporal beamformer. These systems consist of array antennas and tapped-delay lines at each branch of the array to deal with the received signal in time-domain (Junjie, Yongyi, and Henry, 2005; Ishii and Kohno, 1994). However the number of tapped-delay lines increase according to the bandwidth of utilized frequency. Next category relies on space-frequency signal processing. This is an alternative approach to perform wideband beam-formation without the use of tapped-delay lines. In this method the received signal will be decomposed into non-overlapping narrowband component using band-pass filters (Hefnawi and Delisle, 2001). However, for wideband signal, the systems require a large number of frequency filters. The last category utilizes only spatial signal processing, so called wideband spatial beamformer. This is a new method for wideband smart antennas. In the part of signal processing, weighting coefficients are calculated using two-dimensional Inverse Discrete Fourier Transform (IDFT) technique applied to the required radiation pattern. The obtained weighting coefficients become real-values which can be simply realized by attenuators or amplifiers (Uthansakul and Bialkowski, 2005). The main advantage of this wideband spatial beamformer is that its design does not require phase shifters, delay circuits or

frequency filters. This is of considerable practical advantage over the other types of beamformer employing complex weighting coefficients (Uthansakul and Bialkowski, 2005). However, the range between maximum and minimum values of weighting coefficients (attenuation or amplification) is relatively wide and they are not integer number. This is considerably impractical for hardware implementation. Therefore, the aim of this thesis is to round all real-valued weights to integer number and reduce the range between maximum and minimum weighting coefficients while maintaining some important radiation characteristics. The initial weighting coefficients are obtained from original beamforming algorithm employed in fully spatial wideband beamformer. The proposed method is so called refinement algorithm for weighting scheme of fully spatial wideband beamformer. Then, design and construction for a full prototype of smart antenna systems are revealed in order to validate the proposed method.

1.2 Research objectives

The objectives of this research are as follows:

1.2.1 To study a beam formation of smart antenna systems for fully spatial beamformer.

1.2.2 To develop a refinement method to reduce the range of weighting coefficients for fully spatial beamformer.

1.2.3 To design and construct a full prototype of wideband fully spatial beamformer to validate the proposed method.

1.3 Scope and limitation of the study

1.3.1 Refinement algorithm for weighting coefficients based on fully spatial signal processing and its simulated results are presented using MATLAB.

1.3.2 Refinement algorithm concerns with five input parameters to control radiation pattern. These parameters are maximum weighting coefficient, wideband signal, main-beam's direction, beamwidth and average minor lobe level.

1.3.3 The prototype of fully spatial wideband beamformer operates in frequencies from 1.9 to 2.4 GHz.

1.3.4 The array antennas are designed and constructed in the form of 4×4-lattice and planar monopoles is employed to be antenna elements.

1.3.5 This thesis compares the obtained results from simulation results to experimental results.

1.4 Contributions

1.4.1 To obtain a refinement algorithm for weighting coefficients of fully spatial wideband beamformer in order to reduce the range of overall weighting coefficients.

1.4.2 To obtain a prototype of spatial wideband beamformer, which is not complex and able to operate in wide frequency range.

1.5 Thesis organization

The remainder of this thesis is organized as follows. Chapter 2 presents a classification of smart antenna systems. Then, this section investigates the impact of

wideband signal on smart antenna systems. In addition, details of three types of wideband smart antennas are presented.

Chapter 3 describes the concept and configuration of spatial signal processing for wideband smart antenna systems and then, presents designing for low side lobe level. Furthermore, wideband multi beam formation is presented in this chapter.

Chapter 4 provides a development for refinement algorithm in order to reduce range of weighting coefficients for fully spatial wideband beamformer and demonstrates a simulation results to confirm the proposed concept.

Chapter 5 presents the practical implementation of the spatial wideband beamformer. The full prototype is constructed and tested in an anechoic chamber to validate the beamformer algorithm proposed in Chapter 4. The prototype of smart antenna systems consists of array antennas, weighting networks and control devices. For the last two sections of chapter, characteristics of each component both in simulation and measurement are described.

In Chapter 6, experimental setup and the obtained results are presented. This chapter shows the simulation carried out using refinement method for weighting coefficients of fully spatial beamformer. Then, the full prototype is tested in an anechoic chamber and the obtained results are compared with simulation results.

In last chapter, Chapter 7 provides conclusion of the research work and suggestion for further study.

CHAPTER II

LITERATURE REVIEW

2.1 Introduction

This chapter presents literature review for the proposed research. The basic concept of smart antenna systems and classification of smart antennas are presented. Then, impact of wideband signal on smart antenna systems and algorithm related to wideband signal on smart antennas are presented.

2.2 Smart antenna systems

Smart antenna systems consist of an antenna array combined with signal processing. The concept of using antenna array cooperating with signal processing is not new to radar and aerospace technology. Until recent years, cost effectiveness has prevented their use in commercial systems. The advent of very fast and low cost digital signal processors has made smart antennas practical for cellular land or satellite-mobile communication systems (Chryssomallis, 2000). Nowadays, the applications of smart antennas have been suggested for mobile communication systems, to overcome the problem of limited channel bandwidth. In general, smart antennas help improving the system performance by increasing channel capacity and spectrum efficiency, extending range coverage, steering multiple beams to track mobile terminals (Alastalo and Kahola, 2003; Boonpoonga, Sirisuk and Krariksh,

2006) They also reduce delay spread, multipath fading, co-channel interference and Bit Error Rate (BER). The delay spread occurs in multipath propagation environments when desired signal is arriving from different direction. Smart antenna systems are capable of forming beams in certain directions and nulls in the others, thereby canceling some of the delayed arrivals as shown in Figure 2.1. Smart antennas can be generally divided into two types: switched-beam systems and adaptive antenna systems which are described as follows (Rameshwar, 2005).

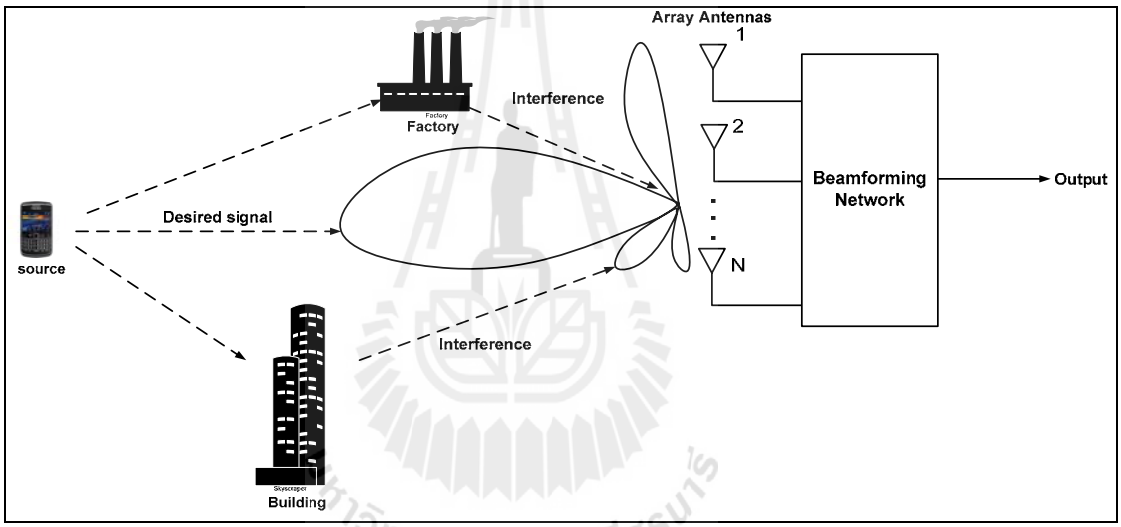

Figure 2.1 Smart antenna systems

2.2.1 Switched-beam antenna systems

Switched-beam antenna systems consist of three major interconnected subsystems. The subsystems are array antennas, beamforming network and beam selector (Bhobe and Perini, 2001; Koubeissi, Decroze, Monediere and Jecko 2005). Figure 2.2 shows the block diagram of switched-beam systems. It is assumed that the incoming signal is incident on the array antennas, then beamforming network forms

beams by adjusting the received signal at in term of amplitude and phase. Finally, the beam selector chooses one beam having the strongest signal strength.

The switched-beam antennas rely on a fixed beam network that produces a set of predefined beams. Probably the most popular solution for fixed beamforming network is a Butler matrix (Ibrahim and Rahim 2007; Liberti and Rappaport, 1999). Figure 2.3 presents the block diagram of 4×4 Butler matrix which consists of 4 linear array antennas spaced by half wavelength, hybrid couplers, phase shifters and crossovers (Lai, M., Wu, T., Hsieh, J., Wang, C, and Jeng, S. 2008). As seen in the figure, the 4 output ports represent the received signal from 4 different directions.

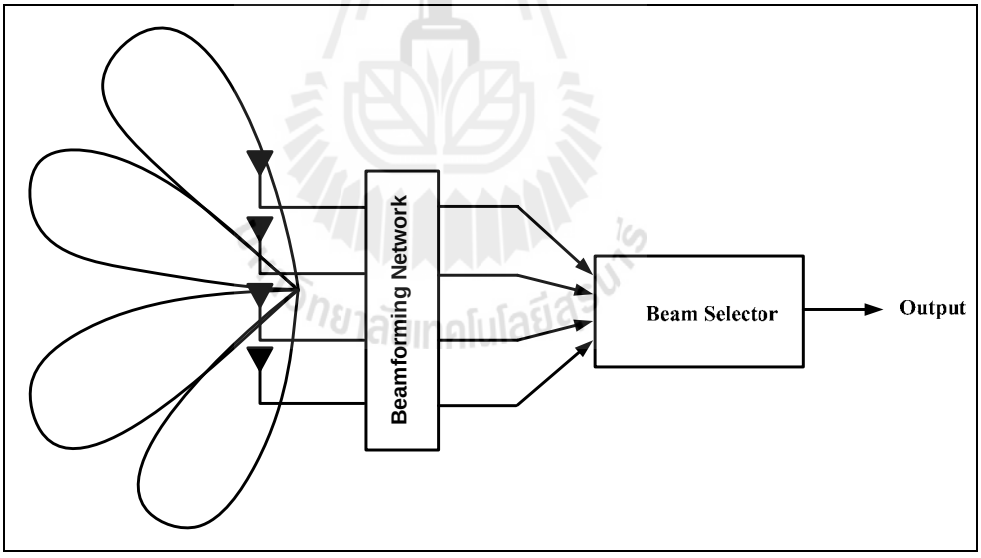

Figure 2.2 Structure of switched-beam antennas.

Butler matrix takes signal from antenna arrays, shifted them in phase and combined them for produce 4 beams with a constant angular separation. Table 2.1 shows the element phasing, beam directions and inter-element phasing at each port for

Butler matrix. This beamforming network can form beams into 4 directions, which are $139°, 104°, 76°$ and $41°$. The radiation patterns obtained from Butler matrix are shown in Figure 2.4.

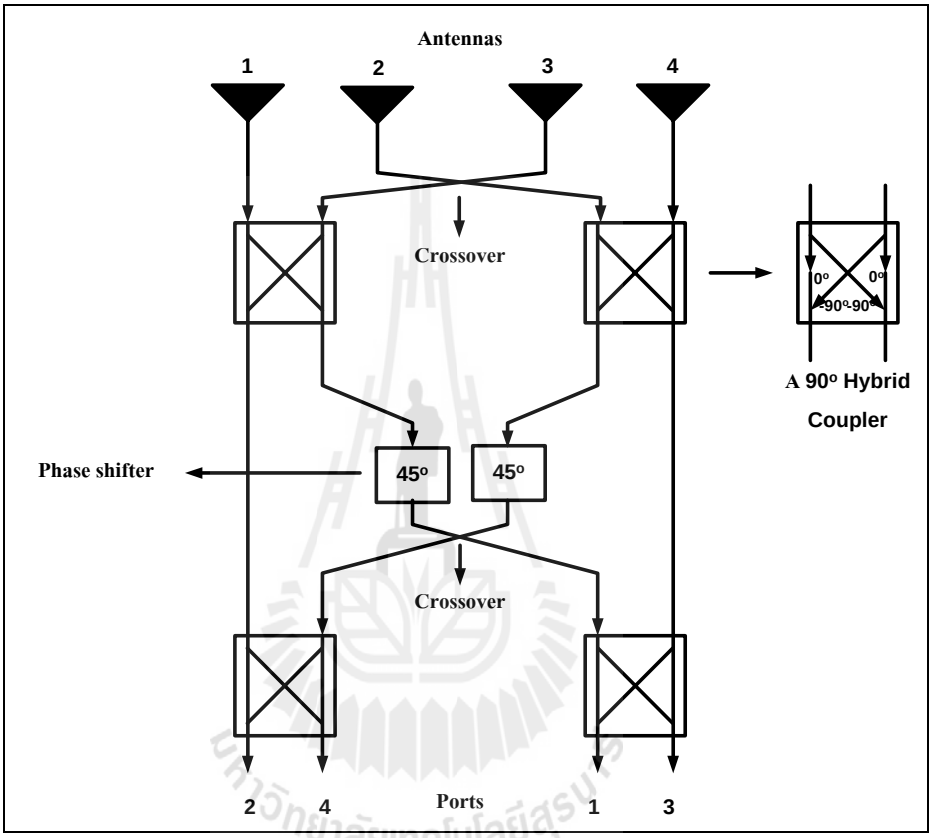

Figure 2.3 Configuration of Butler matrix.

Table 2.1 Element phasing, beam direction, and inter-element phasing for the Butler matrix (Liberti and Rappaport, 1999).

	Antenna 1	Antenna 2	Antenna 3	Antenna 4	Beam direction	Inter-Element Phasing
Port 1	-45°	-180°	45°	-90°	139°	-135°
Port 2	-135°	-45°	-90°	-135°	104°	-45°
Port 3	-135°	-90°	-45°	0°	76°	45°
Port 4	-90°	45°	-180°	-45°	41°	135°

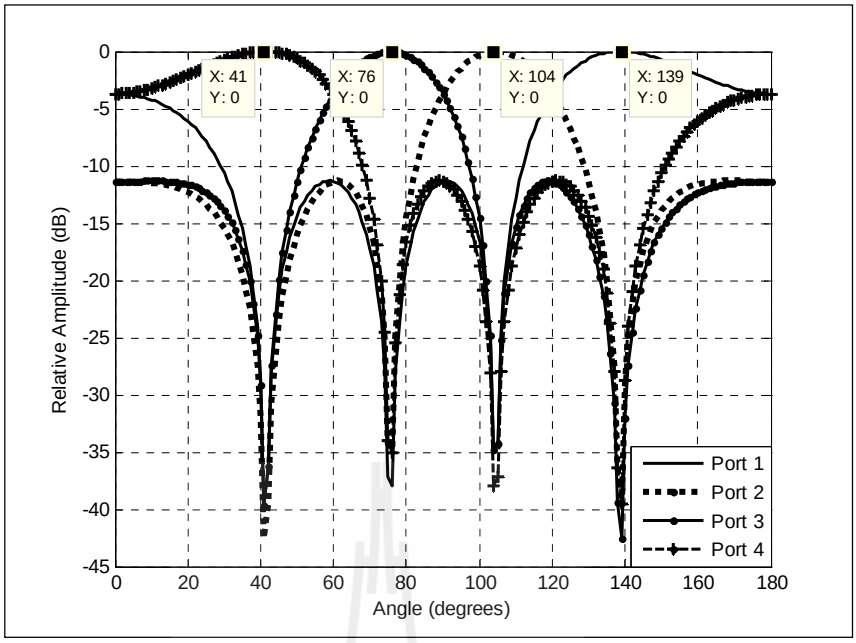

Figure 2.4 Four beam-patterns produced by Butler matrix.

The advantage of switched-beam systems is that it is easy to implement because it is not complex and low of cost. However the drawback of these systems is that they are unable to provide any protection from multipath component which arrives with Direction-Of-Arrivals (DOAs) nearby that of the desired component (Ngamjanyaporn and Krairikh, 2002).

2.2.2 Adaptive antenna systems

One alternative approach for smart antenna systems is adaptive antenna systems. Figure 2.5 illustrates block diagram of these systems consisting of two main parts. The first part is array antennas and another part is adaptive signal processor. The array antennas consist of a number configuration of identical antenna elements which are usually placed in a linear or circular. The individual antenna pattern is assumed to be identical. The signal impinging on array antennas are multiplied by complex weights at each antenna elements and then they are combined together. The complex

weights are continuously adjusted by the adaptive signal processor employing all available information such as pilot, or training sequences, or knowledge of the properties of the signal to calculate the weights. As the result, the systems steer main-beam to desired direction and place nulls in the direction of interferences.

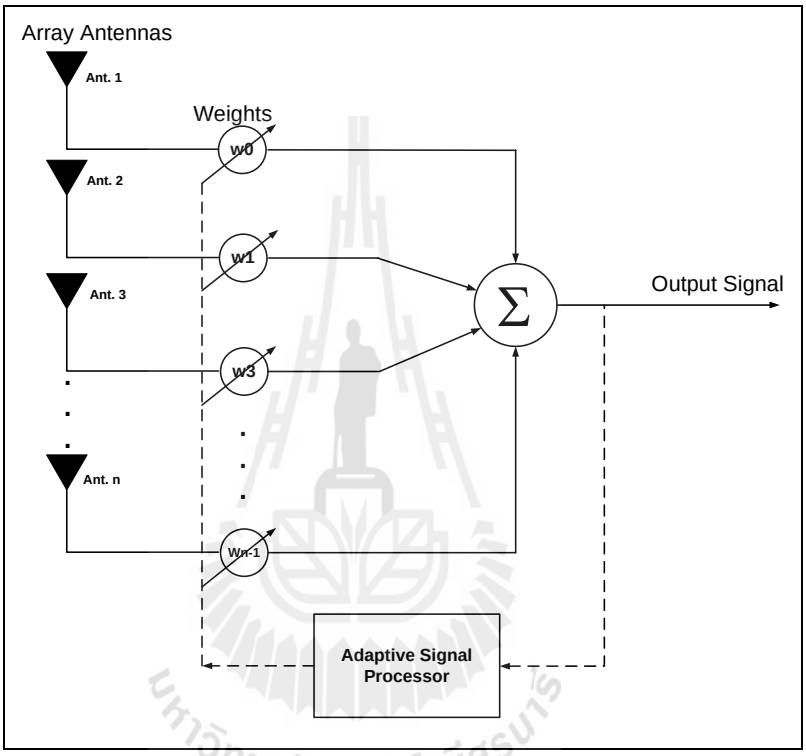

Figure 2.5 Block diagram of adaptive antenna systems.

However, adaptive antenna systems require determination for Direction of Arrival (DOA) of received signal. From literatures, many algorithms have been proposed estimating the DOA, e.g. Multiple Signal Classification (MUSIC) and Estimate Signal parameter via a rotational invariant technique (ESPRIT) (Yoshinaga, Taromaru and Akaiwa, 1999; Fujimoto, Nishikawa and Sato, 1995 and Roy, 1998). Basically, the DOA reveals the direction of arrival of all the incoming signals by

computing time delay, afterwards the adaptive algorithm computes the appropriate weights for the systems.

From the literatures as seen in Petermann, Kuhn and Kammeyer (2000) and Lavate (2010) the adaptive algorithm based on information requirement can be classified into two categories. The first category is reference signal based algorithm or non blind adaptive algorithm. This is based on minimization of the mean square error between the received signal and the reference signal. Therefore, non blind adaptive algorithm requires a reference availability of a reference signal, which has high correlation with the desired signal. Examples of this algorithm are Least Mean Square (LMS) algorithm, Recursive Least Square (RLS) and Sample Matrix Inversion (SMI) (Bhavishya, Sagar, Jain, Prasad, Ramakrishna and Kumar, 2010; Bouacha, Debbat and Bendimerad, 2008). The other category is called blind adaptive algorithm. This algorithm does not require any reference signal information. They themselves generate the required reference signal from the received signal to get the desired signal. Examples are Constant Modulus Algorithm (CMA), Cyclostationary algorithm and Decision-Directed algorithm.

Adaptive array antenna systems have many advantages such as antenna beams adaptively track desired signal direction and a null can be placed in the direction of interferences. These systems do not face a problem of intra-cell hand off because main-beam continually tracks the desired user, thus they have better capability over switched-beam systems. However, adaptive array antenna systems have disadvantage in complication and expend (Fakoukakis, Diamantis, Orfanides and Kyriacou, 2005; Morgan, 2008).

2.3 Impact of wideband signal on smart antenna systems

Most of the smart antenna techniques proposed in the literatures relate to narrowband beamformer. The antenna spacing of narrowband array is usually half of the wavelength of the incoming signal which assumed to have a Fractional Bandwidth (FB) of less than 1%. By definition, the FB of a signal is the ratio of the bandwidth to the center frequency as follows:

$$FB = \frac{f_h - f_l}{(f_h + f_l)/2} \times 100\% \tag{2.1}$$

where f_h and f_l are the highest and the lowest frequencies of the signal, respectively. Wideband arrays are designed for FB up to about 50 percent and ultra-wideband (UWB) arrays are proposed for FB of 50 to 200 percent (Ghavami, 2002). The most of works on smart antennas have concerned narrowband systems, which are characterized by a fractional bandwidth of the order of a few percent. The beamforming techniques used in these narrowband systems are difficult to apply to wideband system because they cause adverse effects, such as main beam squinting and null shifting (Uthansakul and Bialkowski, 2005). As a result, wideband array antennas using narrowband beamforming schemes are unable to steer the main beam to a desired user, and to form nulls or low sidelobes toward interference, over the wide frequency band. To illustrate this problem, literature of Uthansakul and Bialkowski, 2004 has pointed out the impact of wideband signals on a narrowband smart antenna in which the computer simulation results concerning ability to form main-beam and nulls to the desired and interference directions, and signal quality are examined. The dipole antenna has been used to be an antenna element and the Least Mean Square

(LMS) algorithm is employed to achieve the optimum weighting scheme. The 7 dipoles equally spaced by half-wavelength at 2 GHz are employed and the desired signal and interference are coming from 30° and 40° off the array boresight direction, respectively. Figures 2.6 and 2.7 show the radiation pattern employing optimum narrowband weighting scheme but in different signal bandwidth, 10 MHz and 500 MHz respectively. As shown in Figure 2.6, the antenna can effectively steer main beam and null to the desired and interference directions. The array antenna provides good response in this case. In contrast, Figure 2.7 has pointed out that the ability to steer main beam and null of the antenna is degraded while the signal bandwidth is increases.

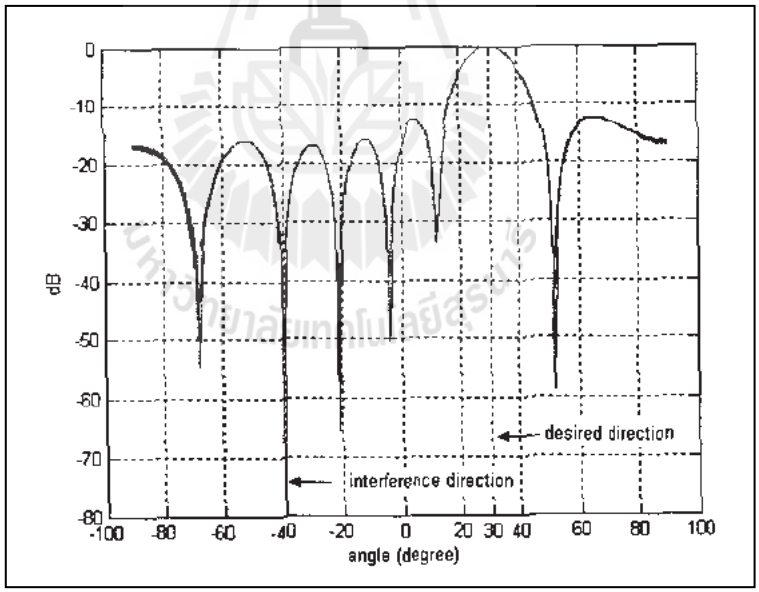

Figure 2.6 Radiation pattern of smart antennas associated with narrowband weighting scheme in presence of narrowband incoming signalhaving bandwidth of 10 MHz (Uthansakul and Bialkowski, 2004)

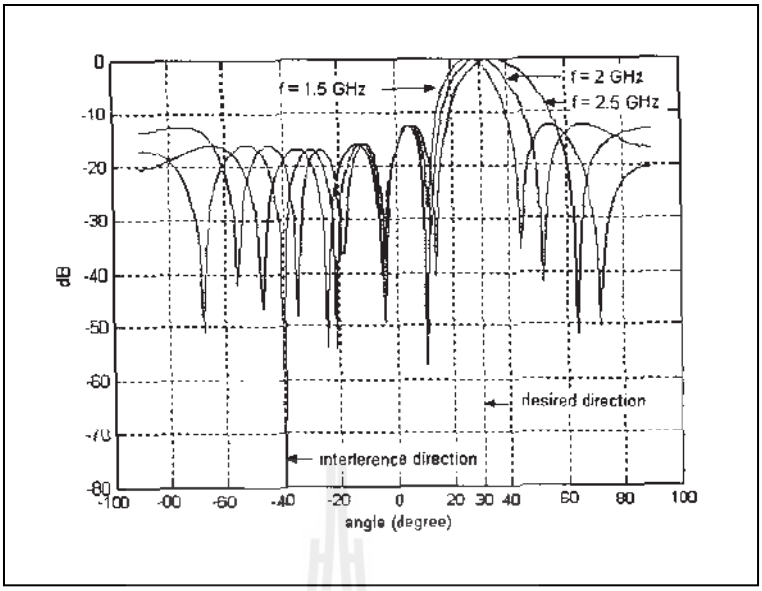

Figure 2.7 Radiation pattern of smart antenna associated with narrowband weighting scheme in presence of wideband incoming signal having bandwidth of 500 MHz (Uthansakul and Bialkowski, 2004)

2.4 Wideband smart antennas

This section presents the concept and configuration of beamforming techniques for wideband smart antenna systems. The advantage and disadvantage of these techniques are also pointed out. The wideband beamforming techniques can be divided into three major categories. The first category is a space-time signal processing or space-time beamformer, second category is a space-frequency signal processing. The first two categories are unattractive for wireless communication systems, because they require tapped-delay networks or large banks of filters. In order to overcome the shortfall of conventional wideband beamformer, the last category, so called a fully spatial signal processing, the wideband beam formation can be

performed using a rectangular array and simple feeding network employing only attenuators or amplifiers.

2.4.1 Space-time signal processing

A space time signal processor, also called spatio-temporal processor, for wideband smart antennas is adaptive array systems. This system combines array antennas and Tapped Delay Lines (TDLs) at each antenna element as shown in Figure 2.8 (Kohno, Wang and Imai, 1992; Kim and Weiss, 1990). The output signal of systems is the weighted sum of signals which has different delays in spatial and temporal domain. In spatial domain, the delays depend on the arrival angle at local and individual of each antenna element while in temporal domain, the received signals are delayed by taps. The TDLs in smart antenna systems were first suggested by Widrow et al. (1967) and have since been studied by several others. In one study, Rogers and Compton (1979) have compared the performance of a two element array with two-, three-, and five-tapped delay-lines using real weights to that of an array with a single complex weight behind each element. In addition, Mayhan, Simmons and Commings (1987) have presented a mathematical analysis of how the number of elements and the number of delay-line taps affect the interference cancellation ratio as a function of bandwidth. Also, Compton (1987) has presented his research again in the topic of how the number of taps and the amount of delay between taps should be chosen in adaptive array to achieve a given bandwidth performance. From these literatures, a suitable number of TDLs are required to control the quality of response in the whole band. For time processing, a TDLs is used on each branch of array, which allows each element to have a phase response that varies with frequency. This is required because lower frequency signal component have less phase shift for a given

propagation distance, whereas higher frequency signal components have greater phase shift as they travel in the same distance. This configuration can be considered as an equalizer, which makes response of all array elements the same across different frequencies (Materum and Marciano, 2003; Bojanapaaly and Kshetrimayum, 2010).

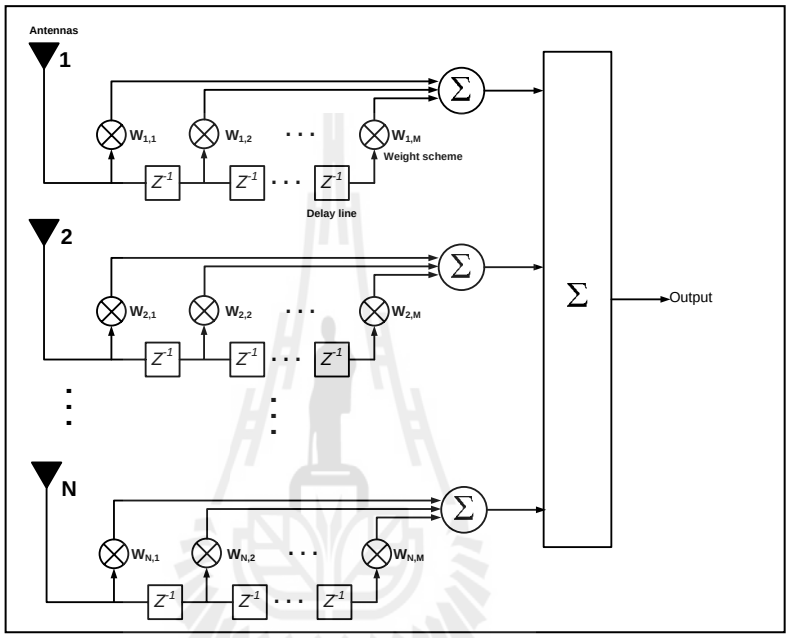

Figure 2.8 Configuration of space-time signal processing.

2.4.2 Space-frequency signal processing

One alternative approach to perform wideband beamforming without using TDLs is space-frequency beamformer. In this method, array antennas are treated as a sensor. The signal received by each antenna element is converted to an intermediate frequency and decomposed into non-overlapping narrowband component using bandpass filters, for example as shown in Figure 2.9 (Mostafa Hefnawi and Gills Y. Delise, 2001). The decomposed signals are weighted with a conventional narrowband weighting scheme. Its shortcoming is due to the requirement of a large

number of filters which add up to the cost of the systems. Also imperfect operation of filters might introduce other problems (Uthansakul and Bialkowski, 2004).

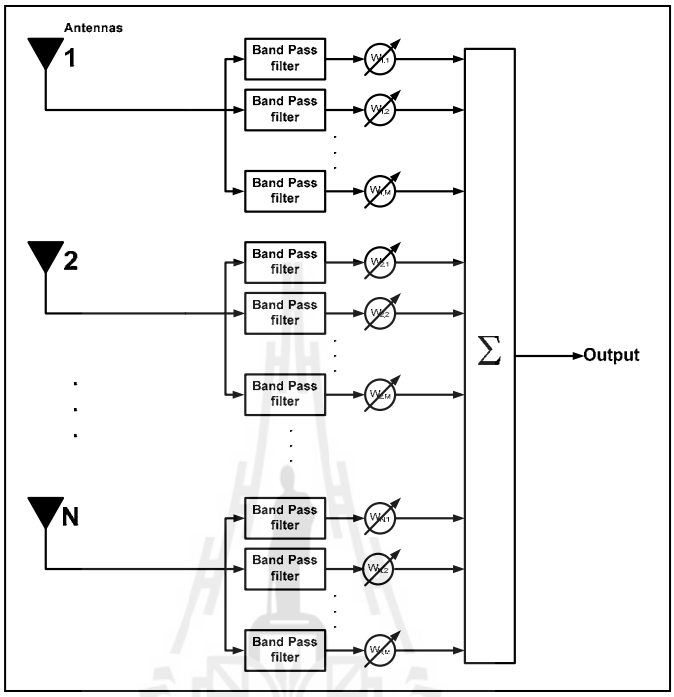

Figure 2.9 Configuration of space-frequency signal processor.

2.4.3 Fully spatial signal processing

The last category for wideband beamformer utilizes fully spatial processing in wideband operation. This is a new method which removes delay networks or frequency filters. This technique relies on the use of a rectangular array to steer beam in azimuth over a large frequency band as shown in Figure 2.10. The purpose of using a 2-D instead of 1-D array is explained as follows. As the signal is assumed to arrive from direction not perpendicular to the array's plane, the array's elements receive the signal's replicas with the different phases. This results in a set of signals, which can be used for processing both in frequency and angular domains. The

obtained set of signals requires only constant real-valued weighting coefficients to form an approximately constant radiation pattern over a wide frequency band. More detail for this type of beamformer is described later on in Chapter 3.

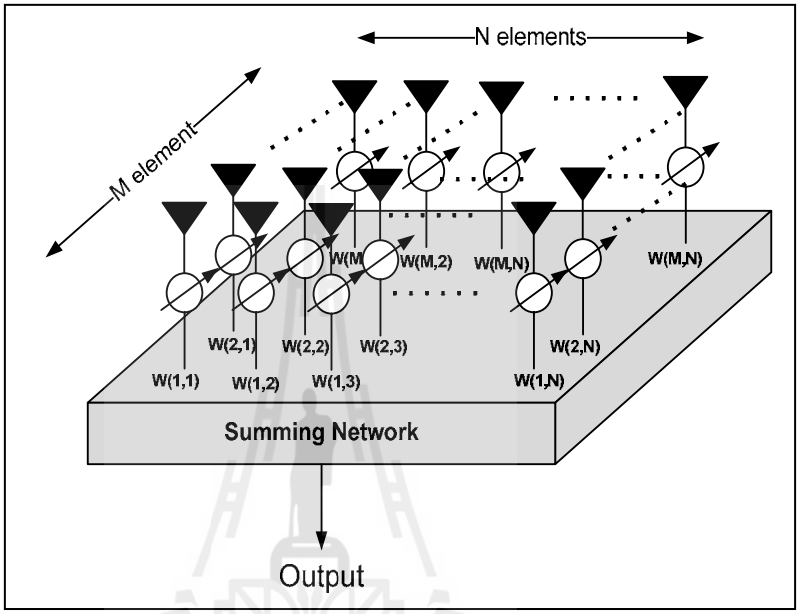

Figure 2.10 Configuration of fully spatial signal processor.

2.5 Chapter summary

This chapter gives a detail and literature surveys of smart antenna systems. Basically, description of smart antenna is used in the wireless communication to represent many signal processing technologies that use multiple antennas on one or both ends of the wireless communication link. This chapter discusses the different types of smart antenna using switched-beam smart antenna and adaptive array. However, smart antenna has concerned narrowband systems, the beamforming techniques used in narrowband systems are difficult to apply for wideband systems because they cause adverse effect, e.g. main beam squinting and null shifting. Thus,

this chapter is presented beamforming algorithms for wideband smart antennas. There are three basic ways to improve the performance: space-time beamforming, space frequency beamforming and full spatial beamforming. The first two types are unattractive to communication system because of the use of large bank of filters or tapped delay networks. In order to overcome this hurdle, fully spatial wideband beam forming techniques can be applied to the smart antenna systems.

CHAPTER III

BACKGROUND THEORY

3.1 Introduction

The purpose of this chapter is to describe a wideband beamforming algorithm using fully spatial signal processing in which its operation relies on the use of an Inverse Discrete Fourier Transform (IDFT) technique. The obtained weighting coefficients are real numbers which can be realized by amplifiers or attenuators. This is considerably advantage over some conventional beamforming algorithms as they result in complex-valued weights. Afterwards, reduction in sidelobe level is discussed following by the concept to produce multiple beams for this kind of beamformer. Finally, last section summaries the chapter.

3.2 Wideband fully spatial beamformer

This section presents concept of wideband beamformer utilizing only spatial signal processing, so called wideband fully spatial beamformer. Figure 3.1 shows the configuration of this kind of beamformer which is constituted by a uniform rectangular array followed by amplifiers or attenuators and summing network. The antenna array is formed by $N_1 \times N_2$ antenna elements where d_1 and d_2 represent array inter-element spacing in two orthogonal directions. It has to be noted that when the array antennas arrange in a square shape for $N_1 = N_2$ and $d_1 = d_2$. The spacing is chosen as half-wavelength $(\lambda / 2)$ at the highest frequency of a given frequency band.

The antenna elements are denoted by indices (m_1,m_2), where $-M_1 \leq m_1, \leq M_1$ and $-M_2 \leq m_2, \leq M_2$. The relation between N and M is $M_i = (N_i\text{-}1)/2$.

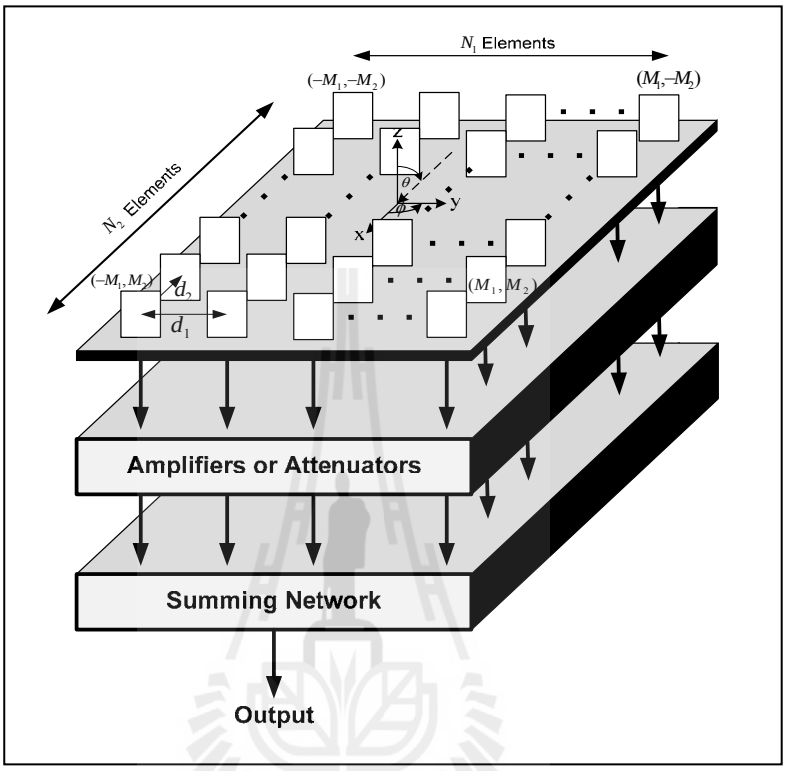

Figure 3.1 Layout of array configuration for fully spatial beamformer.

Assuming that the signal is incident or transmitted in azimuth direction ϕ when $\theta = 90°$, the phase of the signal at element (m_1,m_2) obtained with reference to the array center is given by

$$\psi(m_1,m_2) = \left(\frac{2\pi f}{c}\right)(d_1 m_1 \sin\phi + d_2 m_2 \cos\phi) \tag{3.1}$$

where f is the frequency variable and c is the velocity of an electromagnetic wave in free space. When the array elements are identical, the array frequency-angle response can be written as

$$H(f,\phi) = G(f,\phi) \cdot \sum_{m_1=-M_1}^{M_1} \sum_{m_2=-M_2}^{M_2} w_{m_1,m_2} e^{j\psi} \tag{3.2}$$

where w_{m_1,m_2} are the signal weighting coefficients and $G(f,\theta)$ is the frequency-angle function dependent gain of an antenna element. This function is herein assumed to be an even function of ϕ for $-90° < \phi < 90°$ with the maximum value at $\phi = 0°$ at the center frequency. Then, two auxiliary functions are introduced as follows.

$$u_1 = \left(\frac{fd_1}{c}\right)\sin\phi \tag{3.3}$$

$$u_2 = \left(\frac{fd_2}{c}\right)\cos\phi \tag{3.4}$$

These two functions are related by

$$\frac{u_1}{u_2} = \frac{d_1}{d_2}\tan\phi \tag{3.5}$$

The weighting coefficients can be calculated by taking IDFT to this symmetrical function defining required radiation pattern, so called objective function $\left(H(u_1,u_2)\right)$. Substituting (3.3) and (3.4) into (3.2), the objective function becomes

$$H(u_1,u_2)=\sum_{u_1=-0.5}^{0.5}\sum_{u_2=-0.5}^{0.5}G(u_1,u_2)w_{m_1,m_2}e^{j2\pi(u_1m_1+u_2m_2)} \tag{3.6}$$

The u_1-u_2 region is limited for both u_1 and u_2 to (-0.5, 0.5) which can be derived using two auxiliary parameters and desired frequency band where f_l and f_h are the lowest and highest frequency, respectively. Therefore, the boundary for both u_1 and u_2 can be computed as follows.

$$|u_1|=\left|\frac{fd_1}{c}\sin\phi\right|\le\frac{fd_1}{c}\le\frac{f}{c}\frac{\lambda_{\min}}{2}=\frac{f}{c}\frac{c}{2f_h}\le 0.5 \tag{3.7}$$

$$|u_2|=\left|\frac{fd_2}{c}\cos\phi\right|\le\frac{fd_2}{c}\le\frac{f}{c}\frac{\lambda_{\min}}{2}=\frac{f}{c}\frac{c}{2f_h}\le 0.5 \tag{3.8}$$

where $\lambda_{\min}$ is the wavelength at the highest frequency. However, in the presented case, variables u_1 and u_2 depend on the value of desired frequency band and the array's look angle ϕ.

Then the weighting coefficients can be given by applying the orthogonal property of IDFT to (3.6) and using two auxiliary functions as expressed by

$$w_{m_1,m_2}=\left(\frac{1}{N_{u_1}N_{u_2}}\right)\sum_{u_1=-0.5}^{0.5}\sum_{u_2=-0.5}^{0.5}(H(u_1,u_2)/G(u_1,u_2))\cdot e^{-j2\pi u_1m_1}e^{-j2\pi u_2m_2} \tag{3.9}$$

where N_{u_1} and N_{u_2} are the number of sampling point on u_1-u_2 plane as $\Delta u_1=1/N_{u_1}$ and $\Delta u_2=1/N_{u_2}$. The weights presented in (3.9) are obtained from the assumed H/G characteristic over a wide frequency band. However, the number of sampling points

on the $u_1 - u_2$ plane is larger than the numbers of antenna elements. Therefore, assuming that the number of samples on $u_1 - u_2$ plane is $N_{u_1} = 2N_1$ and $N_{u_2} = 2N_2$ because the radiation pattern is stable both in the angular and frequency domains for an arbitrary size of this array (Uthansakul and Bialkowski, 2006).

If φ is the polar angle of the $u_1 - u_2$ plane, then it can be given by

$$\tan(\varphi) = \frac{u_1}{u_2} = \frac{d_1}{d_2}\tan\phi \tag{3.10}$$

Thus,

$$\varphi = \tan^{-1}\left(\frac{d_1}{d_2}\tan\phi\right) \tag{3.11}$$

Equations (3.3) and (3.4) are raised both sides to second power, then they become

$$\left(\frac{u_1}{fd_1/c}\right)^2 = \sin^2\phi \tag{3.12}$$

$$\left(\frac{u_2}{fd_2/c}\right)^2 = \cos^2\phi \tag{3.13}$$

Then, they can be summed as

$$\left(\frac{u_1}{fd_1/c}\right)^2 + \left(\frac{u_2}{fd_2/c}\right)^2 = \sin^2\phi + \cos^2\phi = 1 \tag{3.14}$$

Equation (3.14) demonstrates an ellipse with the center at $u_1 = u_2 = 0$. In special case having $d_1 = d_2 = d$, it presents circle behavior which can be written as

$$u_1^2 + u_2^2 = \left(\frac{fd}{c} \right)^2 \tag{3.15}$$

where $\left(\frac{fd}{c} \right)$ is radius of the circle. The equations (3.11) and (3.14) represent the loci of constant angle and constant frequency, respectively. The plot of loci for constant angle and constant frequency is shown in Figure 3.2.

Assuming that an array antenna system is designed for direction of main beam $\phi = \phi_0$ and frequency $f_l < f < f_h$ having its center frequency at $f = f_0$. The location of the desired points on $u_1 - u_2$ plane is limited by

$$\varphi_0 = \tan^{-1}\left(\frac{d_1}{d_2} \tan\phi_0 \right) \tag{3.16}$$

and

$$r_l = \frac{f_l}{c} \bar{d} \tag{3.17}$$

$$r_h = \frac{f_h}{c} \bar{d} \tag{3.18}$$

where $r_l < |r| < r_h$ and $\bar{d} = \sqrt{d_1^2 \sin^2 \phi_0 + d_2^2 \sin^2 \phi_0}$. The symmetry of the loci with respects to the origin of $u_1 - u_2$ plane results in real values for multipliers w_{m_1,m_2} of each antenna element (Ghavami, 2002).

Figure 3.2 shows simulation of two loci plot which represents desired frequency band from 1.9 GHz to 2.4 GHz having its center frequency at 2.15 GHz. The array spacing is chosen by half-wavelength at 3 GHz, $d_1 = d_2 = 5cm$. It is assumed that the array is square in shape and formed by 4×4 elements. The desired main beam direction is $45°$.

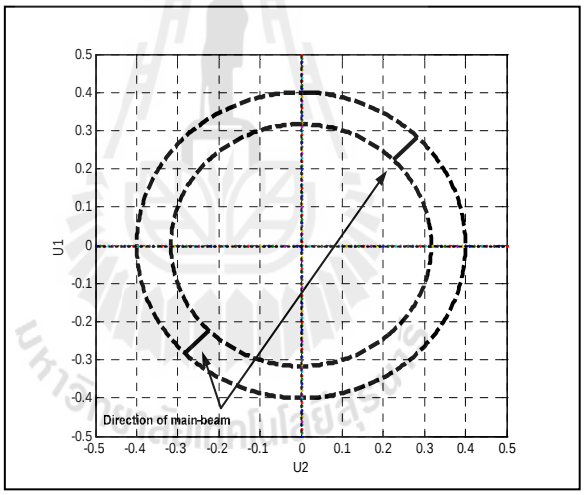

Figure 3.2 Location of desired points on the intersection of the constant angle and constant frequency loci.

From (3.6), the objective function $H(u_1, u_2)$ is assumed using Sinc function to obtain maximum gain in DOA of the desired signal (ϕ_0). As a result of this assumption, the following objective function is written as

$$H(u_1,u_2)=\frac{\sin\left[\alpha\pi\left(\frac{u_1}{u_2}-\tan\phi_0\right)\right]}{\alpha\pi\left(\frac{u_1}{u_2}-\tan\phi_0\right)}\cdot\begin{cases}1 & ,r_l<|r|<r_h\\ \frac{1}{\sqrt{10}} & ,otherwise\end{cases} \tag{3.19}$$

This function is defined only in the region of $r_l<|r|<r_h$ and $\varphi_0=\tan^{-1}\left(\frac{d_1}{d_2}\tan\phi_0\right)$. The factor $1/\sqrt{10}$ is introduced to have a 10 dB drop of signal outside the desired frequency band and α is related to the main beam first null width $\Delta\phi$ which is defined as

$$\Delta\phi=\tan^{-1}\left(\tan\phi_0+\frac{1}{\alpha}\frac{d_2}{d_1}\right)-\tan^{-1}\left(\tan\phi_0-\frac{1}{\alpha}\frac{d_2}{d_1}\right) \tag{3.20}$$

and α is

$$\alpha=\frac{\left(\frac{d_1}{d_2}\tan\Delta\phi\right)}{-1+\sqrt{1+\tan^2\Delta\phi+\tan^2\Delta\phi\tan^2\phi_0}} \tag{3.21}$$

Using these relations, the parameter α is 1.5206 to obtain $\Delta\phi=40°$ when the main beam is pointed to direction of $\phi_0=45°$. The simulation pattern on u_1-u_2 plane is shown in Figure 3.3 and their weighting coefficients can be determined form equation (3.9) as shown in table 3.1.

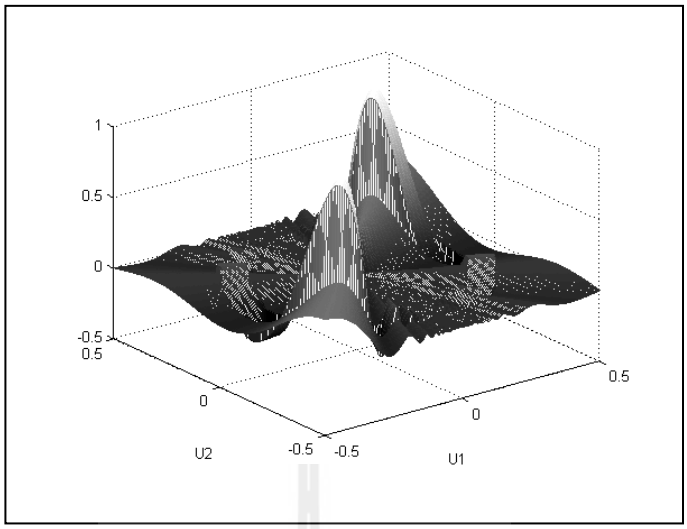

Figure 3.3 Plot of objective function using Sinc created on $u_1 - u_2$ plane for frequencies from 1.9 to 2.4 GHz.

Table 3.1 Weighting coefficients for 4×4 beamformer when desired direction is $45°$

Element Number	Attenuation Factor (dB)	Element Number	Attenuation Factor (dB)
1	13.9602	9	-15.0232
2	-9.9055	10	0
3	-11.6663	11	-11.6983
4	0.2822	12	-7.3688
5	-7.3688	13	0.2822
6	-11.6983	14	-11.6663
7	0	15	-9.9055
8	-15.0232	16	13.9602

From table 3.1, note that negative attenuators mean $180°$-phase shifting, the simulated radiation pattern for the beamformer with its main beam pointed to $45°$ for frequencies from 1.9 to 2.4 GHz is shown in Figure 3.4.

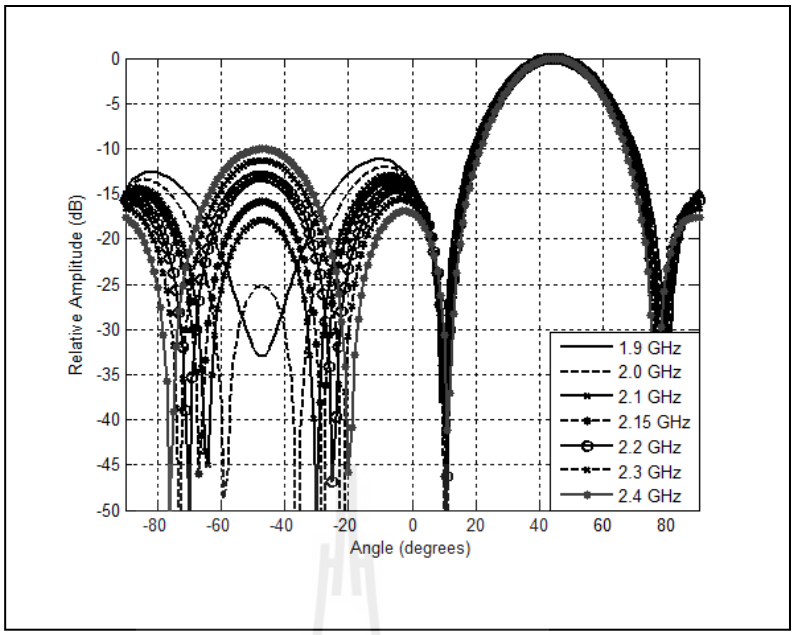

Figure 3.4 Simulated radiation pattern of 4×4 beamformer represented by Sinc plotted for frequencies from 1.9 to 2.4 GHz when the desired Main beam direction is $45°$.

3.3 Designing for low side lobe level

For the fully spatial beamformer mentioned earlier, the objective function $H(u_1, u_2)$ is a key design representing a predefined radiation pattern giving maximum gain at a desired direction. This function is also stable over a designated wide frequency band. As presented in last section, only one main beam is achieved but its side lobe levels are relative high as can be seen in Figure 3.4. Therefore, in this section, the objective function is created using Chebyshev polynomial instead of Sinc function in order to reduce side lobe level (Uthansakul and Bialkowski, 2005)

The chebyshev polynomial function can be expressed as

$$H(u_1,u_2)=\begin{cases} X & ,desired\ \ frequency band \\ \dfrac{1}{\sqrt{10}} & ,otherwise \end{cases} \tag{3.22}$$

where

$$X=\begin{cases} (-1)^N \cosh(N\cdot \arccos h|x|) & ,x<-1 \\ \cos(N\cdot \arccos x) & ,|x|\le 1 \\ \cosh(N\cdot \arccos h\, x) & ,x\ge 1 \end{cases} \tag{3.23}$$

and

$$x=x_0\cos(u/2) \tag{3.24}$$

$$x_0=\cosh\frac{arccoh SLL_{dB}}{N-1} \tag{3.25}$$

$$u=\left(\frac{2\pi}{\lambda}\right)d\sin\phi \tag{3.26}$$

SLL_{dB} is the desired side lobe level in decibels

Therefore

$$x=x_0\cos\left(\left(\left(\frac{2\pi}{\lambda}\right)d\sin\phi\right)/2\right) \tag{3.27}$$

or

$$x = x_0 \cos\left(\left(\pi \sin\left[a \tan(u_1 / u_2 - \phi_0)\right]\right)/2\right) \tag{3.28}$$

Where ϕ_0 stands for the direction at which the main-beam is to be directed and N is the number of antennas.

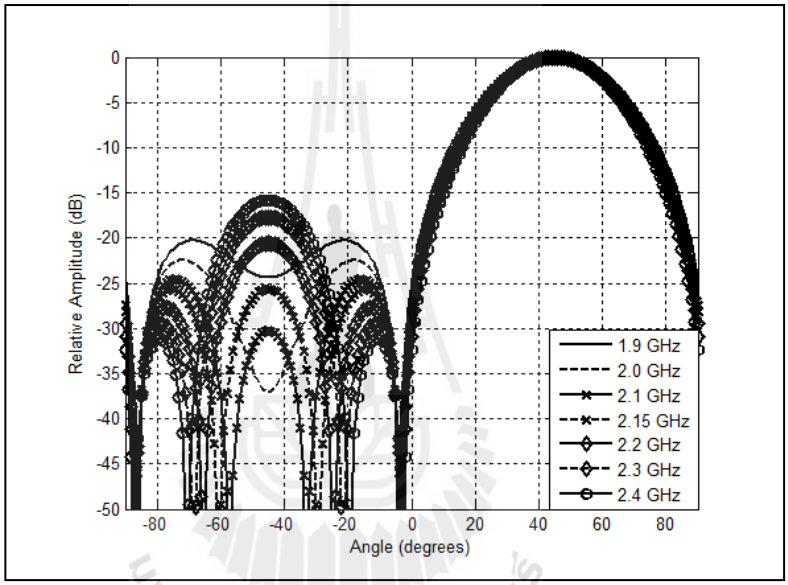

Figure 3.5 Radiation pattern of 4×4 beamformer using Chebyshev polynomial plotted for frequencies from 1.9 to 2.4 GHz when desired main beam direction is $45°$.

The comparison of the radiation patterns when $H(u_1, u_2)$ is assumed in the form of Sinc function and Chebyshev polynomial are shown in the Figures 3.4 and 3.5, respectively. The designated frequency band is herein chosen from 1.9 to 2.4 GHz. The array is square in shape and form by 4×4 antenna elements. The simulation results in term of radiation pattern presented in Figures 3.4 and 3.5 indicate that its

main beam is correctly directed towards $45°$ while side lobe level shown in Figure 3.5 is lower than the one shown in Figure 3.4 throughout the desired frequency band. Thus, the wideband spatial beamformer offers low side lobe level by applying the Chebyshev polynomial to synthesize its radiation pattern.

3.4 Multi-beam formation

This section presents the concept to produce multiple beams for fully spatial beamformer. Only one beam production may introduce an energy loss in unused areas when utilizing for indoor purposes. For instance in the hospital, we loss energy in some unused areas e.g., housekeeping laundry. Moreover, the generated wireless signal becomes interferers in some restricted areas e.g., ECG room, pathology room, or operating rooms, which are prohibited areas and all equipment in those rooms needs a very accurate operation. However, those impairments can be eliminated using a system capable of producing multiple beams. Then, energy can be efficiently used. Also, we can avoid interference signals in some particular areas. Nonetheless, these antenna systems must be low of cost and simple. To support incoming integrated service mentioned before, the systems has to be able to operate in wide frequency band. This is a motivation of this section. The key of this proposal is to have more degree of freedom in objective function as written in (3.29).

$$H(u_1,u_2) = H_{d_1}(u_1,u_2) + H_{d_2}(u_1,u_2) + ... + H_{d_n}(u_1,u_2) \tag{3.29}$$

Where $H_{d_1}(u_1,u_2), H_{d_2}(u_1,u_2),..., H_{d_n}(u_1,u_2)$ standard for objective function in which the main beams are directed to $d_1, d_2,..., d_n$, respectively. Assuming that, desired radiation pattern can form two main beam directions directed to $-65°$ and $65°$ off

boresight direction over the frequency range from 1.9 to 2.4 GHz. The antenna array is formed by 8×8 antenna elements. Also the objective functions are created using Chebyshev polynomial. Thus (3.29) can reduced to

$$H(u_1, u_2) = H_{d_1}(u_1, u_2) + H_{d_2}(u_1, u_2) \tag{3.30}$$

The simulation pattern on $u_1 - u_2$ plane and the obtained radiation pattern are presented in Figures 3.6 and 3.7, respectively.

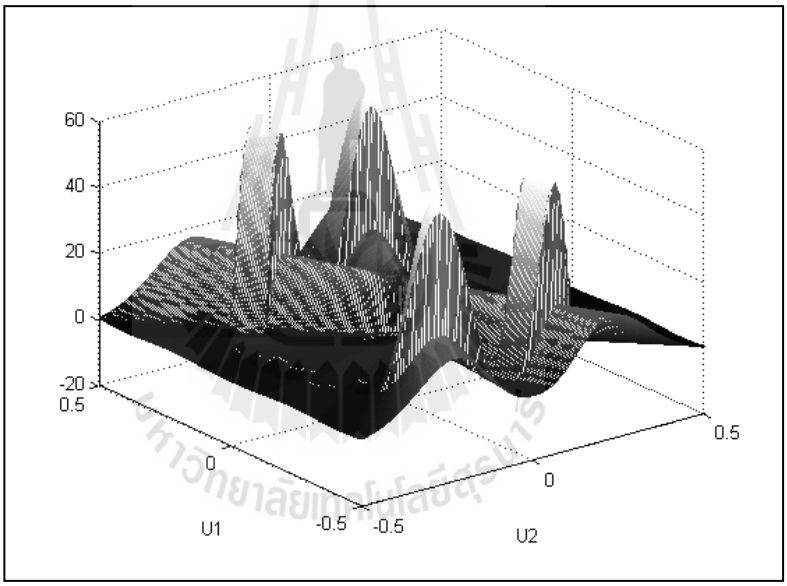

Figure 3.6 Plot of $H(u_2, u_2)$ when desired beam angle are $-65°$ and $65°$

As we can see in Figure 3.7, the beamformer is able to make its maximum gain to the designated directions, $-65°$ and $65°$. Also, the average level of side lobes is low. This behavior is quite stable throughout the designated frequency band.

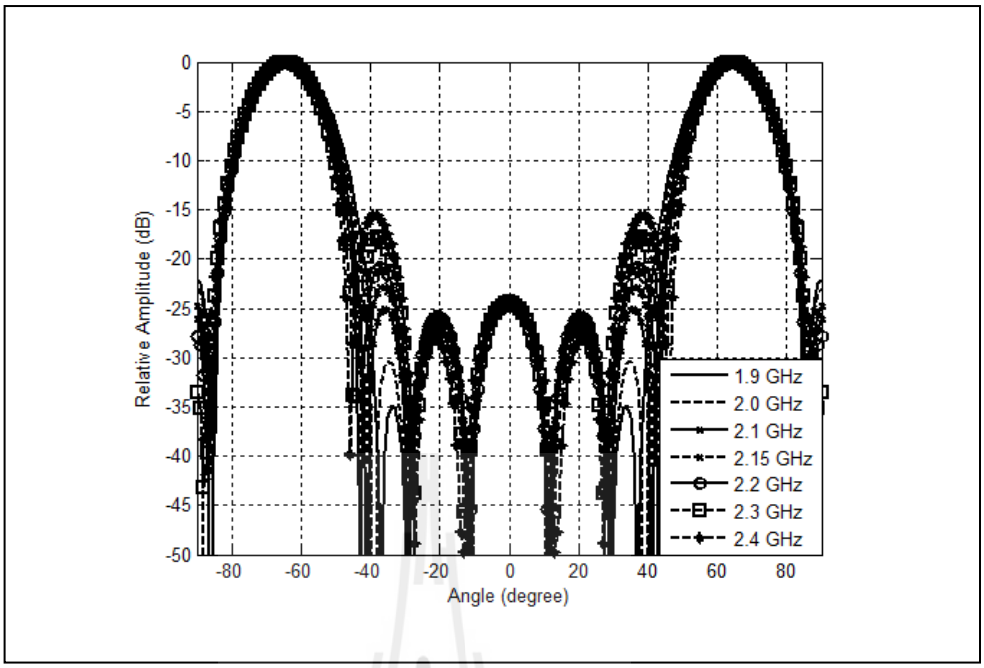

Figure 3.7 Radiation pattern of 8×8-beamformer for desired direction of $-65°$ and $65°$ plotting for frequencies from 1.9 to 2.4 GHz.

From running a number of simulations, multi-beam formation concept works well when employing a number of antenna elements more than 8×8. The reason is that much wider main beam is obtained when utilizing lower number of antenna elements causing overlapping between two formed main beams.

3.5 Chapter summary

This chapter has presented the concept of fully spatial beamformer which is able to steer beam in azimuth over a wide frequency band without the use of phase shifts, frequency filters or delay networks. From the theory is shown that it requires only real-values weights at individual antenna elements which in practice can be realized by amplifier or attenuator. Then, a modification is made to objective function

in order to lower side lobe levels. Before ending the chapter, the concept of muti-beam formation has been introduced. To confirm the concepts, some simulation results have been demonstrated.

CHAPTER IV

REFINEMENT ALGORITHM FOR WIDEBAND FULLY SPATIAL BEAMFORMER

4.1 Introduction

From the last chapter presenting the general background of wideband fully spatial beamformer, this kind of beamformer has a major contribution as its weighting coefficients are real-valued in which can be simply realized by attenuators or amplifiers. However, so far, the range of attenuation or amplification is relatively large which is not practical for hardware realization. Therefore, this chapter proposes a concept to reduce the range of weighting coefficients while maintaining some major characteristic of radiation. Also, the proposed algorithm is validated in term of radiation pattern comparing the ones obtained from IDFT method.

4.2 Refinement algorithm

The weighting coefficients calculated using IDFT method as detailed in last chapter are here defined as

$$W_o = \left\{ w_{o,1}, w_{o,2}, w_{o,3}, \ldots, w_{o,N} \right\} \tag{4.1}$$

$$W_o = \{ w_{o,i} \} \qquad ,i = 1,2,3,\ldots,N \tag{4.2}$$

Where N is number of array antennas. Usually, the value of W_o is general number, then weighting coefficients obtained from IDFT method are rounded to integer-valued weights (W_r) as

$$W_r = \{w_{r,1}, w_{r,2}, w_{r,3}, \ldots, w_{r,N}\} = \{w_{r,i}\} \tag{4.3}$$

or

$$W_r = Int\{w_{o,j}\} \tag{4.4}$$

Then, the required main beam direction (ϕ_0), average level of minor lobe (MLL_0), width of main beam (δ_0) and weighting coefficient (W_r) are given. Next, the algorithm carries out the following steps:

(1) Determine the maximum of W_r, that is

$$w_{\max}^{(k)} = \max_{i=1}^{N}\{w_{r,i}\} \tag{4.5}$$

where $k = 1,2,3,\ldots$ which is the order of iteration.

(2) Decrease maximum of weighting coefficient $(w_{\max}^{(k)})$ by increasing a step size, where $\Delta w > 0$. This results in integer number for weighting coefficients.

$$w_{\max,j}^{(k)} = \left\| w_{\max}^{(k)} - \Delta w \right\| \tag{4.6}$$

where $j = 1,2,3,\ldots$. Then, replace $w_{\max,j}^{(k)}$ with $w_{\max}^{(k)}$ in the set of W_r.

$$w_{\max,j}^{(k)} \Rightarrow w_{\max}^{(k)} \tag{4.7}$$

(3) Multiply W_r to steering vector ψ , the array output can obtained as

$$y_j^{(k)} = \sum_{i=1}^{N} w_{r,i} e^{\psi} \tag{4.8}$$

$$y_j^{(k)} = \sum w_r (\exp((2\pi f / c)(d_1 p \sin\phi + d_2 q \cos\phi))) \tag{4.9}$$

where (p,q) is index of antenna elements, d_1 and d_2 represent inter-element spacing in the two orthogonal direction, f is the frequency and c is the velocity of an electromagnetic wave.

(4) Now, the radiation patterns obtained from (4.9) and then check some significant parameters such as main beam direction $(\phi_r^{(k)})$, average minor lobe level (MLL_r^k) and beamwidth $(\delta_r^{(k)})$ according to the following conditions.

$$w_{\max}^k \le w_0 \tag{4.10}$$

$$\phi_0 - \Delta\phi \le \phi_r^{(k)} \le \phi_0 + \Delta\phi \tag{4.11}$$

$$MLL_r^{(k)} \le MLL_0 + \Delta MLL \tag{4.12}$$

$$\delta_r^{(k)} \le \delta_0 + \Delta\delta \tag{4.13}$$

where w_0 is desired maximum of weighting coefficients.

$\Delta\phi$ is deviation of main beam angle.

ΔMLL is deviation of average minor lobe level.

$\Delta\delta$ is deviation of the first null beamwidth.

(5) Repeat steps 1 to 4 until the set of weighting coefficient is zero according to (4.10) to (4.13), then a set of new solution (w_r) is obtained for the refinement method.

From refinement algorithm, the obtained weights are all integer number and also the range between the minimum and maximum values is narrower while maintaining some characteristics of radiation pattern. Moreover, this is considerably practical for hardware implementation which is low cost and saving energy for obtained narrow range of weighting coefficients.

4.3 Performance evaluation of refinement algorithm

This section shows the performance evaluation of refinement algorithm using my own developed program in MATLAB. The utilized antennas are arranged in 4×4-lattice and the operating frequencies are given from 1.9 to 2.4 GHz. The initial weighting coefficients are computed using IDFT method when the objective function is created using Chebyshev polynomial. Some significant parameters are assumed as follows: decreasing step size of weighting coefficient is 1, desired maximum of weighting value is 30 dB and steering angle is varies from 0 to 90 degrees. The 6-cases with different variables are assumed in simulation as shown in Table 4.1.

Table4.1 Parameters given in simulation for refinement algorithm.

Parameters	Cases of Refinement					
	I	**II**	**III**	**IV**	**V**	**VI**
$\Delta\phi$ (degrees)	0	1	2	3	4	4
ΔMLL (dB)	0	1	2	3	4	4
$\Delta\delta$ (degrees)	0	1	2	3	4	5
Maximum weighting coefficients (dB)	54	54	54	54	34	29
Number of directions	67	71	77	86	90	91

Table 4.1 shows 6 cases for simulation to validate the performance of proposed refinement method for fully spatial beam-former. Some parameters e.g. maximum weighting coefficients (w_0), deviation of main-beam angle $(\Delta\phi)$, deviation of average minor lobe level (ΔMLL) and deviation of first-null beamwidth $(\Delta\delta)$ are different in each case. For case I, all parameters are assumed for ideal case with error free. Running some simulations show that 67 cases (directions) out of 91 cases $(0° - 90°)$ are successful for the proposed refinement method. This means that there are only 67 directions out of 91 directions in which there is no error in main beam direction, minor lobe level and beamwidth. However, the algorithm cannot be refined the obtained maximum weighting coefficient is 54 dB which still maintains. For case II, III and IV, this condition allows a slight error in main-beam direction, average minor lobe level and first-null beamwidth. It has been found that the number of success cases increase from 67 to 71, 77, 86 directions for case II, III, and IV, respectively nevertheless maximum of weight is still 54, as shown in Table 4.1. The rapidly increasing number of success cases is demonstrate in case V from 86 to 90 and obtained maximum weight is reduce to 34 dB. For case VI, 100% success can be achieved and desired maximum weight is 29 dB when systems allow error in main beam direction up to 4°, minor lobe level up to 4 dB and beamwidth up to 5° for some direction. From this

table, the trend for decreasing of maximum weights is narrower range when the system allowed higher error for these parameters.

For example, the main beam direction is chosen at 35° and parameters are $\Delta\phi = 4°, \Delta MLL = 4dB$ and $\Delta\delta = 5°$. As a result, after performing refinement method, its dynamic range of weights can be reduced from 28 dB to 26 dB. In addition, there are 12 groups of obtained weights as shown in Table 4.2.

Table 4.2 The attenuations and parameters of refinement algorithm from simulation when desired direction is 35°.

Group Number	Element Number								Parameters			
	1,16	2,15	3,14	4,13	5,12	6,11	7,10	8,9	$\Delta\phi$ (degree)	ΔMLL (dB)	$\Delta\delta$ (degree)	w_{max} (dB)
1	27	7	8	8	7	19	0	12	3	3	4	27
2	27	7	8	8	7	19	0	12	3	3	5	27
3	27	7	8	8	7	19	0	12	3	4	4	27
4	27	7	8	8	7	19	0	12	3	4	5	27
5	27	7	8	8	7	19	0	12	4	3	4	27
6	27	7	8	8	7	19	0	12	4	3	5	27
7	27	7	8	8	7	19	0	12	4	4	4	27
8	27	7	8	8	7	19	0	12	4	4	5	27
9	26	7	8	8	7	19	0	12	3	3	5	26
10	26	7	8	8	7	19	0	12	3	4	5	26
11	26	7	8	8	7	19	0	12	4	3	5	26
12	26	7	8	8	7	19	0	12	4	4	5	26

From Table 4.2, 9th to 12th groups are candidates as they provide the minimum dynamic range reflected from obtained w_{max}. However, in practice, one group has to be chosen. For this research work, the 9th is chosen as it provide minimum dynamic range of weights while giving minimum error in main beam direction, sidelobe level and beamwidth.

Next, the behavior of $\Delta\phi$, ΔMLL and $\Delta\delta$ when focusing on achievement in reducing dynamic range of weight is detailed. To show one example, main beam direction is chosen at 26° when employing 4×4-antenna array. The maximum weights obtained from IDFT is 42 dB. The parameters given for refinement method are $\Delta\phi = 4°, \Delta MLL = 4\,dB$ and $\Delta\delta = 5°$.

Firstly, the behavior of error in main beam direction ($\Delta\phi$) is in focus. For this case $\Delta MLL = 4dB, \Delta\delta = 5°$ when deviation or error of main beam direction is given from 0º to 20 º. The obtained simulation result is shown in Figure 4.1. As we can see, the dynamic range of weights (ratio between IDFT and refined weights) is narrower when higher error in main beam direction is allowed. However, the mentioned ratio is stable at 0.4761 when the error in main beam direction is higher than 7º. The cause of this stability is as follows. The ratio between refined and IDFT weights can be reduced to a certain value depending on the initial values, for this case $\Delta MLL = 4dB, \Delta\delta = 5°$. This means that the mentioned ratio can be smaller if ΔMLL and $\Delta\delta$ are changed.

Secondly, deviation of average minor lobe level (ΔMLL) is in focus. For this case $\Delta\phi = 4°, \Delta\delta = 5°$ when the mentioned deviation is given from 0 to 20 dB. The obtained simulation result is plotted in Figure 4.2. As we can see, the dynamic range reduces continually when deviation of average minor lobe level increases from 0 dB to 13 dB. This means that the dynamic range of weights can be reduced from 42 dB to 11 dB when 13 dB of error in *MLL* is allowed. However, the reduction of dynamic range is stable at 0.260. This means that up to this point the variation of weights can be altered by $\Delta\phi$ and $\Delta\delta$ instead of ΔMLL.

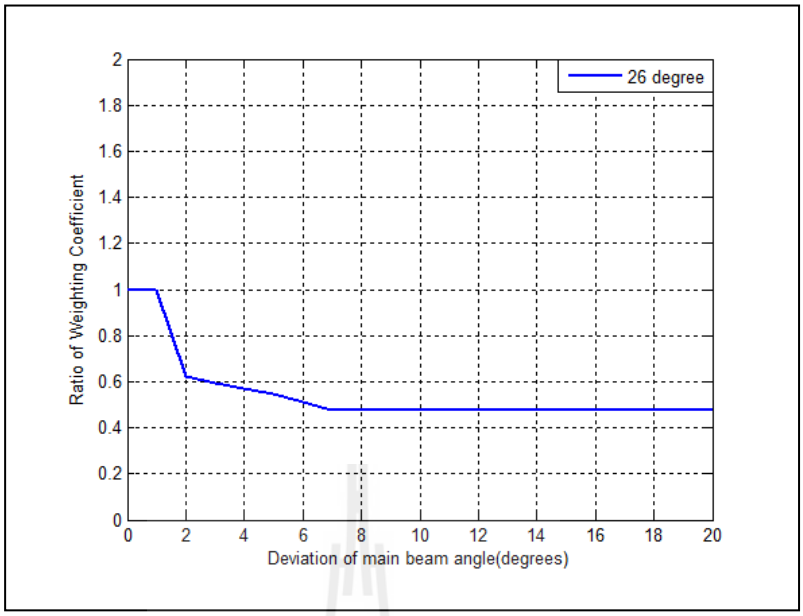

Figure 4.1 Relative between ratio of weighting coefficient and deviation of main beam direction.

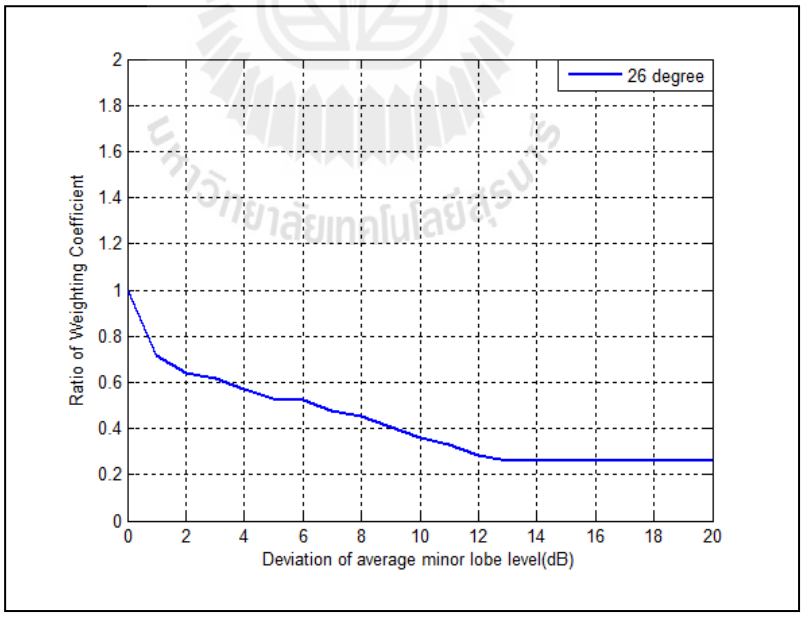

Figure 4.2 Relative between ratio of weighting coefficient and deviation of average minor lobe level.

Lastly, the deviation of first null beam width ($\Delta\delta$) is in focus. For this case $\Delta\phi = 4°, \Delta MLL = 4dB$ when the deviation of first null beamwidth varies from 0º to 20º. Its behavior is plotted in Figure 4.3. As we can see, the ratio of weighting coefficient reduces continually when deviation of average minor lobe level increases from 0 dB to 7 dB reflecting the reduced dynamic range from 42 dB to 23 dB. As expected, the reduction of dynamic range is stable at 0.50. This means that up to this point the variation of weights can be altered by $\Delta\phi$ and ΔMLL instead of $\Delta\delta$.

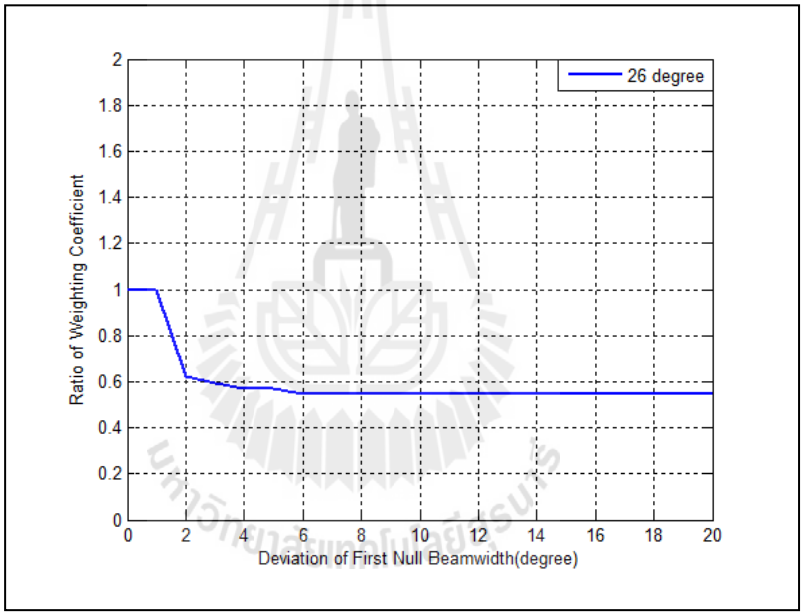

Figure 4.3 Relative between ratio of weighting coefficient and deviation of first null beamwidth.

Table 4.3 shows 16 values of weighting coefficients comparing between IDFT method and proposed refinement method when the desired main beam direction is given at 45°. For the refinement method, the parameters of system are given as: $w_0 = 18\,dB, \Delta\phi = 0^o, \Delta MLL = 3\,dB$ and $\Delta\delta = 0^o$. As shown in Table 4.3, the

maximum weighting coefficient reduces from 22.78 to 18 dB which means that the range of attenuation or amplification decreases.

Table 4.3 The comparison value of attenuation factors using IDFT method and refinement method.

Element number	Attenuation (dB)		Element number	Attenuation (dB)	
	IDFT	Refinement		IDFT	Refinement
1	22.78	18	9	-21.47	-18
2	-6.83	-7	10	0	0
3	-21.47	-18	11	-16.80	-17
4	5.87	6	12	-6.83	-7
5	-6.83	-7	13	5.87	6
6	-16.80	-17	14	-21.47	-18
7	0	0	15	-6.83	-7
8	-21.47	-18	16	22.78	18

Figure 4.4 shows beamforming performance for case shown in Table 4.3 at frequency 2.15 GHz comparing between using IDFT method and proposed refinement method. The obtained result shows that after the refinement method is done the main beam direction is still pointed to 45° and there is no error in beamwidth. Also, the error in average minor lobe level is within 3 dB.

Figures 4.5 and 4.6 show beamforming performance of the beamformer throughout the designated band using IDFT and proposed refinement methods, respectively. As we can see, the beamforming performance for both cases is similar while we can decrease the range of attenuation or amplification up to 4.78 dB (22.78-18 dB).

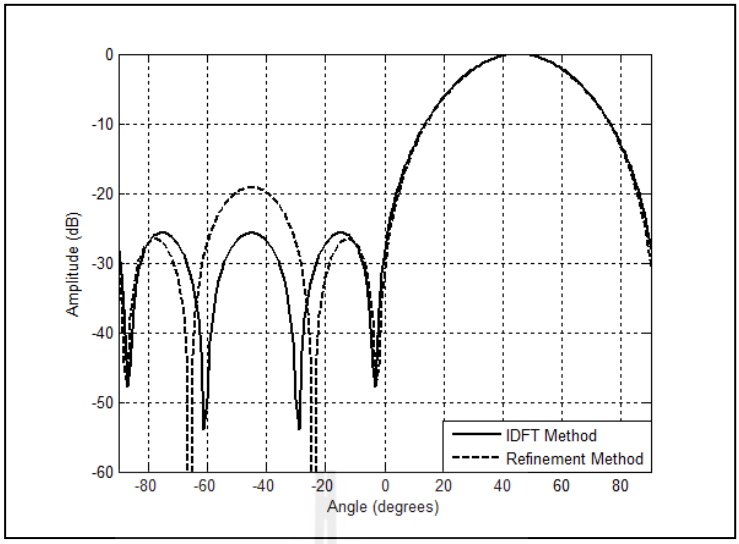

Figure 4.4 The comparison of radiation performance using IDFT method and Refinement method at 2.15 GHz when the main beam is pointed to 45°.

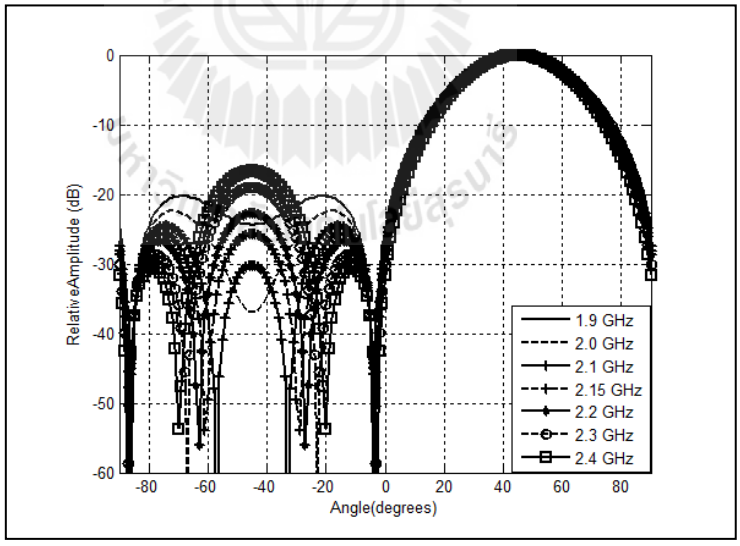

Figure 4.5 Radiation pattern using IDFT method for frequencies from1.9 to 2.4 GHz when main beam is pointed to 45°.

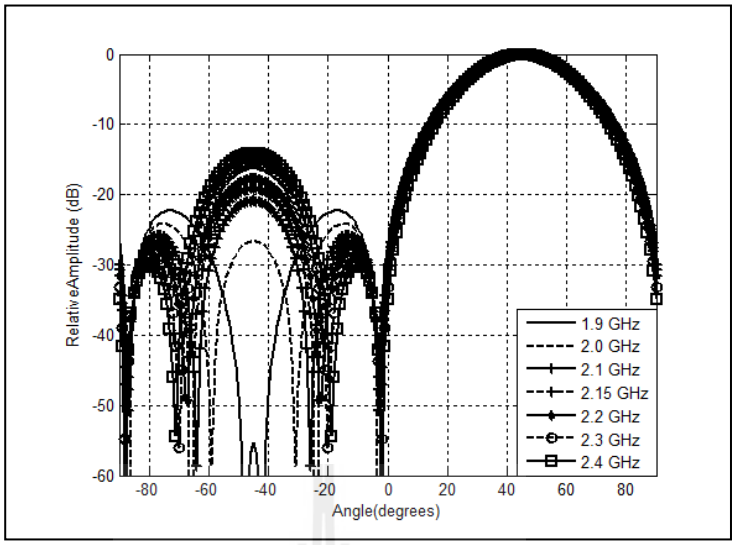

Figure 4.6 Radiation pattern using proposed refinement method for frequencies 1.9 to 2.4 GHz when main beam is pointed to 45°.

The set of the best weights for refinement algorithm for $0° - 90°$ is shown in table 4.4 when the system allowed maximum weighting coefficients (w_0), deviation of main beam angle $(\Delta\phi)$, deviation of average minor lobe level (ΔMLL) and deviation of first null beamwidth $(\Delta\delta)$ are not over 29 dB, 4°, 4 dB and 5°, respectively.

Table 4.4 The weighting coefficients for refinement algorithm

Angle	Attenuation Factor (dB)							
	Element number							
	1,16	2,15	3,14	4,13	5,12	6,11	7,10	8,9
0	-4	0	0	-4	6	3	3	6
1	-4	0	0	-4	6	3	3	5
2	-4	0	0	-4	7	4	2	4
3	-4	0	0	-4	7	4	2	4
4	-5	0	0	-4	10	5	2	3
5	-5	-1	0	-4	9	5	2	3
6	-5	-1	0	-5	13	6	1	2

Table 4.4 The weighting coefficient for refinement algorithm (Continued.)

Angle	Attenuation Factor (dB)							
	Element number							
	1,16	**2,15**	**3,14**	**4,13**	**5,12**	**6,11**	**7,10**	**8,9**
7	-5	-1	0	-5	12	6	1	2
8	-6	-1	0	-5	15	7	1	2
9	-6	-1	0	-6	22	7	1	1
10	-6	-1	0	-6	-24	8	0	1
11	-7	-1	0	-7	-17	9	0	1
12	-8	-2	0	-7	-14	10	0	1
13	-8	-2	0	-8	-13	10	0	1
14	-9	-2	-1	-9	-11	11	0	1
15	-10	-2	-1	-11	-11	11	0	1
16	-11	-3	-1	-12	-12	13	0	2
17	-12	-3	-1	-14	-11	14	0	2
18	-13	-3	-2	-14	-10	14	0	2
19	-14	-4	-2	-14	-10	14	0	2
20	-15	-4	-2	-19	-9	19	0	3
21	-16	-4	-3	-19	-9	19	0	3
22	-17	-4	-3	21	-8	21	0	3
23	-19	-5	-3	26	-8	27	0	4
24	-20	-5	-4	21	-8	21	0	4
25	-21	-5	-4	18	-7	-	0	5
26	-24	-5	-4	16	-7	-24	0	5
27	-23	-6	-5	14	-7	-23	0	6
28	-23	-6	-5	13	-7	-23	0	6
29	-20	-6	-5	12	-7	-20	0	7
30	-20	-6	-6	11	-7	-20	0	8
31	29	-6	-6	10	-7	-23	0	8
32	26	-6	-7	9	-7	-22	0	9
33	-	-6	-7	9	-7	-16	0	10
34	27	-6	-8	8	-7	-20	0	11
35	26	-7	-8	8	-7	-19	0	12
36	22	-7	-9	7	-7	-19	0	13
37	20	-7	-10	7	-7	-18	0	15
38	18	-7	-11	7	-7	-18	0	17
39	18	-7	-12	7	-7	-18	0	18
40	18	-7	-13	6	-7	-17	0	18
41	19	-7	-14	6	-7	-17	0	19
42	22	-7	-15	6	-7	-17	0	22

Table 4.4 The weighting coefficient for refinement algorithm (Continued.)

Angle	Attenuation Factor (dB)							
	Element number							
	1,16	**2,15**	**3,14**	**4,13**	**5,12**	**6,11**	**7,10**	**8,9**
43	17	-7	-17	6	-7	-17	0	-17
44	17	-7	-17	6	-7	-17	0	-17
45	17	-7	-17	6	-7	-17	0	-17
46	17	-7	-17	6	-7	-17	0	-17
47	17	-7	-17	6	-7	-17	0	-17
48	21	-7	21	6	-7	-17	0	-15
49	18	-7	18	6	-7	-17	0	-14
50	17	-7	17	6	-7	-17	0	-13
51	17	-7	17	7	-7	-17	0	-12
52	17	-7	17	7	-7	-17	0	-11
53	17	-7	15	7	-7	-17	0	-10
54	17	-7	13	7	-7	-17	0	-9
55	14	-7	12	8	-7	-14	0	-8
56	14	-7	11	8	-6	-14	0	-8
57	-	-7	10	9	-6	-16	0	-7
58	15	-7	9	9	-6	-15	0	-7
59	16	-7	8	10	-6	-16	0	-6
60	-18	-7	8	11	-6	-18	0	-6
61	-17	-7	7	12	-6	-17	0	-5
62	-18	-7	6	13	-6	-18	0	-5
63	-18	-7	6	14	-6	-18	0	-5
64	-20	-7	5	16	-5	-20	0	-4
65	-21	-7	5	18	-5	-	0	-4
66	-20	-8	4	21	-5	21	0	-4
67	-19	-8	4	23	-5	23	0	-3
68	-17	-8	3	21	-4	21	0	-3
69	-16	-9	3	-18	-4	18	0	-3
70	-15	-9	3	-17	-4	17	0	-2
71	-13	-10	2	-13	-4	13	0	-2
72	-13	-10	2	-13	-3	13	0	-2
73	-11	-11	2	-11	-3	11	0	-1
74	-11	-11	2	-11	-3	11	0	-1
75	-10	-10	1	-10	-2	10	0	-1
76	-9	-12	1	-9	-2	12	0	-1
77	-8	-12	1	-8	-2	10	0	0
78	-8	-13	1	-7	-2	10	0	0

Table 4.4 The weighting coefficient for refinement algorithm (Continued.)

Angle	Attenuation Factor (dB)							
	Element number							
	1,16	**2,15**	**3,14**	**4,13**	**5,12**	**6,11**	**7,10**	**8,9**
79	-7	-17	1	-7	-1	9	0	0
80	-6	-26	1	-6	-1	8	0	0
81	-6	15	1	-6	-1	7	1	0
82	-6	12	2	-5	-1	7	1	0
83	-5	10	2	-5	-1	6	1	0
84	-5	10	2	-5	-1	6	1	0
85	-5	8	3	-4	-1	5	2	0
86	0	0	0	0	0	0	0	0
87	0	0	0	0	0	0	0	0
88	0	0	0	0	0	0	0	0
89	0	0	0	0	0	0	0	0
90	0	0	0	0	0	0	0	0

From Table 4.3, note that negative attenuators mean 180° -phase shifting, the minus sign means no signal and 0 dB means no attenuation.

4.4 Chapter summary

This chapter has presented the core concept of refinement algorithm proposed in this thesis. The proposed concept is to reduce the range of weighting coefficient for fully spatial beamformer. This has been validated through some simulations. It can be found that the more errors e.g. main beam direction, minor lobe level and beamwidth are allowed, the higher number of success cases for refinement can be achieved. To practically confirm the proposed concept, next section shows some experiment results.

CHAPTER V

PROTOTYPE OF WIDEBAND FULLY SPATIAL BEAMFORMER

5.1 Introduction

The previous chapter has focused on the concept of refinement method and also the idea was confirmed through simulation results. The aim of proposed method is to reduce the range of weighting coefficients which can be realized using variable attenuators or amplifiers. This chapter presents the design and construction of beamformer prototype in order to validate the proposed refinement method. The prototype is designed for operating frequencies from 1.9 to 2.4 GHz. The prototype diagram is shown in Figure 5.1. The prototype is a digitally controlled beamforming system and it consists of three functional blocks: antenna array, weighting network, and control devices. The block diagram of the beamformer starts from 4×4 antenna array receiving the incident signals. The received signal is weighted in weighting network to adjust its amplitude. Then, the signal is summed at power combiner to form the system output.

This chapter is organized as follows: firstly, an antenna element is designed using CST Microwave studio. Then, the antenna element is fabricated to confirm its characteristic. The simulation and experimental results are confirmed. Next, the

design of weighting network is discussed. Finally, the part of control devices containing microprocessors to control components in weighting network is explained.

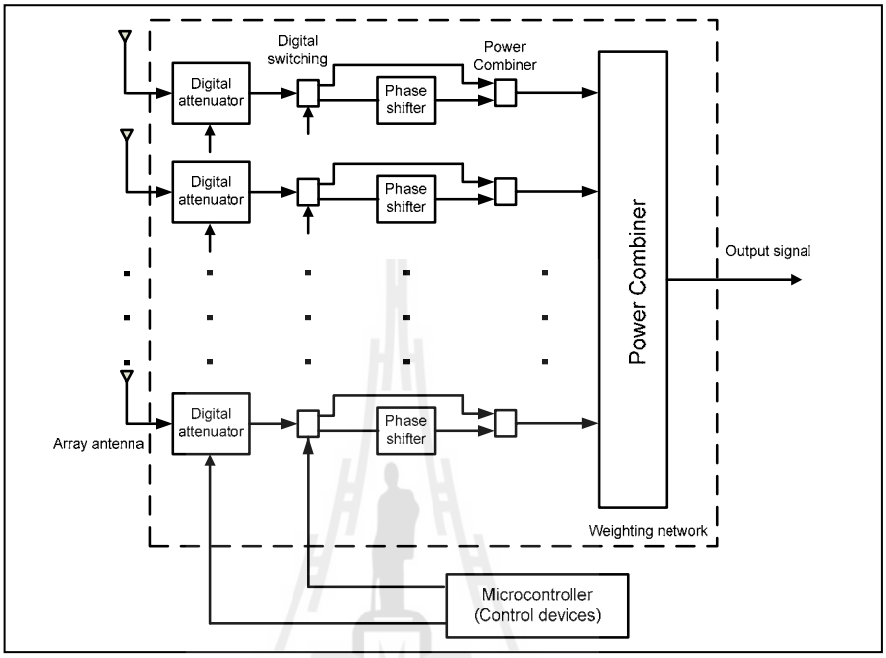

Figure 5.1 Prototype diagram of wideband spatial beamformer.

5.2 Antennas

This section shows the design of antenna element following the design in array form. The simulation and experimental results are compared to confirm their characteristic.

5.2.1 Design of antenna element

A planar monopole antenna is chosen to be antenna element. The reason is that this type of antenna works well in wide frequency range. Also, it is compact enough to be arranged to form the array having inter-element spacing of half wavelength. Thegeometrical configuration of a planar monopole antenna is shown in Figure 5.2. For the design studied here, the radiation element and the feed line are

printed on the same side of a microstrip patch having substrate FR4 of thickness 1.6 mm while the other side is the ground plane of antenna. As appeared in Figure 5.2, the feed line is 25-mm in length and ground plane is sized by 25×40 mm^2.

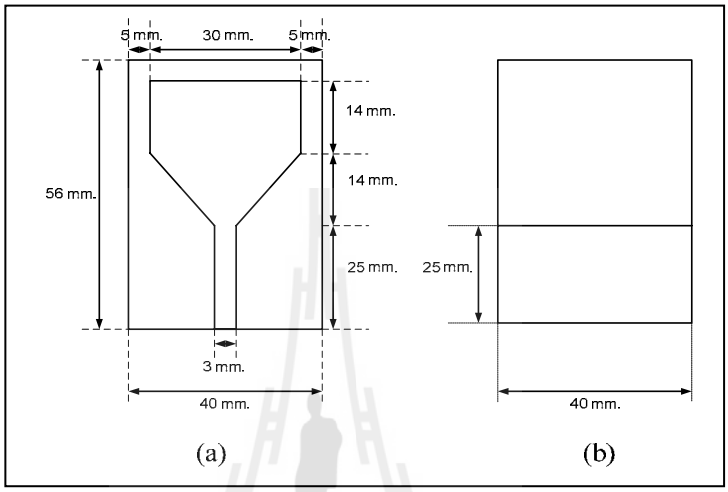

Figure 5.2 Planar monopole antenna structure at (a) front view (b) back view.

The designed antenna shown in Figure 5.2 is simulated using CST Microwave Studio to see its characteristic. The location of planar antenna is shown in Figure 5.3. A single antenna places on z-x plane (perpendicular to the y-axis) which is ground plane. Its simulated return loss throughout the frequencies from 1.5 to 3 GHz is shown in Figure 5.4. As we can see, the designed antenna has return loss lower than -10 dB throughout the designated band, from 1.9 to 2.4 GHz.

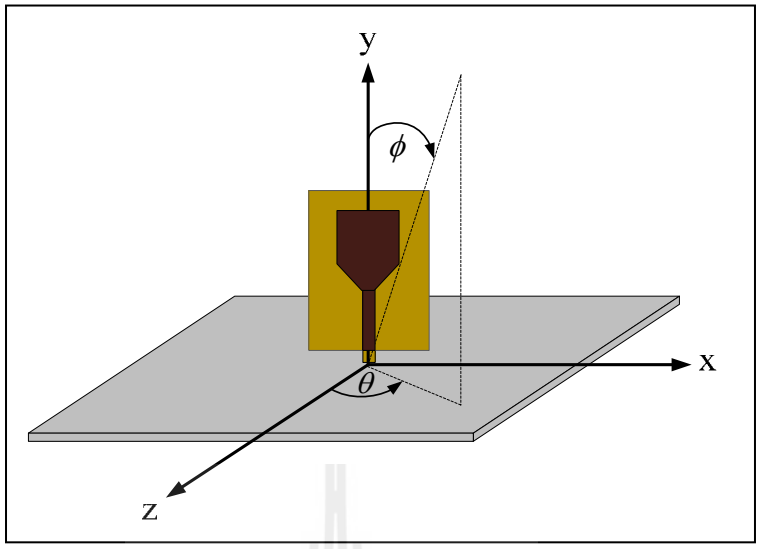

Figure 5.3 Geometry of a planar antenna and its coordinate system.

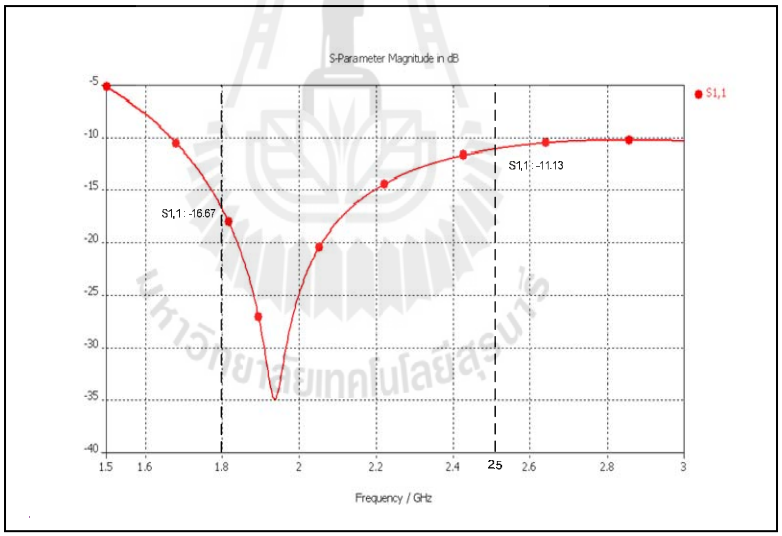

Figure 5.4 Simulated return loss of the designed antenna shown in Figure 5.2.

In addition, its simulated radiation patterns at 2.15 GHz are plotted for E-plane and H-plane as shown in Figures 5.5 and 5.6, respectively. It can be observed that both H-plane and E-plane are relatively omnidirectional as expected for general monopole antenna.

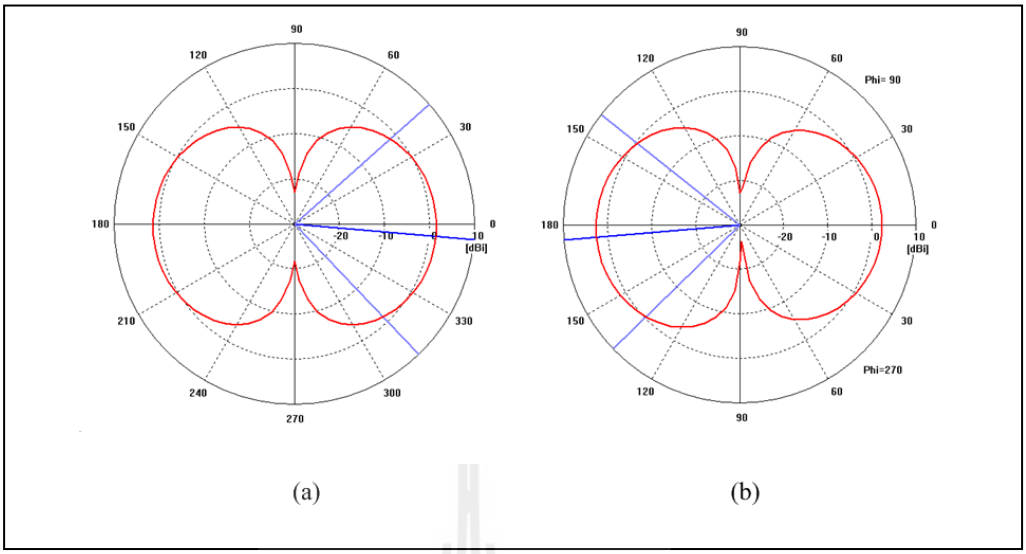

Figure 5.5 Simulated for E-plane pattern (a) y-z plane (b) x-y plane.

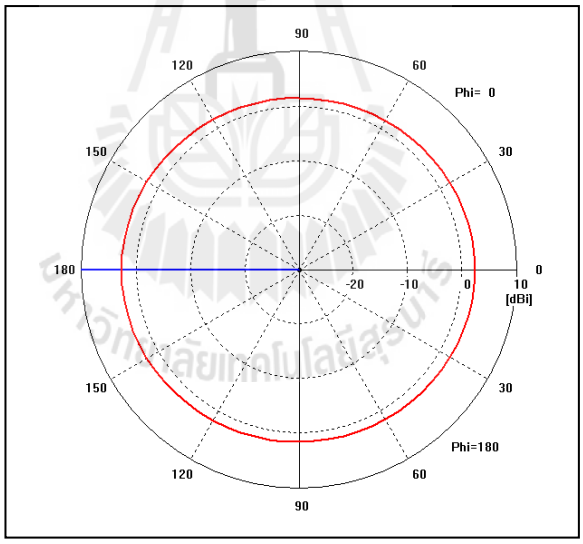

Figure 5.6 Simulated for H-plane (x-z plane) patterns.

5.2.2 Practical realization

- **Antenna element**

The planar monopole antenna designed from last section is fabricated using single-layer FR-4 substrate with dielectric constant of 4.4. The photograph of the manufactured antenna including coaxial feeding port using SMA connector is shown in Figure 5.7.

Figure 5.7 Photograph of fabricated wideband planar monopole antenna.

The actual return loss of the antenna fabricated on a $40 \times 56\, mm^2$ substrate is measured using Hewlett Packard 87220 50MHz-40 GHz network analyzer is shown in Figure 5.8. The measured frequency is spanned from 1 to 3 GHz. As we can see, the fabricated antenna has return loss under -10 dB for throughout the designated band from 1.9 to 2.4 GHz. This measurement result has shown that the proposed design of planar monopole work well within the designated

band. In addition, both measured and simulated results in return loss (dB) of the antenna are in good agreement.

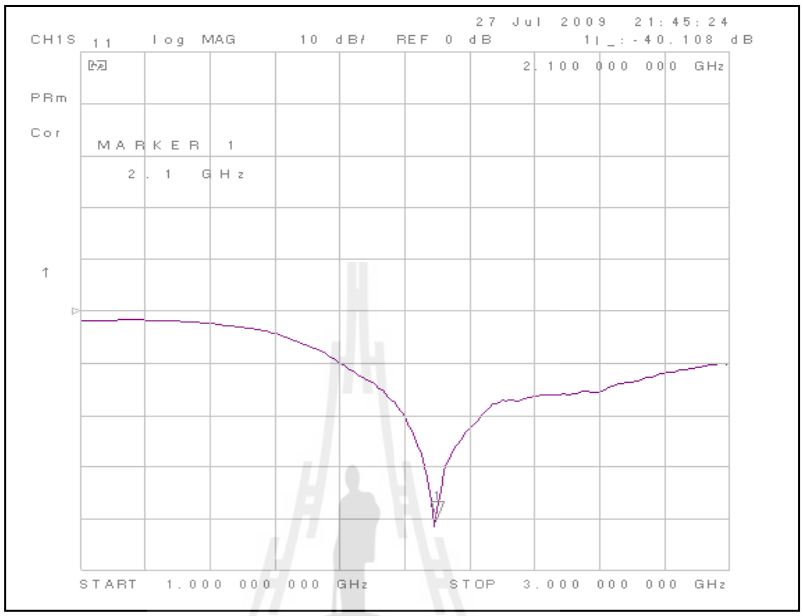

Figure 5.8 Measured return loss of the designed antenna Figure 5.7

Figures 5.9 and 5.10 show the measured radiation pattern of fabricated antenna in H-plane and E-plane, respectively. Comparing with the ones shown in Figures 5.5 and 5.6, the good agreement between simulation and measurement is achieved in which the designed antenna behaves similar to conventional monopole antenna. However, as we can see in Figure 5.10, the antenna gain is dropped in the region of boresight direction. This may be caused by unsymmetrical structure occurred when fabricating the antenna.

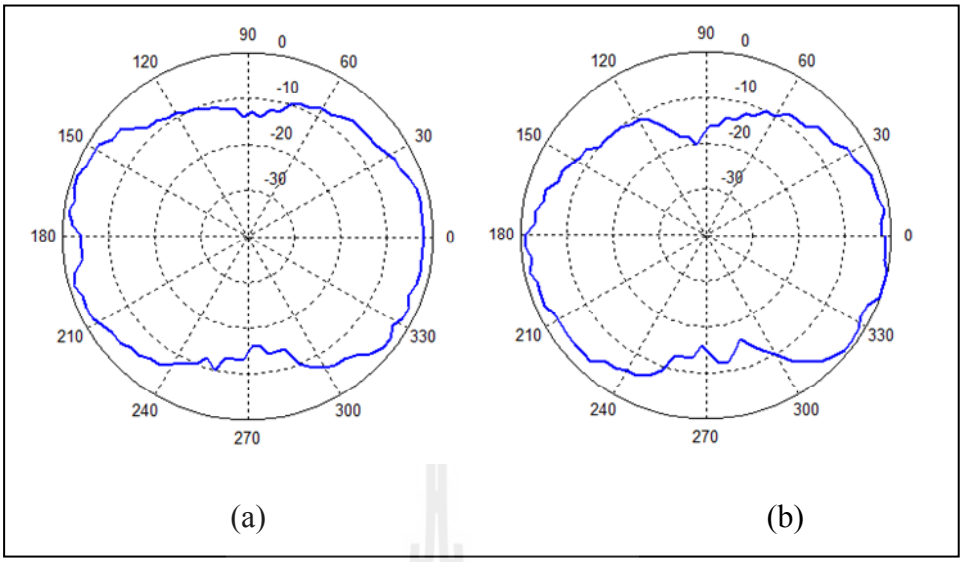

Figure 5.9 Measured E-plane pattern (a) y-z plane (b) x-y plane.

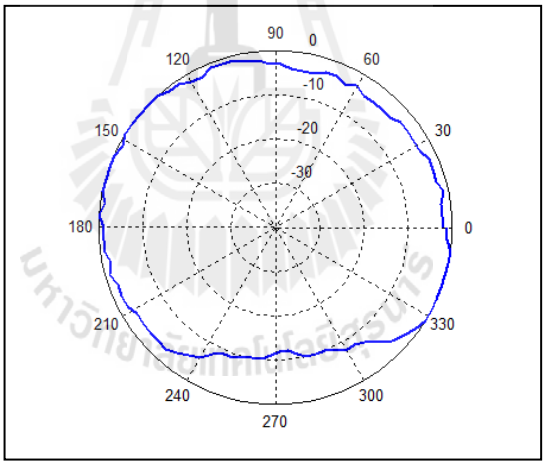

Figure 5.10 Measured for H-plane (x-z plane) patterns.

- **Array element**

Having completed the design of a single antenna element, this section concerns the design and construction of a 4×4 array antenna which is capable of beam steering in the azimuth direction over an increased operational

bandwidth. The design focuses on the frequency band covering 1.9 to 2.4 GHz. The antenna elements are spaced by half wavelength at 3 GHz (50 mm), which is higher than the highest frequency of the assumed band (2.4 GHz). The use of this higher frequency (3 GHz) is required in the beamforming algorithm to avoid the edge effect when finding the weighting coefficients is performed. Figure 5.11 shows the photograph of fabricated 4×4-array antenna. The array is supported by 200 mm^2 ground plane.

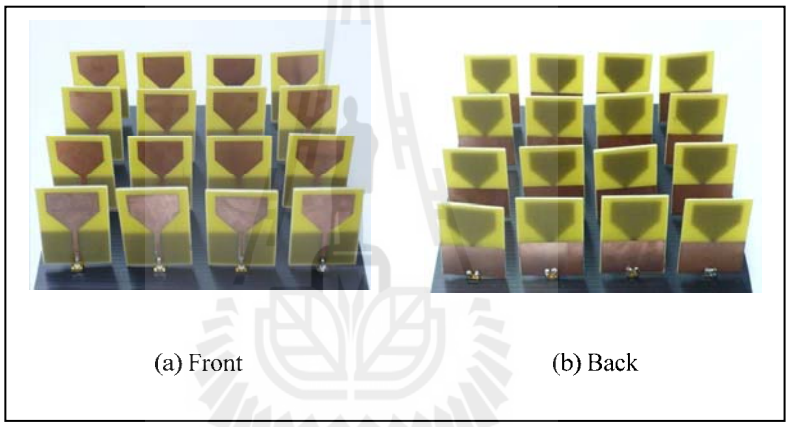

Figure 5.11 Photograph of fabricated 4×4-array antenna.

5.3 Weighting networks

In the prototype, weighting networks consist of two major components: weighting systems and control devices which are explained in this section.

5.3.1 Weighting systems

The weighting systems consist of four components: digital attenuators, digital switching, phase shifters and power combiners. Each component operates very

well over wide range of frequency covering frequencies from 1.9 to 2.4 GHz. The detail of each component is shown as follows:

(1) The first component is an attenuator. The received signal from each antenna is weighted by attenuator which is digital step attenuator. The utilized attenuator is a 50-Ω RF digital step attenuator offering an attenuation range up to 31.5 dB with 0.5 dB step controlled by 6 bit serial interface. The operating frequency covers from DC to 2.4 GHz. The photograph of digital step attenuator is shown in Figure 5.12 which is model number ZX76-31R5-SN+ from Minicircuit©. The operation of digital step attenuation can be explained using simplified schematic illustrated in Figure 5.13. The attenuation state can be selected using different control bit as shown in Table 5.1.

Figure 5.12 Photograph of Digital step attenuator.

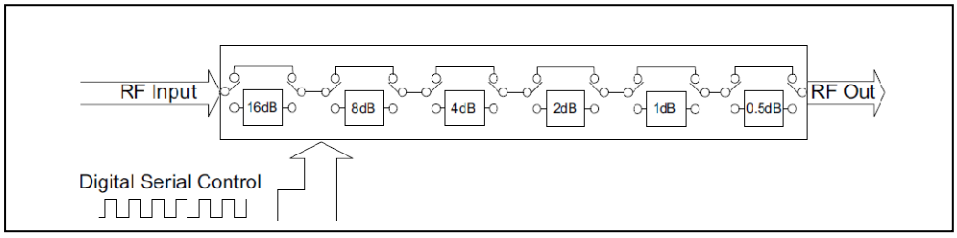

Figure 5.13 Simplified schematic of digital step attenuator**.**

Table 5.1 64 possible combinations of C0.5-C16 for digital step attenuator

State	Control Bit						Attenuation State (dB)
	C16	C8	C4	C2	C1	C0.5	
1	0	0	0	0	0	0	Reference
2	0	0	0	0	0	1	0.5
3	0	0	0	0	1	0	1
4	0	0	0	0	1	1	1.5
5	0	0	0	1	0	0	2
6	0	0	0	1	0	1	2.5
7	0	0	0	1	1	0	3
8	0	0	0	1	1	1	3.5
9	0	0	1	0	0	0	4
10	0	0	1	0	0	1	4.5
11	0	0	1	0	1	0	5
12	0	0	1	0	1	1	5.5
13	0	0	1	1	0	0	6
14	0	0	1	1	0	1	6.5
15	0	0	1	1	1	0	7
16	0	0	1	1	1	1	7.5
17	0	1	0	0	0	0	8
18	0	1	0	0	0	1	8.5
19	0	1	0	0	1	0	9
20	0	1	0	0	1	1	9.5
21	0	1	0	1	0	0	10
22	0	1	0	1	0	1	10.5
23	0	1	0	1	1	0	11
24	0	1	0	1	1	1	11.5
25	0	1	1	0	0	0	12
26	0	1	1	0	0	1	12.5
27	0	1	1	0	1	0	13
28	0	1	1	0	1	1	13.5
29	0	1	1	1	0	0	14
30	0	1	1	1	0	1	14.5
31	0	1	1	1	1	0	15
32	0	1	1	1	1	1	15.5
33	1	0	0	0	0	0	16
34	1	0	0	0	0	1	16.5
35	1	0	0	0	1	0	17
36	1	0	0	0	1	1	17.5
37	1	0	0	1	0	0	18

Table 5.1 64 possible combinations of C0.5-C16 for digital step attenuator (Continued.)

State	Control Bit						Attenuation State (dB)
	C16	C8	C4	C2	C1	C0.5	
38	1	0	0	1	0	1	18.5
39	1	0	0	1	1	0	19
40	1	0	0	1	1	1	19.5
41	1	0	1	0	0	0	20
42	1	0	1	0	0	1	20.5
43	1	0	1	0	1	0	21
44	1	0	1	0	1	1	21.5
45	1	0	1	1	0	0	22
46	1	0	1	1	0	1	22.5
47	1	0	1	1	1	0	23
48	1	0	1	1	1	1	23.5
49	1	1	0	0	0	0	24
50	1	1	0	0	0	1	24.5
51	1	1	0	0	1	0	25
52	1	1	0	0	1	1	25.5
53	1	1	0	1	0	0	26
54	1	1	0	1	0	1	26.5
55	1	1	0	1	1	0	27
56	1	1	0	1	1	1	27.5
57	1	1	1	0	0	0	28
58	1	1	1	0	0	1	28.5
59	1	1	1	0	1	0	29
60	1	1	1	0	1	1	29.5
61	1	1	1	1	0	0	30
62	1	1	1	1	0	1	30.5e
63	1	1	1	1	1	0	31
64	1	1	1	1	1	1	31.5

The attenuation of digital step attenuator is tested using network analyzer as shown in Figure 5.14 and the measurement result of attenuation factor for 0.5, 1, 2, 4, 8 and 16 dB at 1.9, 2.0, 2.1, 2.15, 2.2, 2.3 and 2.4 GHz is shown in Figure 5.15.

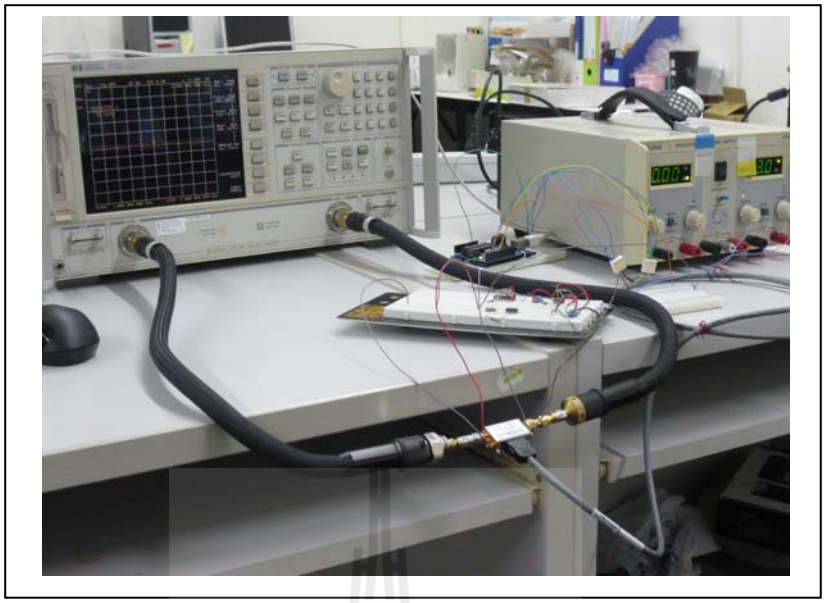

Figure 5.14 Set up for digital step attenuator testing.

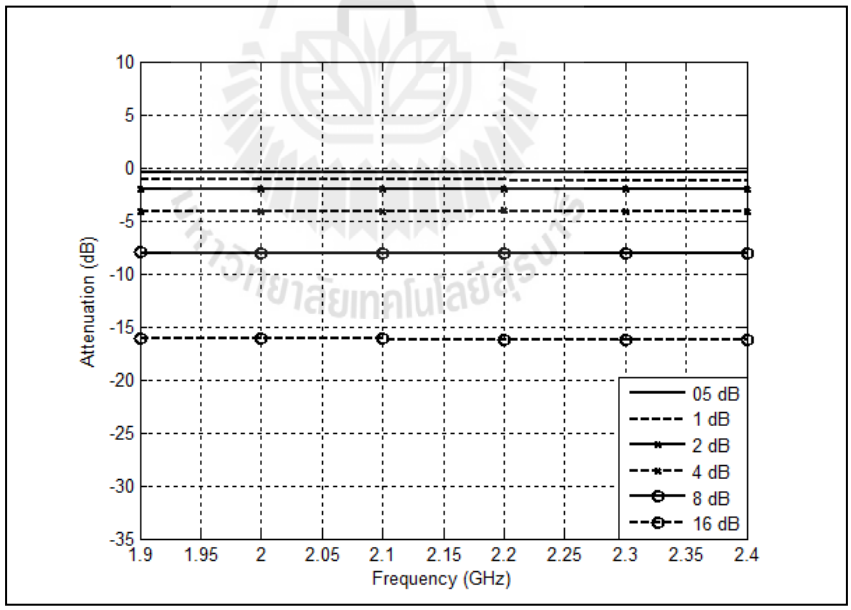

Figure 5.15 Measured attenuation factors of digital step attenuator.

(2) RF switch is designed for receiving signal from attenuator and transmitting signal to phase shifter or power combiner. A 50-Ω high isolate SPDT RF switch from Minicircuit© having model number of ZX80-DR230+ shown in Figure 5.16 is utilized. It works well from DC up to 3 GHz.

Figure 5.16 Photograph of RF-switch.

This product includes an internal CMOS control driver with two-pin control and its circuit is shown in Figure 5.17. The RF control bits select the desired switch-state as show in Table 5.2

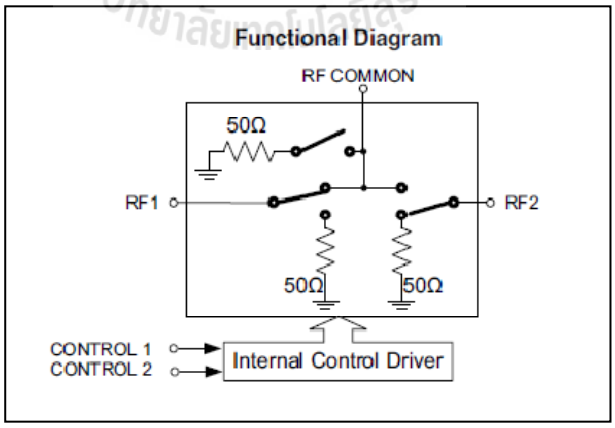

Figure 5.17 Functional diagram of the RF switch.

Table 5.2 The RF control bits select the desired switch-state

State	Control input		RF Input/output	
	Control 1	**Control 2**	**RF1 to RF Common**	**RF2 to RF Common**
1	Low	Low	OFF	OFF
2	Low	High	OFF	ON
3	High	Low	ON	OFF
4	High	High	N/A	N/A

Remark : Case I: When either of the RF1 or RF2 port is closed (ON state), the closed port is connect to the RF Common port.

Case II: When either of the RF1 or RF2 port is open (OFF state), the open port is connect to an internal 50Ω termination.

Case III: When both the RF1 and RF2 port is open (OFF state), the all three RF ports are connected to an internal.

(3) Phase shifters using FR-4 substrate were designed from CST Microwave Studio. Its size and dimension is shown in Figure 5.18. This component is utilized to 180°-shift the phase of signal in order to produce the minus sign for some weighting coefficients. The phase shifters were manufactured as its photograph is shown in Figure 5.19.

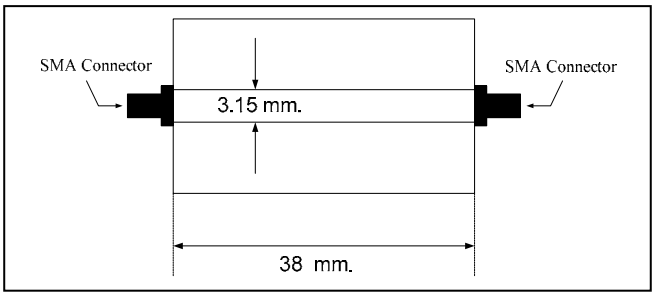

Figure 5.18 Diagram of Phase Shifter.

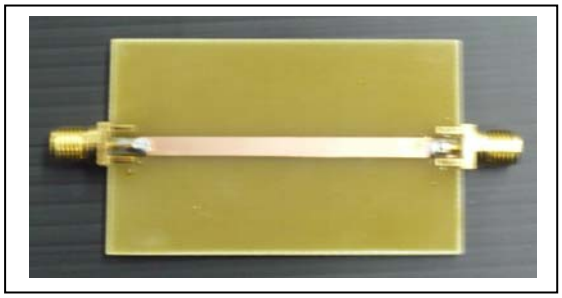

Figure 5.19 Photograph of Phase Shifter.

Figures 5.20 and 5.21 show measured return loss of the phase shifter. The obtain results indicate that its return loss is lower than -10 dB over the designated band. This confirms that the designed phase shifter work well for proposed prototype.

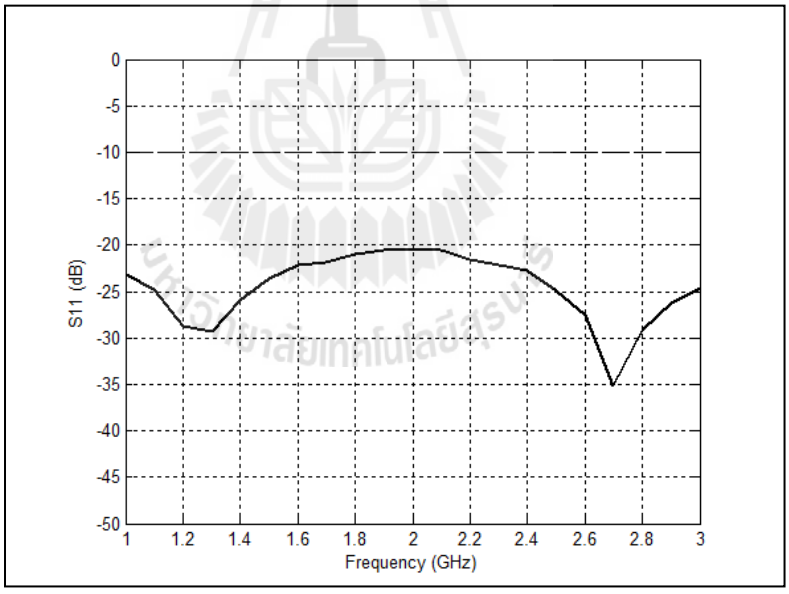

Figure 5.20 Measured return loss (S_{11}) of phase shifter.

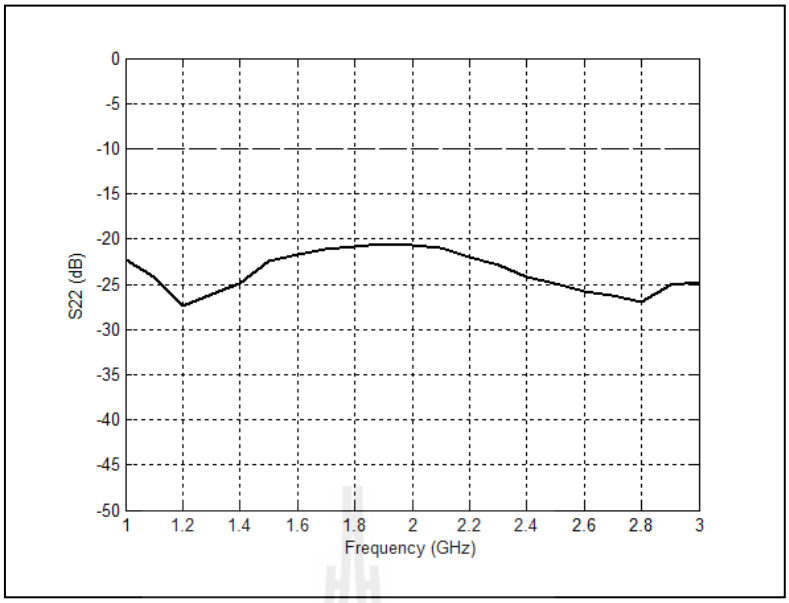

Figure 5.21 Measured return loss (S_{22}) of phase shifter.

In addition, Figure 5.22 shows that the designed phase shifter has a slight insertion loss throughout the designated band. Also, Figure 5.23 shows that output signal has $180°$ phase difference with input signal.

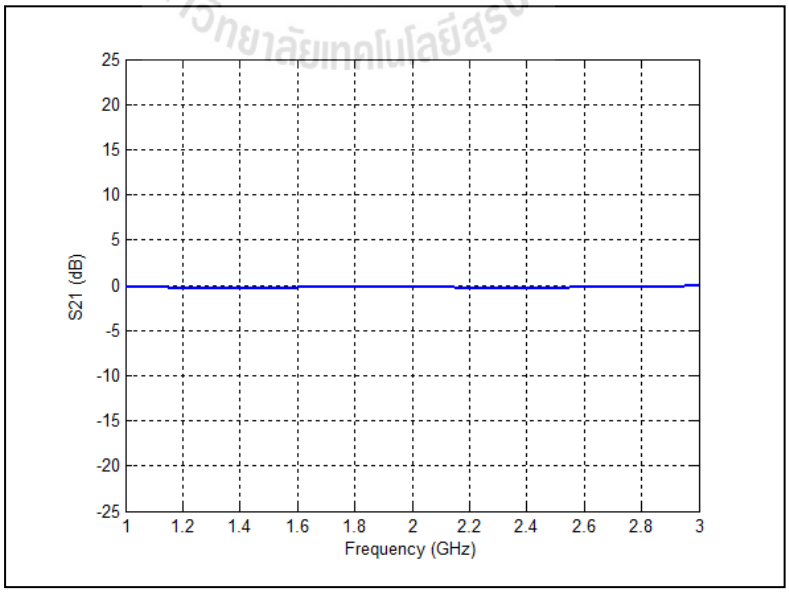

Figure 5.22 Measured insertion loss (S_{21}) of phase shifter.

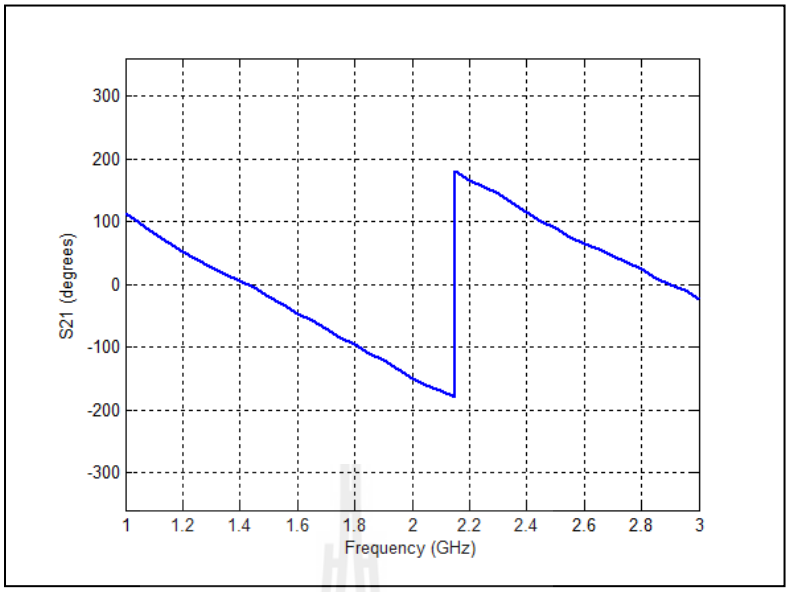

Figure 5.23 Phase difference between input and output signal of phase shifter.

(4) The utilized power combiners shown in Figures 5.24 and 5.25 which are separated into two different types that are 2:1 operating in frequency range from 1.6 to 3.3 GHz and 16:1 operating for frequencies from 1.8 to 2.6 GHz. They are model number ZX10-2-332+ and ZC16PD-2185 from Minicircuit©, respectively. The first type combines signal from RF switch with phase shifter and other type combines all output signals from the first type.

Figure 5.24 Photograph of 2:1 power combiner.

Figure 5.25 Photograph of 16:1 power combiner.

5.3.2 Control device

Twelve Arduino Duemilanoves are utilized to control digital attenuators and digital switches. The reason to choose this type of control device is that it is low of cost but able to meet the requirement in this thesis. Figure 5.26 demonstrates a photograph of Arduino Duemilanove. The Arduino Duemilanove is a microcontroller board based on the ATmega328 which has 14 digital input/output pins (of which 6 can be used as PWM outputs), 6 analog inputs, a 16 MHz crystal oscillator, a USB connection, a power jack, an ICSP header, and a reset button. It can be simply connected to a computer with a USB cable. Also, it can be powered with a AC-to-DC adapter or battery to get started. Table 5.3 shows summary of specification for Arduino Duemilanove.

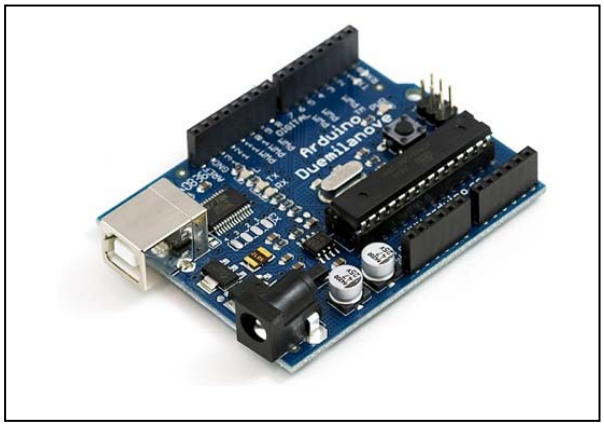

Figure 5.26 Photograph of ATMEGA 328 microprocessor.

Table 5.3 Summary of specification of Arduino Duemilanove.

Parameters	Details
Operating Voltage	5V
Input Voltage (recommended)	7-12V
Input Voltage (limits)	6-20V
Digital I/O Pins	14
Analog Input Pins	6
DC Current per I/O Pin	40 mA
DC Current for 3.3V Pin	50 mA
Flash Memory	32 KB (ATmega328) of which 2 KB used by bootloader
SRAM	2 KB
EEPROM	1 KB
Clock Speed	16 MHz

5.4 Prototype of fully spatial beamformer

All parts discussed in Sections 5.3 and 5.4 are combined forming a prototype of 4×4 wideband spatial beamformer as shown in Figure 5.27. The power supply is located at the bottom of the shelf. This supports needed power to microcontrollers, digital attenuators and digital switches. The control devices as mentioned in last section are located at the 2nd shelf followed by the weighting network which is placed

on the 3rd shelf as shown in Figure 5.27. The top of the shelf is provided for the 4×4 antenna array as mentioned before. Also, the power combiners are placed on the top shelf, which pass the output signal to the computer.

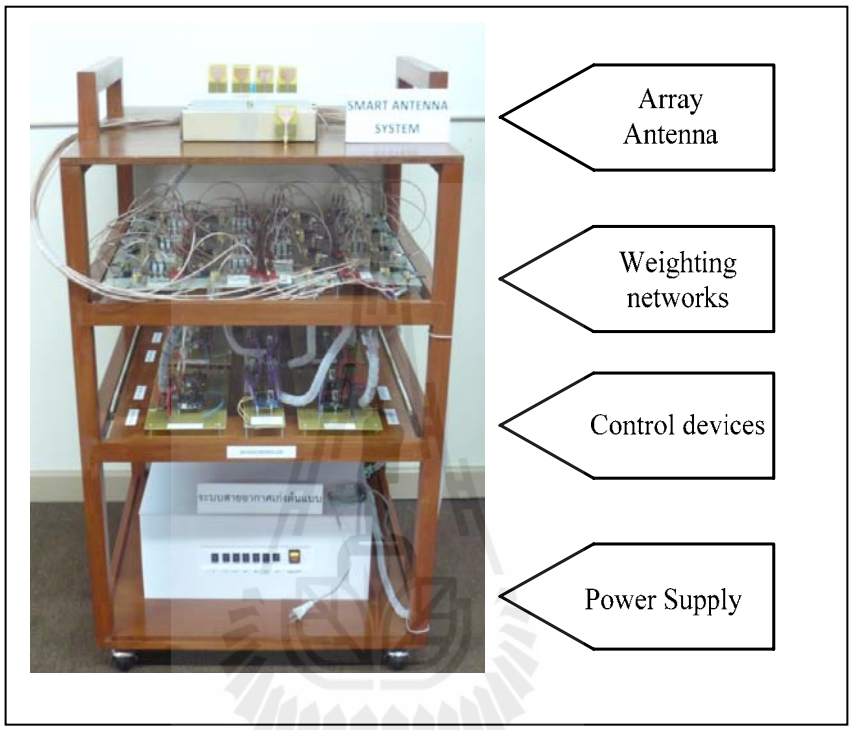

Figure 5.27 Photograph of full prototype of wideband fully spatial beamformer.

5.5 Chapter summary

This chapter has shown the design and the construction the full prototype of wideband fully spatial beamformer which consist of the three core components: antenna and weighting networks and control devices. Each component is discussed and some simulation results confirming its performance have been shown.

CHAPTER VI

EXPERIMENTAL RESULTS

6.1 Introduction

The previous chapter has shown the design and construction of beamformer prototype for wideband array antennas. In order to validate the refinement algorithm proposed in this thesis, the full prototype of the beamformer is assembled in order to test in anechoic chamber. The experimental results are also shown comparing with the ones obtained from computer simulation. The radiation pattern for a designate band is the parameter to indicate the performance of proposed concept.

6.2 Experimental setup

First of all, the twelve microprocessors are programmed in order to control digital attenuators and digital switches according to data presented in Tables 6.1 and 6.2 for 6 desired directions (7°,-17°, 34°, -34°, 57°and 75°). The reason of chosen directions is the need of variation case between ±90º off boresight direction. Table 6.1 shows the weighting coefficients obtained from IDFT method while Table 6.2 presents the ones from proposed refinement algorithm. Also, Table 6.3 shows some parameters which are given in simulation for the refinement method for each desired direction. As we can see the weighting coefficients obtained from proposed refinement has lower dynamic range comparing the ones obtained from IDFT method

The full prototype of the beamformer is assembled and tested in anechoic chamber as shown in Figure 6.1 as operating in receiving mode. The measurement is taken place at a single frequency at a time from 1.9 to 2.4 GHz.

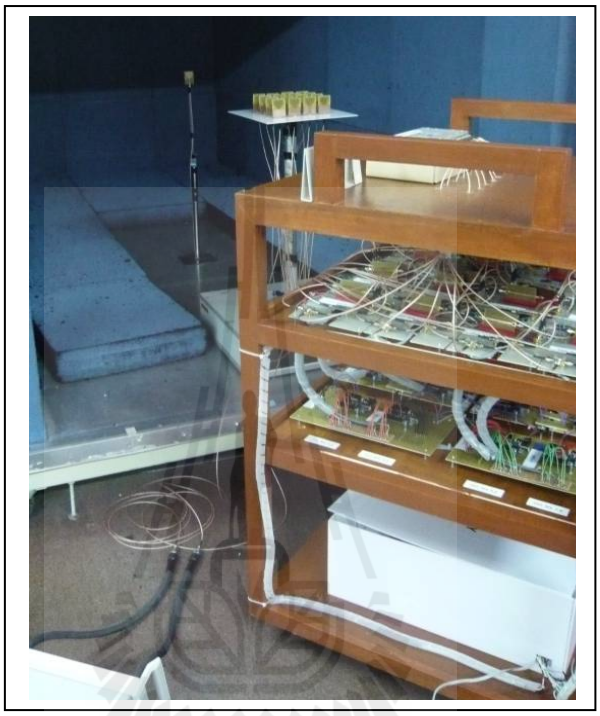

Figure 6.1 Assembly of beamformer prototype tested in anechoic chamber.

Table 6.1 Weighting coefficients (dB) from IDFT method of 4×4 beamformer in 6 directions.

Element Number	**Desired directions**					
	7°	**-17°**	**34°**	**-34°**	**57°**	**75°**
1	-5	-14	30	8	33	-10
2	-1	-1	-6	-8	-7	-13
3	0	-3	-8	-6	10	1
4	-5	-12	8	30	9	-11
5	16	2	-7	11	-6	-2

Table 6.1 Weighting coefficients (dB) from IDFT method of 4×4 beamformer in 6 directions. (Continued.)

Element Number	Desired directions					
	7°	**-17°**	**34°**	**-34°**	**57°**	**75°**
6	6	0	-20	0	-21	13
7	1	15	0	-20	0	0
8	2	11	11	-7	-7	1
9	2	11	11	-7	-7	1
10	1	15	0	-20	0	0
11	6	0	-20	0	-21	13
12	16	2	-7	11	-6	-2
13	-5	-12	8	30	9	-11
14	0	-3	-8	-6	10	1
15	-1	-1	-6	-8	-7	-13
16	-5	-14	30	8	33	-10

Table 6.2 Weighting coefficients (dB) from proposed refinement algorithm of 4×4 beamformer in 6 directions

Element Number	Desired directions					
	7°	**-17°**	**34°**	**-34°**	**57°**	**75°**
1	-4	-14	27	4	14	-2
2	-1	-1	-6	-4	-7	-2
3	0	-3	-8	-4	10	1
4	-4	-12	8	4	9	-2
5	4	2	-7	4	-6	-2
6	4	0	-20	0	-14	2
7	1	14	0	-4	0	0
8	2	-11	11	-4	-7	-1
9	2	-11	11	-4	-7	-1
10	1	14	0	-4	0	0
11	4	0	-20	0	-14	2
12	4	2	-7	4	-6	-2
13	-4	-12	8	4	9	-2
14	0	-3	-8	-4	10	1
15	-1	-1	-6	-4	-7	-2
16	-4	-14	27	4	14	-2

Table 6.3 gives conclusive figure for those assumed 6-cases. As we can see, giving different values of error in mainbeam direction results in unpredictable capability in reducing dynamic range when performing proposed refinement method. However, that dynamic range can be relatively reduced when higher error in average minor lobe level is allowed as can be seen for cases A D and F. In addition, lower dynamic range of weights can be obtained when higher error in first-null beamwidth is allowed as compared between cases C and E.

Table 6.3 The parameters of refinement method for each desired directions

Case	**Desired Direction**	$\Delta\phi$ **(degree)**	ΔMLL **(dB)**	$\Delta\delta$ **(degree)**	**Maximum Weighting coefficients**	
					IDFT Method	**Refinement method**
A	7°	5	11	0	16	4
B	-17°	3	0	4	15	14
C	34°	3	4	5	30	27
D	-34°	2	15	0	30	4
E	57°	3	4	6	33	14
F	75°	3	7	0	13	2

6.3 Experimental results and discussion

This section validates the beamforming performance of the proposed refinement method through the prototype testing as shown in last section. The performance is compared between employing IDFT method and proposed refinement method. There are 6-case examples (6 directions) for this validation as detailed in last section. Please note that the operating frequencies are chosen from 1.9 to 2.4 GHz.

Figure 6.2 shows some examples at 2.15 GHz of refinement performance comparing between simulation and experimental results for cases A (7°) and C (34°). The reason of choosing both cases is that they present maximum and minimum

reduction of dynamic range among all 6 cases. As we can see in the figure, there is a good agreement between simulation and measurement. However, its sidelobe level is higher when performing experiment. This may be caused by mutual coupling effect between antenna elements as the mentioned effect has been neglected in simulation (Dandekar, Ling and Xu, 2002 and Lui, Hui and Leong, 2009).

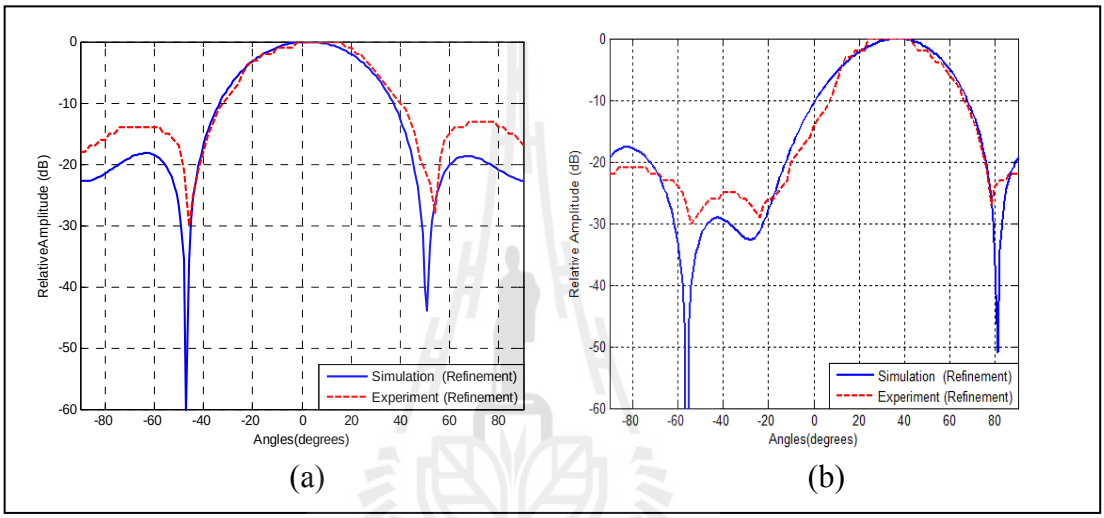

Figure 6.2 Simulated and measured radiation pattern using refinement method for frequency 2.15 GHz when the main beam direction is (a) 7° (Case A) and (b) 34° (Case C).

Figures 6.3 to 6.8 show results for a whole designated band (1.9 to 2.4 GHz) obtained from simulation and measurement for cases A to F. As we can see, their beamforming behavior looks stable throughout band. However, the ones obtained from measurement have slightly error in minor lobe level. This is may be cause by mutual coupling effect between antenna elements.

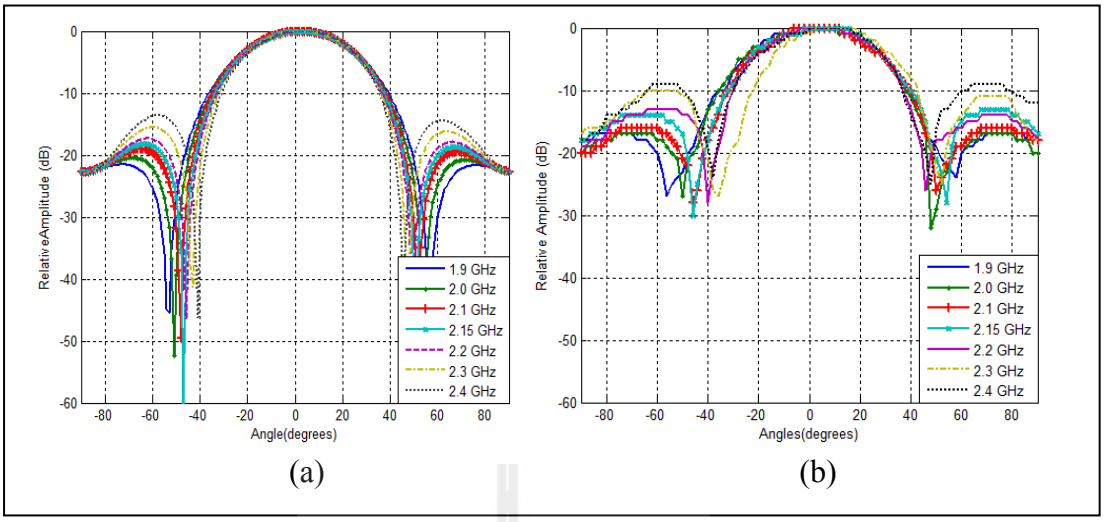

Figure 6.3 (a) Simulated and (b) measured radiation pattern using refinement method for frequencies from 1.9 to 2.4 GHz when the main beam direction is 7° (Case A).

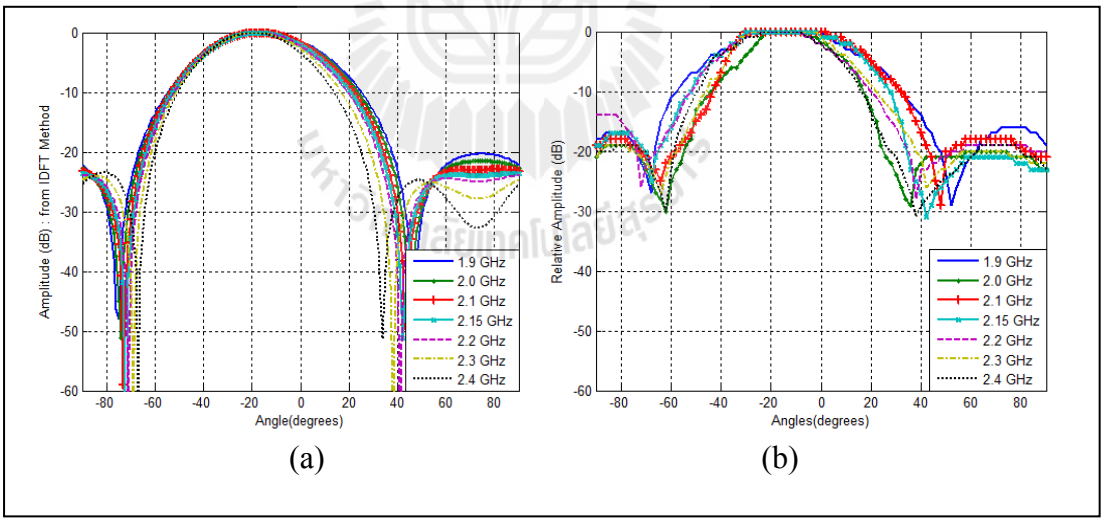

Figure 6.4 (a) Simulated and (b) measured radiation pattern using refinement method for frequencies from 1.9 to 2.4 GHz when the main beam direction is -17° (Case B).

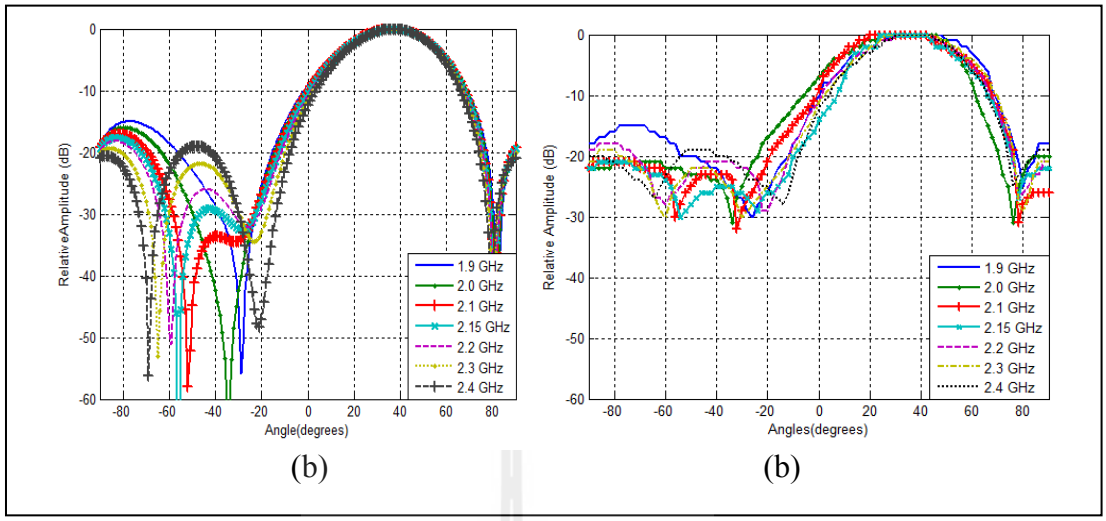

Figure 6.5 (a) Simulated and (b) measured radiation pattern using refinement method for frequencies from 1.9 to 2.4 GHz when the main beam direction is 34° (Case C).

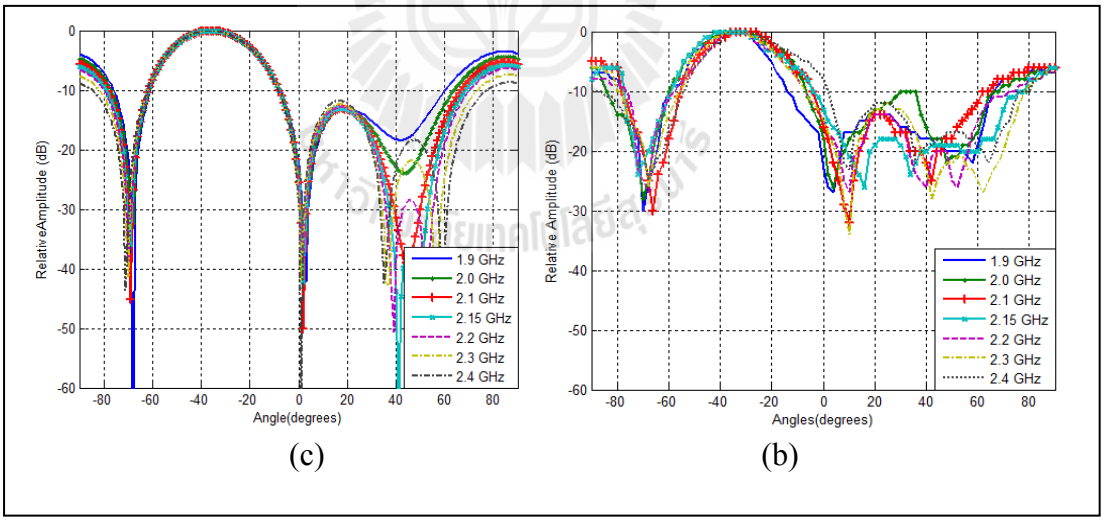

Figure 6.6 (a) Simulated and (b) measured radiation pattern using refinement method for frequencies from 1.9 to 2.4 GHz when the main beam direction is -34° (Case D).

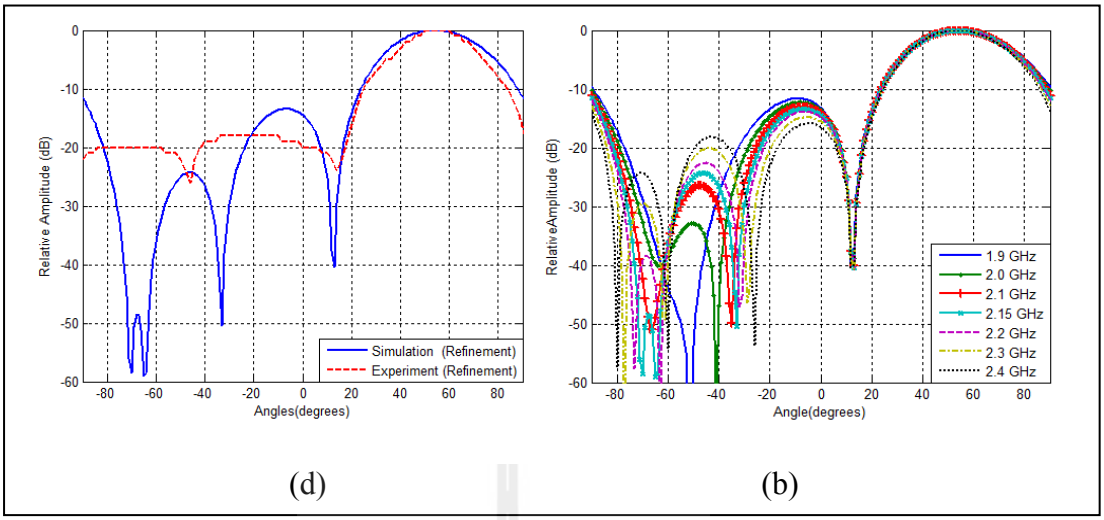

Figure 6.7 (a) Simulated and (b) measured radiation pattern using refinement method for frequencies from 1.9 to 2.4 GHz when the main beam direction is 57° (Case E).

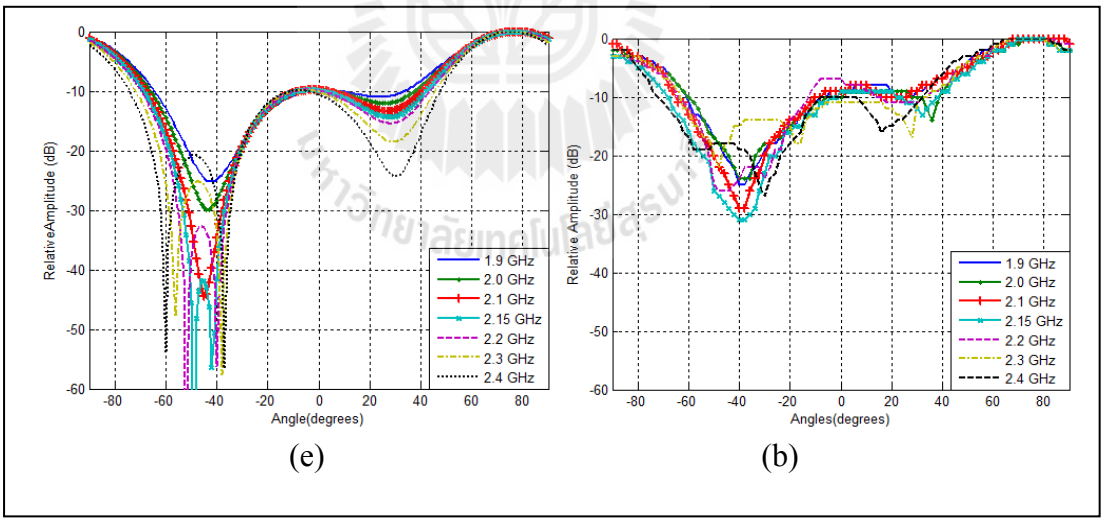

Figure 6.8 (a) Simulated and (b) measured radiation pattern using refinement method for frequencies from 1.9 to 2.4 GHz when the main beam direction is 75° (Case F).

6.4 Error in average minor lobe level

From the experimental results for Cases A to F shown in previous section, the error in maximum deviation of average minor lobe level is pronounced. However, this variation is within 7 dB. Thus, this section is devoted to the reason behind that circumstance. Firstly, the radiation pattern employing IDFT method obtained from simulation and experiment is declared. For this case, the main beam is supposed to be pointed to 2° and the maximum of weighting coefficients is 8 dB when employing IDFT method. After performing refinement method for $\Delta\phi = 2°$, $\Delta MLL = 11dB$, and $\Delta\delta = 0°$, dynamic range of weights can be reduced from 8 to 6 dB.

Figure 6.9 shows its radiation pattern according to the above condition comparing between IDFT (simulation and measurement) and refinement methods (simulation and measurement) at 2.15 GHz. As we can see, higher sidelobe level is obtained when performing experiment. This may be caused by mutual coupling effect between antenna elements as some literatures: Kang and Pozar (1985) and Wyglinski and Blostein (2003) have discussed.

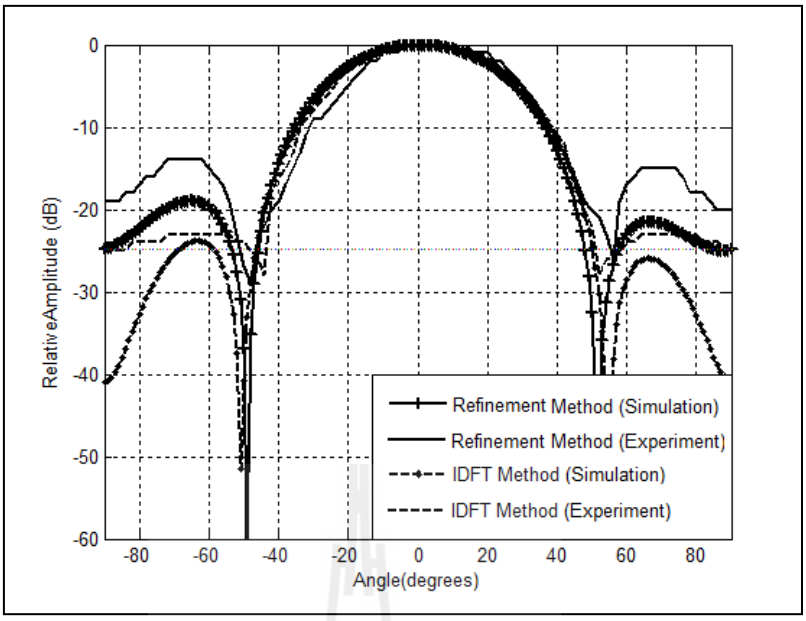

Figure 6.9 Radiation pattern for frequency at 2.15 GHz when the main beam direction is 2°.

6.5 Chapter summary

This chapter has presented a full constructed prototype which validates the beamforming performance of the proposed refinement method. The performance employing proposed refinement method is compared with the one employing IDFT method. The obtained results have indicated that the main beam can be pointed to the designated direction and also the radiation pattern looks stable throughout the designated band. In addition, the proposed refinement method can reduce the dynamic range of weights comparing with the one obtained from IDFT method. However, some obvious errors in minor lobe level can be seen. This is because of the imperfection of measuring environment.

CHAPTER VII

THESIS CONCLUSION

7.1 Conclusion

Due to the explosion of mobile communication demand and the increasing shift to offer new and advance services base on high speed data rate, the third generation (3G) technologies were developed. Although various 3G technologies offer higher data rate and double voice capacity compare with their 2G counterparts, their actual performance is still susceptible to interference, and adverse channel conditions created by multipath propagation and system loading. In order to cope with the demand for high data rate communication in multi-user environments the use of wideband smart antennas is in focus. The term “smart antennas” describes the ability to point its main beam towards a desired user and nulls toward interferences. From literatures, most of the algorithms for smart antennas are dealing with narrowband signal. They are typically divided into two major categories: switched-beam and adaptive systems. Both systems have the same aim as they attempt to increase its gain in the direction of desired user. This could be achieved by directing the main lobe, with an increase gain, to the direction of desired user while pointing nulls to the direction of interferences. Unfortunately the conventional narrowband beamforming schemes cannot be extended to wideband signals as some unexpected manner can be occurred such as beam squinting and null shallowing. From the literatures, the wideband beamformer can be divided into three categories depending on the type of

signal processing schemes: time-space, time-frequency and fully spatial. The first two categories are not attractive for use in wireless communication systems because they require a large number of TDLs and frequency filters to perform the beam formation over wide frequency band. In order to overcome these shortfalls, a wideband spatial beamformer can be used as an attractive alternative. This is because the system results in real-valued weights, thus in practice they can be realized by attenuators or amplifiers. The concept of this fully spatial beamformer has been presented in this thesis in which the weighting coefficients can be calculated using an Inverse Discrete Fourier Transform (IDFT) technique to a objective function describing the desired characteristic radiation pattern for a given designated frequency band. However, the obtained weighting coefficients are not integer and the value between maximum and minimum values (dynamic range) of weighting coefficients is relatively high. Thus, this thesis has proposed an algorithm to overcome these problems, so call refinement algorithm.

For the proposed refinement method, some parameters e.g. error in main-beam direction $(\Delta\phi)$, average minor lobe level (ΔMLL) and beamwidth $(\Delta\delta)$ has to be assumed. From running a number of simulations, the dynamic range of weighting coefficients can be reduced up to 29 dB while some other significant characteristic remains. As a result, the implementation of wideband spatial beamformer is practical. A full prototype of wideband spatial beamformer was developed in order to validate the proposed concept. This prototype consists of 4×4 array of square planar monopoles followed by a feeding network. To realize real-valued weights, digital attenuators controlled by microcontrollers are chosen. In addition, as some weights are negative real values, phase shifters are designed and manufactured to produce a 180°

difference. The prototype was also tested in anechoic chamber. The experiment was performed in 7 different desired directions (2°, 7°,-17°, 34°, -34°, 57°and 75°) on the designated band from 1.9-2.4 GHz. Both from simulation and experimental results, the proposed refinement method can effectively reduce the dynamic range of weighting coefficients for wideband spatial beamformer throughout the designated frequency band. This is considerably helpful to make this kind of smart antennas more practical to the system designer. For future work, the refinement algorithm for multi-beam formation is attractive as diversity in space domain is in focus nowadays. According to this, we can save power radiation in some unused or prohibited areas.

REFERENCES

Alastalo, A.T. and Kahola, M. (2003). Smart-antenna operation for indoor wireless local-area networks using OFDM. **IEEE Transactions on Wireless Communications**. 2(2): 392-399.

Ammann, M.J. (1999). Square planar monopole antennas. **IEE Nat Conf Antenna Propagate.** 37-40.

Ammann, M.J. (2001). Control of the impedance bandwidth of wideband planar monopole antennas using a beveling technique. **Microwave and Optical Technology Letter.** 30(4): 229-232.

Ammann, M.J. (2001). Wideband monopole for reconfigurable multiband radio terminals. **IEEE AP-S International Symposium on Antennas and Propagation.** 1: 170-173.

Ammann, M.J. and Chen Z.N. (2003). Wide-Band shorted planar monopole with bevel. **IEEE Transactions on Antennas and Propagation**, 51(4): 901-903.

Ammann, M.J. and Chen Z.N. (2004). Asymmetrical feed arrangement for improved impedance bandwidth of planar monopole antennas. **Microwave and Optical Technology Letters.** 40(2): 156-158.

Antonino-Daviu, E., Cabedo-Fabres, M., Ferrando-Bataller, M., and Valero-Nogueira, A. (2003). Wideband double-fed planar monopole antennas. **Electronics Letters.** 39(23): 1635-1636.

Bhobe, A. U. and Perini , P. L. (2001). An overview of smart antenna technology for wireless communication**. IEEE Proceedings Aerospace Conference.** 2: 2/875-2/883.

Bojanapally, S. and Kshetrimayum, R. S. (2010). Wideband antenna beamforming using FIR filter. **International Conference on Computing, Communication and Networking Technologies**. 1-4.

Boonpoonga, A., Sirisuk, P., and Krariksh, M., (2006). A switched-beam element phased array antenna for CMA initialization. **Proceeding of the 36th European Microwave Conference.** 772-775.

Bouacha, A., Debbat, F. and Bendimerad, F. T. (2008). Modified blind beamforming algorithm for smart antenna system. **Journal of Radio Electronics.** 1-20.

Chryssomallis, M. (2000). Smart antennas. **IEEE Antenna and Propagation magazine.** 42(3): 129-136.

Compton, R.T., (1988). The bandwidth performance of a two-element adaptive array with tapped delay line processing. **IEEE Transactions on Antennas and propagations.** 36(1): 5-14.

Dandekar, K.R., Ling H. and Xu, G. (2002). Experimental study of mutual coupling compensation in smart antenna applications. **IEEE Transactions on Wireless Communication.** 1(3): 480-487.

Durrani, S. and Bialkowski, M.E. (2004). Effect of mutual coupling on the interference rejection capabilities of linear and cicular arrays in CDMA systems. **IEEE Transactions on Antenna and Propagation**, 52(4): 1130-1134.

Fakoukakis, F.E., Diamantis, S.G., Orfanides, A.P., and Kyriacou, G.A. (2006). Development of an adaptive and a switched beam smart antenna system for wireless communications. **Journal of Electromagnetic Waves and Applications.** 20(3): 399-408.

Fujimoto, M.; Nishikawa, K. and Sato, K. (1995). A study of adaptive array antenna system for land mobile communications. **Proceeding on Vehicles'95.** 36 – 41.

Ghavami, M. (2002). Wideband smart antenna theory using rectangular array structures. **IEEE Transaction on Signal processing.** 50(9): 2431-215.

Hefnawi, M., and Delisle, G. Y. (2000). Impact of wideband CDMA signals on smart antenna systems. **IEEE International Conference on Personal Wireless Communications.** 5-8.

Hefnawi, M., and Delisle, G. Y. (2001). Smart antenna system for wideband CDMA signal. **IEEE International Symposium on Antenna and Propagation Society.** 4: 22-25.

Hefnawi, M., and Delisle, G. Y. (2001). Performance analysis of wideband smart antenna system using difference frequency compensation. **IEEE Symposium on Computers and Communications.** 237-242.

Ibrahim, S.Z., and Rahim, M. (2007). Switched beam antenna using omnidirectional antenna array. **Asia-Pacific Conference on Applied Electromagnetics Proceeding** (Melaka, Malaysia). 1-4.

Ishii, N., and Kohno, R. (1994). Spatial and temporal equalization based on adaptive tapped-delay-line array antenna. **IEEE International Symposium on Personal, Indoor and Mobile Communication.** 1:232-236.

Jana, R. (2000). 3G Wireless capacity optimization for widely spaced antenna arrays. **IEEE Personal Communication**. 7(6): 32-35.

Junjie, G., Yongyi, Y., and Henry S. (2005). Design of the tapped-delay line smart antenna array using vector space projections. **IEEE Workshop on Singnal Processing Advances in Wireless Communications**. 196-200.

Kang, Y.W. and Pozar, D. (1985). Correction of error in reduced sidelobe synthesis due to mutual coupling. **IEEE Transactions on Antenna and Propagation**. 20(3): 288-295.

Kawikar, R.S. and Shevgaonkar, R.K. (2003). Design of smart antenna test bested prototype. **International Symposium on Antenna and Propagation, and EM Theory**. 299-302.

Kawitar, R. and Wakde, D.G. (2005). Advance in smart antenna system. **Journal of Scientific and Industrial Research.** 64: 660-665.

Kim, Y.S. and Weiss, I.M. (1990). Bandwidth performance of phased array with tapped-delay line filter. **International Symposium on Antennas and Propagation Society.** 4: 1696 – 1699.

Kin-Lu Wong, Chih-Hsien Wu, and Saou-Wen (Stephen) Su. (2004). Ultrawide-Band square planar metal-plate monopole antenna with a trident-shaped feeding strip. **IEEE Transactions on Antennas and Propagation.** 53(4): 1262-1269.

Kohno, R., Wang, H. and Imai, H. (1992). Adaptive array antenna conbined with tapped delay line using processing gain for soread-spextrum CDMA system. **IEEE international Symposium on Personal, Indoor and Mobile Radio Communications**. 634 – 638.

Koubeissi, M., Decroze, C., Monediere, T. and Jecko, B. (2005). Switched-beam antenna based on novel design of Butler matrices with broadside beam. **IET Journals & Magazines.** 41(20): 1097-1098.

Lai, M., Wu, T., Hsieh J., Wang, C, and Jeng, S. (2008.) Compact switched-beam antenna employing a four-element slot antenna array for digital home applications. **IEEE Transactions on Antennas and Propagation**. 56(9): 2929-2936.

Lavate, T.B., Kokate, V.K. and Mani, G.S. (2010). Non blind and blind adaptive array smart antenna beam forming algorithm for W-CDMA mobile communication system. **International Conference on Computer Engineering and Applications.** 2: 200-203.

Liberti, J. C. and Rappaport. (1999). **Smart antennas for wireless communication IS-95 and Third Generation CDMA Applications**. New Jersey: Prentice Hall.

Lui, H.S., Hui, H.T. and Leong, M. S. (2009). A Note on the mutual coupling problems in transmitting and receiving antenna array. **IEEE Antenna and Propagation Magazine**. 51(5): 171-176.

Materum, L.Y. and Marciano, J.S. (2003). Wideband nulling capability estimate of a tapped delay line beamformer. **IEEE Topical Conference on Wireless Communications Technology.** 386 – 387.

Mayhan, J., Simmons, A. and Cummings, W. (1981). Wide-band adaptive antenna nulling using tapped delay lines. **IEEE Transactions on Antennas and Propagations.** 29(6): 923-936.

Morgan, D. R. (2008). Wideband equalization using multiple antennas. **IEEEE Wireless Communications and Networking Conference.** 634 – 639.

Ngamjanyaporn, R. and Krairiksh, M. (2002). Switched-beam single patch antenna **Electronics Letters**. 38(1): 7-8.

Petermann, T., Kuhn, V. and Kammeyer, K.D. (2000). Iterative blind and non- blind channel estimation in GSM receivers. **IEEE International Symposium on Personal, Indoor and Mobile Radio Communications.** 1: 554-559.

Ramineni, B., Sagar, G.C., Jain K.A., Prasad, M. S. G., Ramakrishna, T. V. and Kumar K.S. (2012). Comparison and performance evaluation of different adaptive beam forming algorithms in wireless communications with smart antenna. **International Journal of Engineering Research and Applications (IJERA)**. 2(3): 630-633.

Rivas, M., Shuguo, X.L. and Donglin, S. (2010). A review of adaptive antenna techniques for wideband smart antennas. **International Conference on Wireless Communication Network and Mobile Computing.** 1-5.

Rodgers, W.E. and Compton, R.T. (1979). Adaptive array bandwidth with tapped delay-line processing. **IEEE Transactions on Aerospace and Electronic Systems.** 15(1): 21-28.

Roy, R.H. (1998). An overview of smart antenna technology the next wave in wireless communications. **IEEE Aerospace Conference**. 3: 339-345.

Rui, L., Yuchun, G., Xin, Z. and Xiaowei,. S. (2007). An investigation into broadband smart antenna systems for wireless communication. **International Conference on Microwave and Millimeter Wave Technology.** 1-4.

Stine, J.A. (2006). Exploiting smart antennas in wireless mesh network using contention access. **IEEE Wireless Communication.** 13(2):38-39.

Uthansakul, M. and Bialkowski, M.E. (2003). A wideband smart antenna with non-uniform components for a wideband communication system. **In proceeding Asia-Pacific Microwave Conference (APMC)**. 3: 1542-1543.

Uthansakul, M. and Bialkowski, M.E. (2003). DOA estimation by a smart antenna with non-uniform components operating in a wideband frequency band. **International Symposium on DSP and Communication System (DSPCS).** 142-146.

Uthansakul, M. and Bialkowski, M.E. (2003). The effect mutual coupling on performance of a wideband smart antenna with non-uniform components. **International Symposium on Antennas and Propagation.** 2: 621-624.

Uthansakul, M. and Bialkowski, M.E. (2004). Frequency-angle dependent compensation of non-uniform components for wideband smart antenna. **IEEE MTT-S International Microwave Symposium (IMS).** 2: 1253-1256.

Uthansakul, M. and Bialkowski, M.E. (2004). Wideband smart antenna using non-uniform components. **International Conference on Microwave, Radar and Wireless Communications (MIKON).** 1: 70-73.

Uthansakul, M. and Bialkowski, M.E. (2004). Impact of wideband signals on smart antenna system. **International Conference on Microwave, Radar and Wireless Communication. 2: 501-504**

Uthansakul, M. and Bialkowski, M.E. (2004). An Investigation into smart antenna configurations for wideband communication. **International Conference on Microwave, Radar and Wireless Communications (MIKON).** 2: 505-508.

Uthansakul, M. and Bialkowski, M.E. (2005). Designing wideband spatial beamformer for low sidelobe radiation pattern performance. **Asia-Pacific Microwave Conference (APMC).** 3: 1953-1956.

Uthansakul, M., and Bialkowski, M.E. (2005). A wideband beam-steered array antenna utilizing real-valued weighting coefficients. **International Symposium on DSP and Communication System.** 237-241.

Uthansakul, M. and Bialkowski, M.E. (2005). A wideband spatial beamformer employing a rectangular array of planar monopoles. IEEE **International Symposium on Antenna and Propagation Society.** 1B: 303-306.

Uthansakul, M. and Bialkowski, M.E. (2005). Wideband beam forming with a rectangular array. **IEEE Wireless Communications.** 63-66.

Uthansakul, M. and Bialkowski, M.E. (2006). An array antenna with wideband beam steering capability employing spatial signal processing. **International Conference Microwave, Radar and Wireless Communications**. 469-472.

Uthansakul, M. and Bialkowski, M.E. (2006). Fully spatial wide-band beamforming using a rectangular array of planar monopoles. **IEEE Transactions on Antenna and Propagation.** 54(2): 527 – 533.

Widrow, B., Mantey, P.E., Griffiths, L.J. and Goode, B.B. (1967). Adaptive antenna systems. **Proceeding of IEEE Journal and Maggazines.** 55(12): 2143-2159.

Yoshinaga, H., Taromaru, M. and Akaiwa, Y. (1999). Performance of adaptive array antenna with widely spaced antenna elements. **Vehicular Technology Conference (IEEE VTS 50th)**. 1: 72-27.

Wyglinski, A.M. and Blostein, S.D. (2003). On uulink CDMA cell capability: mutual coupling and scattering effecting on beamforming. IEEE Transactions on Antenna and Vehicular Technology. 52(2): 289-304.

APPENDIX A

ANTENNA DESIGN

A.1 Antenna design

From literatures, there are wide varieties of wideband antennas in which many of them are electrically large. However, this thesis focuses on wideband antenna having small size as it has to be constituted for 4×4-lattice. The basic approach to making an electrically small antenna wideband is to make it fat. The bandwidth of an antenna is related to the size of the sphere that just encloses it. By making the antenna fat, more of the spheres are occupied and the antenna bandwidth can be maximized. Some typical fat monopoles are illustrated in Figure A.1. These and other similar shapes have formed the basis for UWB antenna design (Huang, Y and Boyle, K, 2008).

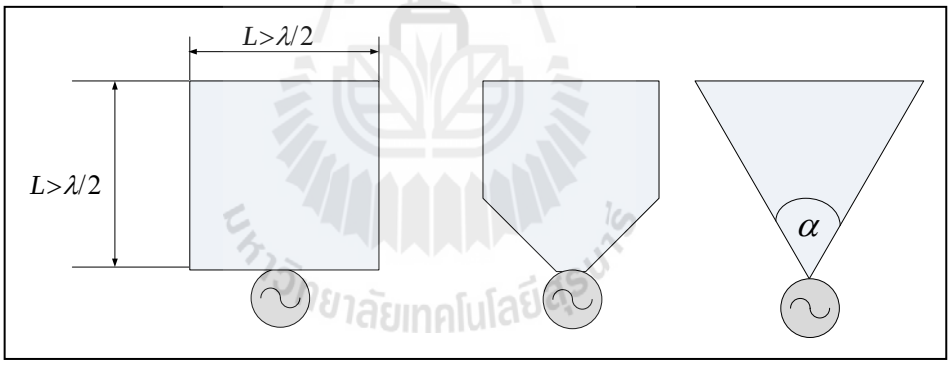

Figure A.1 Some examples of 'fat monopole' antenna

(Huang, Y and Boyle, K, 2008).

Several techniques have been proposed to improve the antenna bandwidth, such as the use of a beveling plate (Ammann and Chen, 2003), a double feed (Antonino-Daviu, Cabedo-Fabres, Ferrando-Bataller and Valero-Nogueira 2003) or asymmetrical feed arrangement (Ammann and Chen, 2004), a trident-shape feeding

strip (Kin-Lu Wong, Chih-Hsien Wu, and Saou-Wen (Stephen) Su. (2004). From the literature of Ammann (2001), the authors have presented an increased bandwidth which can be controlled by beveling the planar geometry as shown in Figure A.2.

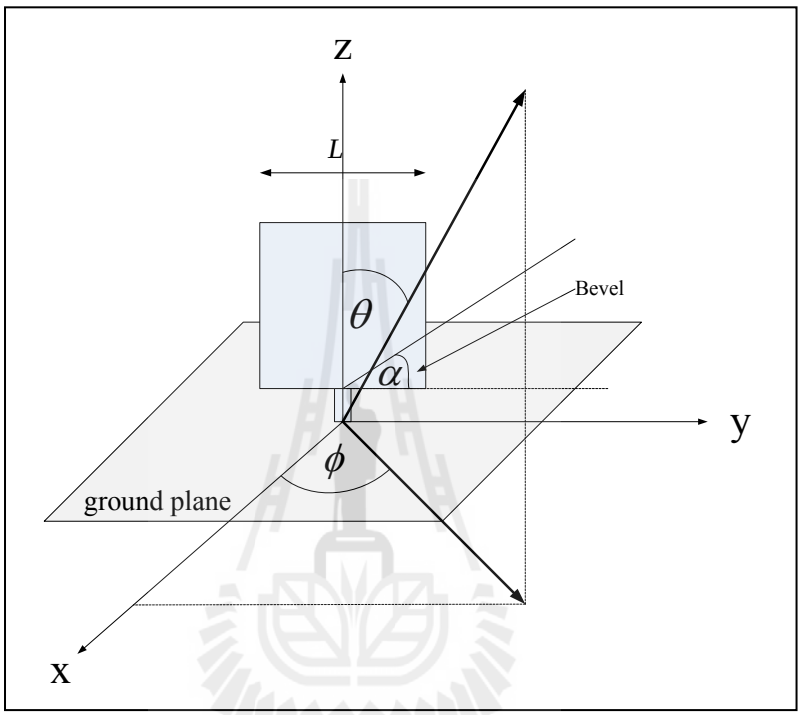

Figure A.2 Symmetry pentagonal planar monopole with monopole with bevel illustrated (Ammann, 2001).

From the mentioned literature, the antenna is constructed using a 25-mm square copper sheet which is 0.2-mm thick and fed via an SMA connector mounted on a 150-mm square ground plane. The beveled is located on one or both sides of the feed probe, yielding asymmetrical or symmetrical pentagonal structure, as shown in Figure A.3. Fine control of the impedance bandwidth is achieved by varying the angle of bevel. The upper and lower edge frequencies of the simple square dimension *L* of 25 mm have been experimentally shown to be 2.35 and 4.95 GHz (Ammann, 1999),

representing an impedance bandwidth ratio (IBR) of 2.1:1. If the square element is beveled by $\alpha = 10°$ on one side of the feed probe, (see Figure A.3) yielding an asymmetrical pentagon, the upper edge frequency is increased to 5.3 GHz. If the bevel is increased to $\alpha = 40°$, the upper edge frequency increases to 6.0 GHz, while the lower edge frequency drops to 2.175 GHz. This represents an IBR of 2.75:1. The measured return loss for the antenna with a single bevel of $\alpha = 10°, 20°, 30°$ and $40°$ is shown in Figure A.4, and the values are tabulated in table A.1. If the planar element is symmetrically beveled on both sides of the feed probe, the upper edge frequency is increased further. For a symmetrical bevel 0f $\alpha = 20°$, the upper edge frequency is found to be 6.75 GHz, and for $\alpha = 30°$, it increases to 7.25 GHz, yielding an IBR of 3.5:1. Symmetrically trimming to $40°$ significantly increase the upper edge frequency to 12.5 GHz, representing an IBR of 5.75:1. The upper and lower edge frequencies for the symmetrically beveled element are tabulated in Table A.2. However, a further increase in bevel does not increase the impedance bandwidth.

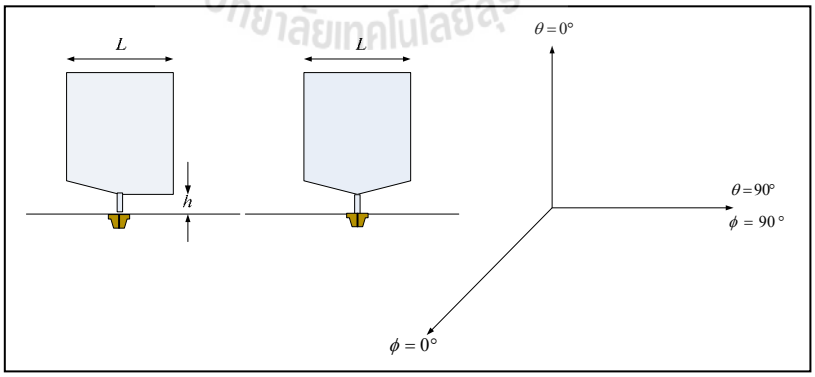

Figure A.3 Simple square geometry with one and two sides beveled, forming Asymmetrical and symmetrical pentagon (Ammann, 2001).

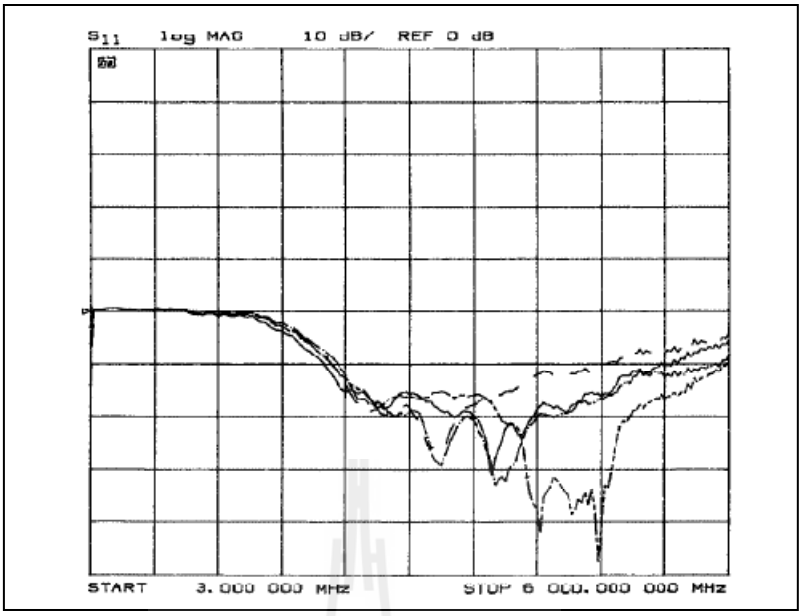

Figure A.4 Measured return loss for the simple square geometry (dashed), with a single 10° (Solid), 20° (dot-dash), 30° (dash-dash) (Ammann, 2001).

Table A.1 Measured impedance bandwidth for the square element beveled on one side of the planar element, showing an increase in upper edge frequency with increase of angle (Ammann, 2001).

Bevel α (degrees)	**Bandwidth (GHz) Asymmetrically Beveled**
0	2.35-4.95
10	2.20-5.30
20	2.19-5.75
30	2.17-5.97
40	2.17-6.00

The results from this literature have shown that a planar monopole employing a beveling technique (increasing of α) can increase the bandwidth. However, the radiation patterns are shown to be quasi-omnidirectional over the impedance bandwidth, as shown in Figure A.5.

Table A.2 Measured impedance bandwidth for the square element beveled on two side of the planar element, showing an increase in upper edge frequency with increase of angle (Ammann, 2001).

Bevel α (degrees)	**Bandwidth (GHz) Symmetrically Beveled**
0	2.35-4.95
10	2.12-5.95
20	2.11-6.75
30	2.10-7.25
40	2.10-12.50

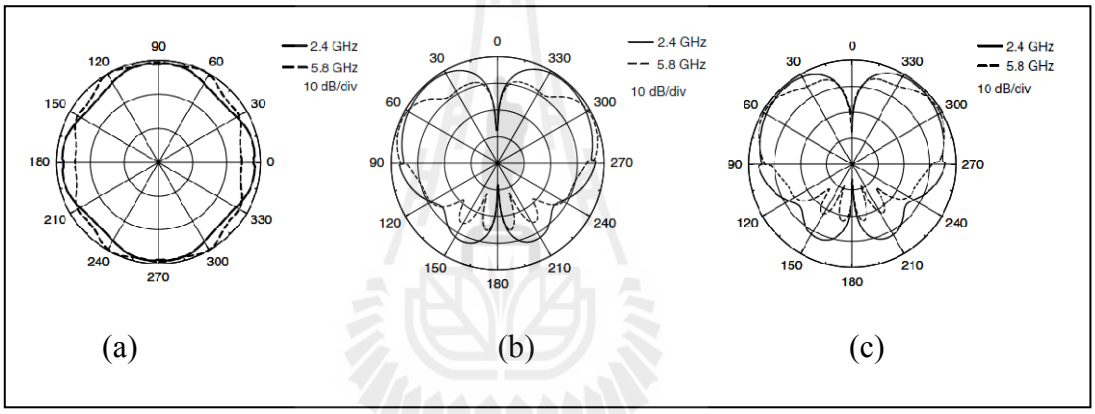

Figure A.5 (a) Normalized *H*-plane pattern $E_\theta(\phi, \theta = 90°)$ for the symmetrically beveled square monopole on a 150 mm. square ground plane.

(b) Normalized *E*-plane pattern $E_\theta(\theta, \phi = 90°)$ for the symmetrically beveled square monopole on a 150 mm. square ground plane.

(c) Normalized *E*-plane pattern $E_\theta(\theta, \phi = 0°)$ for the symmetrically beveled square monopole on a 150 mm. square ground plane.

A wideband planar monopole employing a beveling technique to increase the bandwidth has been investigated and considered to be a solution for this research work. However, the design does not cover the designated band for this thesis (1.9 to

2.4 GHz). In addition, it is relative heavy which is not practical to be arranged in 4×4-lattice. Therefore, some modification is required. According to the mentioned impairment, printed microstrip antenna is attractive because of low profile, small size, light weight, low cost and ease of fabricated and beveling technique as can be seen in literatures of Zaker, Ghobadi and Nourinia (2007).

The work of Al-Husseini, El-Hajj and Kabalan (2008) has presented a printed microstrip antenna in which its geometry is shown in Figure A.6 (a). The FR4-based board is 1.6-mm. in thickness. The feed line is 22-mm. long and 3-wide. The radius of the modified circular patch is 19.2 mm. The coppered edges of the patch are apart. The ground plane is 5-cm. wide and flushed with the feed line. The part of the patch bounded by the coppered edges act like a rectangular patch, which is relayed to the feed line via a "tapered" connection, thus providing better impedance matching. The remaining round-edge part also helps to improve the bandwidth.

From this literature, the design already covers the designated band for this thesis work. However, its size and dimension is large at 3 GHz. Therefore, some reduction in size is done in this thesis work and beveling technique is adopted to extend its bandwidth. Then, the performance of designed antenna is reflected using CST Microwave Studio. Finally, the final design of the antenna covering designated band for this thesis work is presented in Figure A.6 when $\alpha = 37°$. Please note that its radiation pattern is shown in Chapter 5.

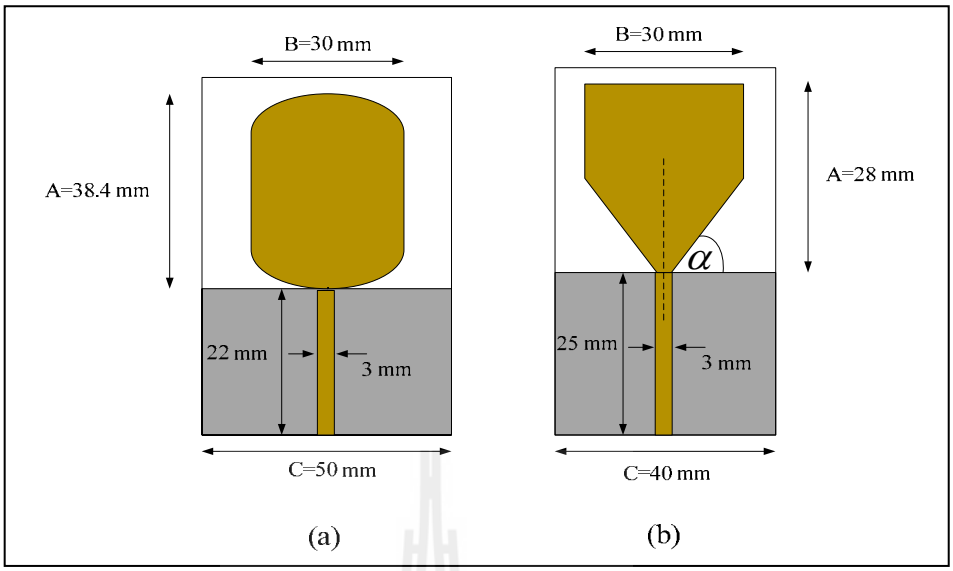

Figure A.6 (a) Antenna structure illustrated in literature of Al-Husseini, El-Hajj and Kabalan. (2008).

(b) Antenna structure designed for this thesis.

APPENDIX B

TECHNICAL PUBLICATION

List of publications

International Journal Paper

Bunsanit, C., Uthansakul, P. and Uthansakul M. (2012). Refinement Method for Weighting Scheme of Fully Spatial Beamformer. **International Journal of Antennas and Propagation**. 2012: 1-13. (ISI Impact factor 0.48)

Uthansakul, M., Attakitmongkol, K., Bunsanit, C. and Uthansakul, P. (2010). Wideband multibeam formation using fully spatial signal processing for indoor communications. **Microwave and Optical Technology Letters.** 52(11): 2423-2427. (ISI Impact factor 0.618)

International Conference Paper

Bunsanit, C., Uthansakul P., Wongsan, R. and Uthansakul, M (2009). Low profile multi-beamformer operating in wide frequency band. **Electrical Engineering/Electronics, Computer, Telecommunications and Information Technology (ECTI) International Conference**. 2: 774-777.

Hindawi Publishing Corporation
International Journal of Antennas and Propagation
Volume 2012, Article ID 359847, 13 pages
doi:10.1155/2012/359847

Research Article

Refinement Method for Weighting Scheme of Fully Spatial Beamformer

Chayanit Bunsanit, Peerapong Uthansakul, and Monthippa Uthansakul

School of Telecommunication Engineering, Suranaree University of Technology, Muang, Nakhon Ratchasima 30000, Thailand

Correspondence should be addressed to Monthippa Uthansakul, mtp@sut.ac.th

Received 10 April 2012; Revised 28 May 2012; Accepted 7 June 2012

Academic Editor: Chih-Peng Li

So far, a wideband spatial beamformer has been proposed. This kind of beamformer has a major contribution as its weighting coefficients are real valued in which they can be simply realized by attenuators or amplifiers. However, so far, the range of attenuation or amplification is relatively large which is not practical for hardware realization. Therefore, this paper proposes a concept to reduce the range of weighting coefficients hence, the hardware realization becomes practical. In this paper, a full prototype of wideband spatial beamformer is constructed to reflect the true beamforming performance of the proposed refinement method. Its radiation patterns obtained from simulation and measurement are compared. As a result, we can reduce the attenuation or amplification range while some radiation characteristic is remained.

1. Introduction

In recent years, wireless communication systems have grown rapidly and contained several technologies operating in different frequencies, for example, WiFi, WiMAX, Bluetooth, and broadband WLAN. From these reasons, the systems are demanded for better coverage, wider frequency range, higher quality of service, and more capacity [1]. So far, smart antenna systems have been envisaged to be the solution. This is because the systems can form one beam towards a desired direction and create nulls or sidelobes towards interference directions. As a result, the greatly improving system performance and also saving energy can be obtained [2]. The smart antenna systems usually consist of antenna array and a suitable signal-processing unit adjusting the weighting coefficients at individual antenna elements to ease the effect of interference signal [3]. The signal processing works according to the utilized algorithms. So far, the beamforming algorithms for smart antennas in wireless communications have concerned only narrowband operation. However, in order to support high data-rate transmission, new efforts are currently required to deal with smart antennas in wide frequency range [4]. From literatures [5–7], wideband smart antenna technology can be classified into three categories. The first category utilizes space-time signal processing, so called spatiotemporal beamformer. These systems consist of array antennas and tapped-delay line at each branch of the array to deal with the received signal in time domain [8]. However, the number of tapped-delay line increases with the bandwidth of utilized frequency. Next category relies on space-frequency signal processing. This is an alternative approach to perform wideband beam-formation without the use of tapped-delay lines. In this method the received signal will be decomposed into non-overlapping narrowband component using band-pass filter. However, for wideband signal, the systems require a large number of frequency filters [9, 10]. The last category utilizes only spatial signal processing, so-called wideband spatial beamformer. This is a new method for wideband smart antennas. In the part of signal processing, weighting coefficients are calculated using two-dimensional Inverse Discrete Fourier Transform (IDFT) technique applied to the required radiation pattern. The obtained weighting coefficients become real values which can be simply realized by attenuators or amplifiers [11–13]. The main advantage of this wideband spatial beamformer is that its design does not require phase shifters, delay circuits, or

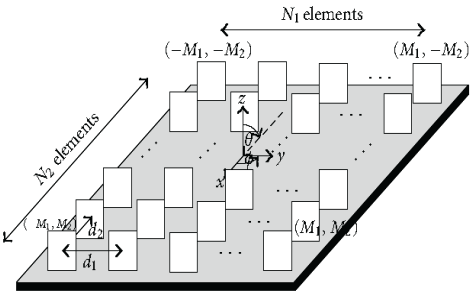

Figure 1: Layout of array configuration for fully spatial beamformer.

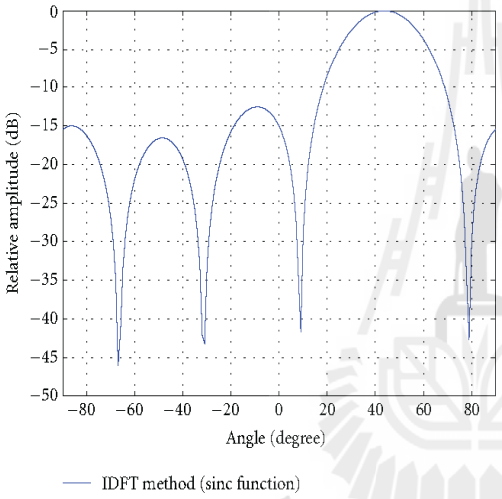

Figure 2: Simulated radiation pattern of 4×4 beamformer at 2.15 GHz, when the main beam direction is 45°.

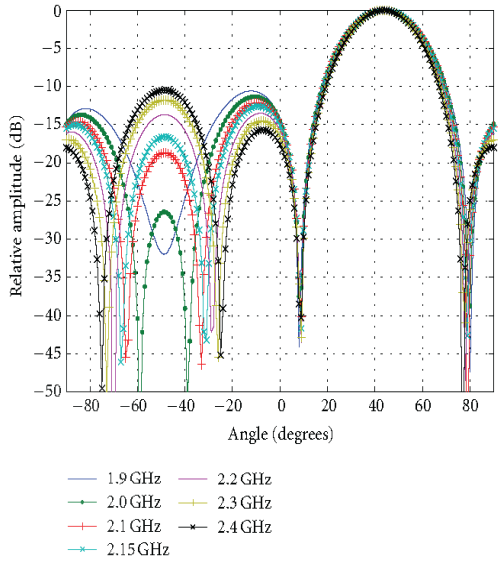

Figure 3: Simulated radiation pattern of 4×4 beamformer for frequencies from 1.9 to 2.4 GHz, when the main beam direction is 45°.

frequency filters. This is of considerable practical advantage over the other types of beamformer employing complex weighting coefficients [14]. However, the range between maximum and minimum values of weighting coefficients (attenuation or amplification) is relatively wide. This is considerably impractical. Therefore, this paper proposes the refinement method for fully spatial beamformer. The aim of the proposed method is to reduce the range of overall weighting coefficients. As a result, the implementation of this kind of beamformer is practical. A full prototype of fully spatial beamformer is developed in order to validate the proposed method.

The remainder of this paper is as follows. After brief introduction showing the background and motivation of the paper, the concept of beam formation in wide range of operating frequency band using only spatial signal processing is described in Section 2. Section 3 proposes the method to make the weights more practical, so-called refinement method. A full prototype of fully spatial beamformer is detailed and constructed in Section 4. Then, its beamforming performance is revealed with the use of proposed refinement method in Section 5. Finally, Section 6 concludes the article.

2. Wideband Beamforming Algorithm Using Fully Spatial Signal Processing

2.1. Fully Spatial Beamformer. The configuration of a wideband beamformer employing a fully spatial signal processing for beam and null steering in azimuth direction is shown in Figure 1. It is constituted by $N_1 \times N_2$ where d_1 and d_2 represent array spacing in two orthogonal directions and are usually chosen as half-wavelength ($\lambda/2$) at the highest frequency of a given frequency band. The antenna elements are denoted by indices (m_1, m_2) where $-M_1 \le m_1 \le M_1$ and $-M_2 \le m_2 \le M_2$. The relationship between M and N is $M_i = (N_i - 1)/2$ [15].

The radiation pattern of the array as a function of angle and frequency can be given by

$$H(f,\phi) = G(f,\phi) \cdot \sum_{m_1=-M_1}^{M_1} \sum_{m_2=-M_2}^{M_2} w_{m_1,m_2} \cdot e^{j(2\pi f/c)(d_1 m_1 \sin\phi + d_2 m_2 \cos\phi)}, \quad (1)$$

where f is the frequency variable, c is the speed of signal, and $G(f,\phi)$ is a function of frequency-angle-dependent gain of each antenna element. Note that signal is incident or transmitted in azimuth direction ϕ and $\theta = 90°$. When ϕ and θ are the azimuth and the elevation angles, respectively.

In order to determinate the weighting coefficients w_{m_1,m_2} in (1), a modified IDFT is applied to H as shown in (2)

$$w_{m_2,m_2} = \left(\frac{1}{N_{u_1} \cdot N_{u_2}}\right) \times \sum_{u_1=-0.5}^{0.5} \sum_{u_2=-0.5}^{0.5} \frac{H(u_1,u_2)}{G(u_1,u_2)} \times e^{-j2\pi u_1 m_1} e^{-j2\pi u_2 m_2}. \quad (2)$$

We define two auxiliary functions as $u_1 = (fd_1/c)\sin\phi$ and $u_2 = (fd_2/c)\cos\phi$. Where N_{u_1} and N_{u_2} are number of sampling points in $u_1 - u_2$ plane in which $N_{u_1} \cong 2N_1$ and $N_{u_2} \cong 2N_2$. The $H(u_1, u_2)$ is the form of Sinc function to obtain maximum gain in the desired direction [16] which can be given as

$$H(u_1,u_2) = \begin{cases} \dfrac{\sin[\alpha\pi(u_1/u_2) - \tan\phi_0]}{\alpha\pi(u_1/u_2) - \tan\phi_0}, & r_l < |r| < r_h, \\ \dfrac{1}{\sqrt{10}}, & \text{otherwise}, \end{cases} \quad (3)$$

where ϕ_0 is the direction at which the main beam to be pointed to which is assumed to be prior known [14], α is the number related to the main beam first-null width, r_l and r_h are defined by the following expressions: $r_l = (f_l/c)\overline{d}$ and $r_h = (f_h/c)\overline{d}$, respectively, when $\overline{d} = \sqrt{d_1^2\sin^2\phi_0 + d_2^2\cos^2\phi_0}$, f_l is lowest frequency and f_h is highest frequency. Referring to the previous work presented in [14], null steering implementation is difficult to perform using IDF method. This is because the obtained weighting coefficients become real valued. Therefore, degree of freedom is relatively limited comparing the ones employing complex weighting coefficients.

To give some simulation examples, we consider 4×4-array operating over frequencies from 1.9 to 2.4 GHz and choose planar monopole having omnidirectional radiation to be an antenna element. From (1) to (3), we calculate weighting coefficients when the main beam is required to be pointed to $\phi_0 = 45°$. The outcomes of beam formation are shown in Figures 2 and 3.

Figures 2 and 3 show the radiation pattern of the 4×4 spatial beamformer in which the objective function as shown in (3) is assumed using Sinc function with the mainbeam pointed to 45° off the array broadside direction. These figures indicate that the main beams are correctly directed towards the desired direction, and the patterns are alike throughout the desired frequency band, from 1.9 to 2.4 GHz. Also, it can be observed that as frequency increases, the array's sidelobe levels increase, and the null locations slightly change with respect to the operating frequency. However, from the results, the validity of the wideband spatial beamforming concept can be confirmed.

2.2. Chebyshev Function. In the previously section, we consider the Sinc function being as an objective function $H(u_1, u_2)$. As a result, the sidelobe level (SLL) is relatively high. Thus, in this section, the objective function is created, using Chebyshev function instead as shown in (4) [17, 18]. We consider

$$H(u_1,u_2) = \begin{cases} X, & \text{desired frequency band} \\ \dfrac{1}{\sqrt{10}}, & \text{otherwise}, \end{cases} \quad (4)$$

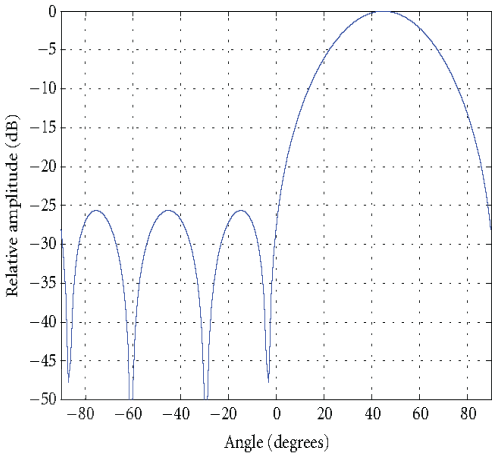

Figure 4: Simulated radiation pattern of 4×4 beamformer plotted at 2.15 GHz, when the main beam direction is 45°, and the objective function is Chebyshev.

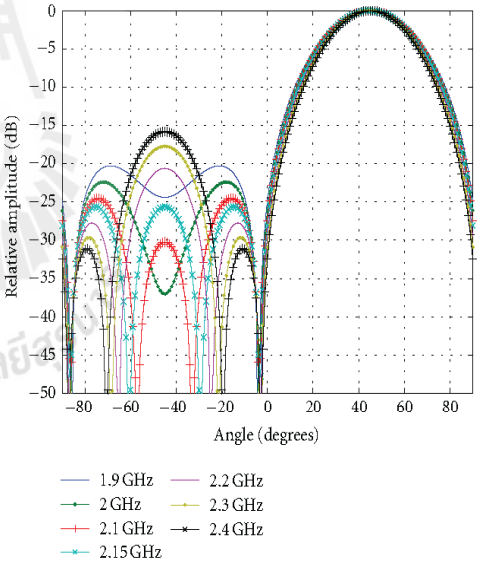

Figure 5: Simulated radiation pattern of 4×4 beamformer for frequencies from 1.9 to 2.4 GHz, when the main beam direction is 45°, and the objective function is Chebyshev.

where

$$X = \begin{cases} (-1)^N \cosh(N \cdot \operatorname{arccosh}|x|), & x < -1 \\ \cos(N \cdot \arccos x), & |x| \le 1 \\ \cosh(N \cdot \operatorname{arccosh} x), & x \ge 1, \end{cases} \quad (5)$$

$$x = x_0 \cos\left\{\frac{2\pi}{\lambda} d \sin\frac{(\theta)}{2}\right\}, \quad (6)$$

$$x_0 = \cosh\left(\frac{\cosh^{-1}\mathrm{SLL_{dB}}}{N} - 1\right), \quad (7)$$

$$N = N_1 = N_2. \quad (8)$$

From (6) direction of arrival on $u_1 - u_2$ plane is

$$\theta = a\tan\left(\frac{u_1}{u_2} - \phi_0\right). \quad (9)$$

Substituting (9) into (6) yields

$$x = x_0 \cos\left\{\frac{2\pi}{\lambda} d \sin\frac{(a\tan(u_1/u_2) - \phi_0)}{2}\right\} \quad (10)$$

or

$$x = x_0 \cos\left\{\pi \sin\frac{(a\tan(u_1/u_2) - \phi_0)}{2}\right\}. \quad (11)$$

In this section, it is easily done by replacing the objective function $H(u_1, u_2)$ appeared in (3) by the one appeared in (4). Therefore, SLL is expected to be lower comparing to the ones shown in Figures 2 and 3. The simulation results for this assumption are shown in Figures 4 and 5.

Comparing between Figures 4 and 5 and Figures 2 and 3 reveals that the sidelobe level when objective function is assumed using Chebyshev polynomial is lower than using Sinc function for all frequencies. In Figure 5, the null location slightly changes when frequency increases as the ones appeared in Figure 3.

3. Refinement Method for Weighting Scheme of Fully Spatial Beamformer

Regarding the previous section, it has shown that we can obtain a value of weighting coefficient of smart antenna by taking IDFT to the desired radiation pattern. One example of the obtained weighting coefficients using both Sinc and Chebyshev functions is shown in Table 1. As we can see they are all real valued in which we can simply utilize attenuators or amplifiers to be weights. However, as we can notice in Table 1, they are not integer numbers, and also the range between the maximum and minimum values is relatively wide. This is considerably not practical for hardware implementation. Therefore, the modification of calculated weighting coefficients is needed while maintaining some important characteristic of radiation pattern.

In this section, we describe the proposed refinement method for weighting scheme of fully spatial beamformer in order to make it practical. This method is implemented after initially calculating the weighting coefficients using IDFT as mentioned before. Some significant properties of radiation behavior are maintained as described below.

3.1. Refinement Algorithm. The main proposal of this algorithm is to decrease the operation range of weighting coefficients as an example shown in Table 1. This algorithm is required because simply squeezing the mentioned range affects some importance radiating characteristics such as main-beam's direction and sidelobe levels. However, obtaining the integer numbers in weighting coefficients is byproduct when performing refinement method.

The weighting coefficient from IDFT method detailed in Section 2.1 is now defined as

$$W_o = \{w_{o,1}, w_{o,2}, w_{o,3}, \ldots, w_{o,N}\} = \{w_{o,i}\}, \quad i = 1, 2, 3, \ldots, N, \quad (12)$$

where N is number of array antennas. Usually, the value of W_o is general number, then we round the weights obtained from IDFT method to integer-valued weights (W_r) as

$$W_r = \{w_{r,1}, w_{r,2}, w_{r,1}, \ldots, w_{r,N}\} = \{w_{r,i}\} = \mathrm{Int}\{w_{o,i}\}. \quad (13)$$

Then, the required mainbeam direction (ϕ_0), average level of minor lobe ($\mathrm{MLL_0}$) and width of main beam (δ_0) and weighting coefficient (W_r) are given. Next, we carry out the following steps.

(1) Determine the maximum of W_r, that is

$$w_{\max}^{(k)} = \max_{i=1}^{N}\{w_{r,i}\}, \quad (14)$$

where $k = 1, 2, 3\ldots$ is order of iteration.

(2) Decrease maximum of weighting coefficient ($w_{\max}^{(k)}$) by decreasing a step size, where $\Delta w > 0$. This results in integer number for weighting coefficients. We have

$$w_{\max,j}^{(k)} = \left\| w_{\max}^{(k)} - \Delta w \right\|, \quad (15)$$

where $j = 1, 2, 3, \ldots$. Then we replace $w_{\max,j}^{(k)}$ with $w_{\max}^{(k)}$ in a set of W_r. We consider

$$w_{\max,j}^{(k)} \Longrightarrow w_{\max}^{(k)}. \quad (16)$$

(3) Multiply W_r by steering vector ψ, and we can get output as follows:

$$y_j^{(k)} = \sum_{i=1}^{N} w_{r,i} e^{\psi}, \quad (17)$$

$$y_j^{(k)} = \sum_{i=1}^{N} w_{r,i}\left(\exp\left(\left(\frac{2\pi}{c}\right)(d_1 p \sin\phi + d_2 q \cos\phi)\right)\right), \quad (18)$$

where (p, q) is index of antenna elements.

(4) Now, we can obtain the radiation pattern from (18). Then we can check some significant parameters such as mainbeam direction ($\phi_r^{(k)}$), average minor-lobe level

Table 1: Weighting coefficients when the required radiation pattern is created using Sinc and Chebyshev functions.

Number of element	Attenuation (dB) Objective		Number of element	Attenuation (dB) Objective	
	Sinc	Chebyshev		Sinc	Chebyshev
1	11.72	22.78	9	22.82	21.47
2	9.68	6.83	10	0	0
3	11.72	21.47	11	11.98	16.80
4	0.94	5.87	12	5.50	6.83
5	5.50	6.83	13	0.94	5.87
6	11.98	16.80	14	11.72	21.47
7	0	0	15	9.68	6.83
8	22.82	21.47	16	11.72	22.78

Table 2: Parameters given in simulation for refinement algorithm of 6 cases.

Parameters	Cases of refinement					
	I	II	III	IV	V	VI
$\Delta\phi$ (degrees)	0	1	2	3	4	4
ΔMILL (dB)	0	1	2	3	4	4
$\Delta\delta$ (degrees)	0	1	2	3	4	5
Number of directions	67	71	77	86	90	91

($\mathrm{MLL}_r^{(k)}$), and beamwidth ($\delta_r^{(k)}$) according to the following conditions:

$$w_{\max}^{k} \le w_0, \tag{19}$$

$$\phi - \Delta\phi \le \phi_r^{(k)} \le \phi + \Delta\phi, \tag{20}$$

$$\mathrm{MLL}_r^{(k)} \le \mathrm{MLL}_0 + \Delta\mathrm{MLL}, \tag{21}$$

$$\delta_0 - \Delta\delta \le \delta_r^{(k)} \le \delta_0 + \Delta\delta, \tag{22}$$

where w_0 is desired maximum of weighing coefficients, $\Delta\phi$ is deviation of main beam angle, ΔMLL is deviation of average minor-lobe level, $\Delta\delta$ is deviation of beamwidth.

(5) Repeat steps 2 to 4 until the set of weighting coefficient is zero according to (19) to (22), and then we can obtain a set of new solution (W_r) for the refinement method.

This proposed algorithm can run in both offline or real time processing depending on the purpose of users. In case of ruing in real-time, we need a suitable DSP board to receive the important information from DFT method then perform 5 steps refinement as shown above. Afterwards, the DSP board feedbacks the weighting coefficients to control the attenuators or amplifiers.

3.2. Simulation Results. In this section we show the efficiency of the proposed refinement method using our own developed program in MATLAB. The utilized antennas are arranged in 4×4 lattice, and the operating frequency is given from 1.9 to 2.4 GHz. We also assume the decreasing step size of weighting coefficient of 1, desired maximum of weight value of 32 dB, and steering angle from 0 to 90 degrees. Some parameters are given in simulations for 6 cases as shown in Table 2.

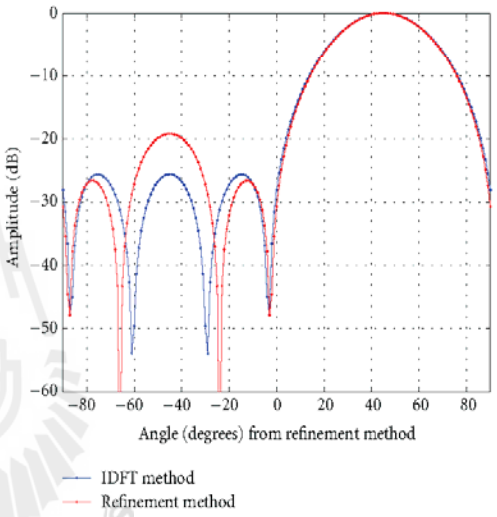

Figure 6: The comparison of radiation patterns at 45° using IDFT method and Refinement method at frequency 2.15 GHz.

Table 2 shows 6 cases for the proposed refinement method. Some parameters, for example, maximum weighing coefficients, deviation of mainbeam angle ($\Delta\phi$), deviation of average minor lobe level (ΔMLL), and deviation of beamwidth ($\Delta\delta$) are differently given in each case. For case I, we set the conditions not to have any error in the parameters mentioned earlier. From running some simulations, we have found that 67 directions or cases out of 91 directions, 0°–90°, are succeeded for refinement. This means that there are only 67 directions out of 91 directions in which we can maintain no error in mainbeam direction, minor lobe level and beamwidth. For case II, we allow the slight error in mainbeam direction, minor lobe level and beamwidth as shown in Table 2. We have found that the number of success cases increases from 67 to 71 directions. Also, higher error in mainbeam direction, minor lobe level, and beamwidth is allowed as shown in Table 2 for cases III, IV, V, and VI. As we can see, the number of success cases increase as we allow more error in mainbeam direction, minor-lobe level

Table 3: The comparison value of attenuator factors between IDFT method and refinement method.

	Attenuation (dB)			Attenuation (dB)	
Number of element	IDFT	Refinement	Number of element	IDFT	Refinement
1	22.78	18	9	21.47	18
2	6.83	7	10	0	0
3	21.47	18	11	16.80	17
4	5.87	6	12	6.83	7
5	6.83	7	13	5.87	6
6	16.80	17	14	21.47	18
7	0	0	15	6.83	7
8	21.47	18	16	22.78	18

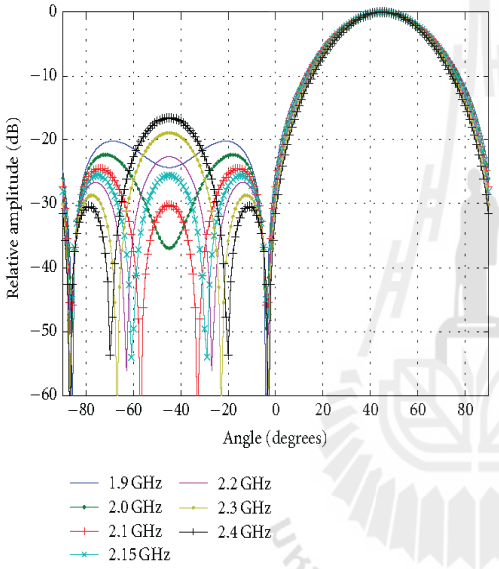

Figure 7: Radiation pattern at 45° using IDFT method from frequencies 1.9 to 2.4 GHz.

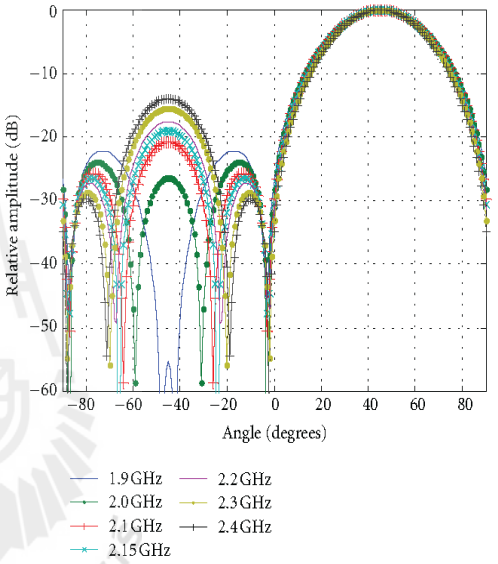

Figure 8: Radiation pattern at 45° using proposed refinement method from frequencies 1.9 to 2.4 GHz.

and beamwidth. For case VI, 100% success can be achieved when we allow error in mainbeam direction of 4°, minor lobe level of 4° and beamwidth of 5°. For this case, the maximum weighting coefficients can be decreased from 54 dB to 32 dB.

Table 3 shows 16 values of weighting coefficients comparing between IDFT method and proposed refinement method when the desired mainbeam direction is given at 45°. For the refinement method, we set $w_0 = 18$ dB, $\Delta\phi = 0°$, ΔMLL = 3 dB and $\Delta\delta = 0°$. As we can see in Table 3, we can decrease maximum weighting coefficient from 22.78 dB to 18 dB which mean the range of attenuation or amplification decreases.

Figure 6 shows beamforming performance for case shown in Table 3 at frequency 2.15 GHz comparing between using IDFT method and proposed refinement method. The obtained result shows that after the refinement method is done, the mainbeam direction is still pointed to 45°, and there is no error in beamwidth. Also, the error in average minor lobe level is within 3 dB.

Figures 7 and 8 show beamforming performance of the beamformer throughout the designated band using IDFT method and proposed refinement method, respectively. As we can see, the beamforming performance for both cases is similar while we can decrease the range of attenuation or amplification up to 4.78 dB (22.78–18 dB).

4. Practical Realizations

The full prototype employing 4 × 4 array antennas for the proposed antenna systems is designed for the operating frequencies from 1.9 to 2.4 GHz as shown in Figure 9. The prototype is a digitally controlled analog beamforming system, and it consists of three functional blocks: antenna array, weighting network, and control devices. A block diagram of smart antenna systems starts from the received incident signals at 4 × 4-antenna array. The received signals are weighted in weighting network which is controlled

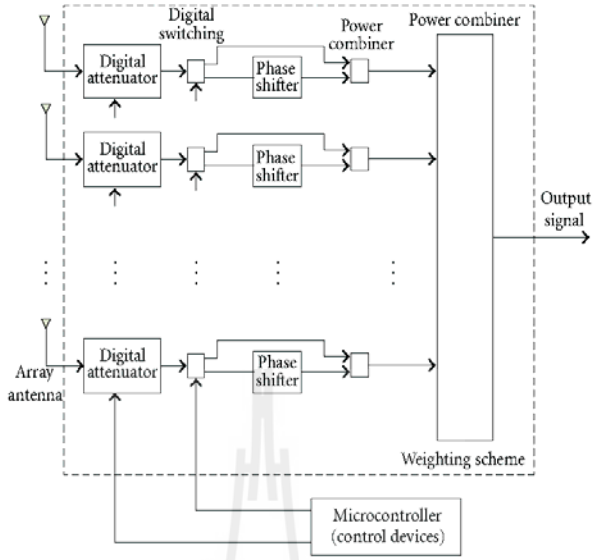

Figure 9: Diagram of smart antenna system.

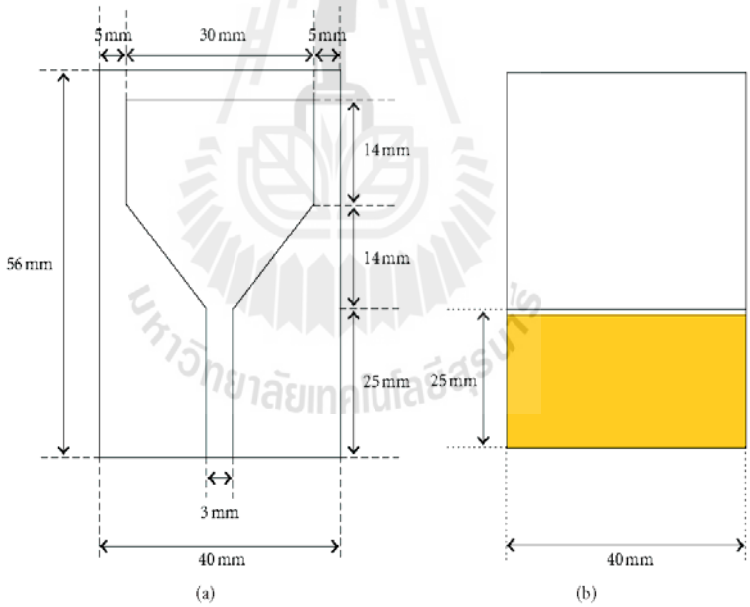

Figure 10: Printed monopole antenna structure at (a) front view and (b) back view.

by control devices. Then, the signals are summed at the combiner device.

4.1. Antenna

4.1.1. Single Element. A printed monopole antenna as shown in Figure 10 is chosen to be the antenna element for this paper. The reason is that this type of antenna is compact enough to be arranged to form the array having interelement spacing of half-wavelength. As appeared in Figure 10, the feed line is 25-mm in length, and ground plane is sized by $25 \times 40\ \text{mm}^2$. The fabricated antenna is shown in Figure 11 using single-layer FR-4-based board having its thickness of 1.6 mm. This antenna was designed to be able to operate in 1.9–2.4 GHz band. Figure 12 shows the measured return loss of the antenna. As we can see, the antenna provides return loss lower than −10 dB within the designated band. Also, its radiation is omnidirectional over the designated band.

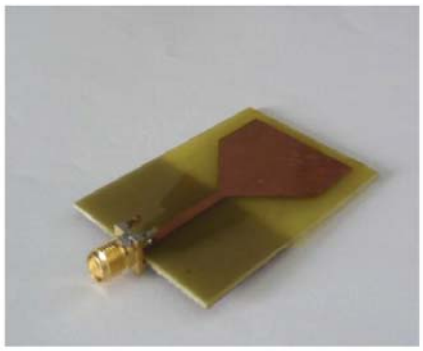

Figure 11: Photograph of the printed monopole antenna fabricated on a 40 × 50 mm^2 single-layer FR-4 substrate.

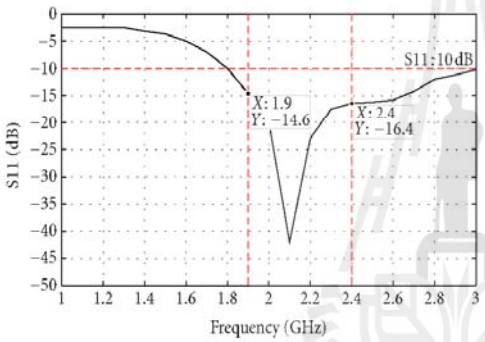

Figure 12: Measured return loss of the antenna shown in Figure 11.

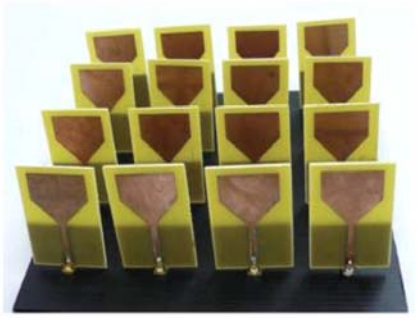

Figure 13: Photograph of fabricated 4 × 4-array antenna.

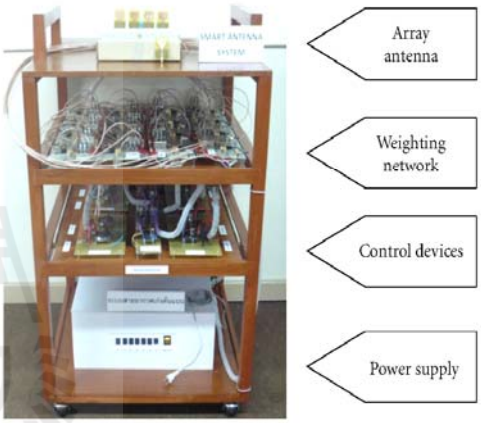

Figure 14: Photograph of full prototype for 4 × 4 spatial beamformer consisting of antenna array, weighting network, control devices, and power supply.

4.1.2. Antenna Array. Here we present the design and development of a 4 × 4-array antenna which is capable of beam steering in the azimuth direction over an increased operational bandwidth. The design focuses on the frequency band from 1.9 to 2.4 GHz. The photograph of constructed antenna array is presented in Figure 13 when the antenna elements are spaced by half-wavelength at 3 GHz (50 mm), which is higher than the upper frequency of the assumed band (2.4 GHz). The use of this higher frequency (3 GHz) is required in the beamforming algorithm to avoid the edge effect when finding the weighting coefficients.

4.2. Weighting Network. The weighting networks consist of four major components: digital attenuators, digital switching, phase shifters, and power combiners. Each component operates very well over wide range of frequency covering frequencies from 1.9 to 2.4 GHz. The detail of each component is shown as follows.

(1) The utilized attenuator is a 50-Ω RF digital step attenuator offering an attenuation range up to 31.5 dB with 0.5 dB step controlled by 6 bit serial interface. The operating frequency covers from DC to 2.4 GHz.

(2) The digital switching is 50-Ω high isolate SPDT RF switch designed for wireless application, covering a broad frequency range from DC up to 3 GHz with low insertion loss.

(3) Phase shifters using FR-4 substrate were designed from CST microwave studio. These components are utilized to 180°-shift the phase of signal in order to produce the minus sign for some weighting coefficients.

(4) The power combiners are separated into two different types which are 2 : 1 operating in frequency range from 1.6 to 3.3 GHz and 16 : 1 operating for frequencies from 1.8 to 2.6 GHz.

4.3. Control Devices. Twelve ATMEGA328 microprocessors are utilized to digital attenuator and digital switching. The reason to choose this type of control device is that it is low of cost but be able to meet the requirement in this paper.

4.4. Spatial Beamformer. The prototype of 4 × 4 spatial beamformer is constructed to test the validation of the proposed method as shown in Figure 14. The power supply is located on the bottom of the shelf. This supports needed power to microcontrollers, digital attenuators, and digital switches. The control devices as mentioned in last section are

FIGURE 15: Testing the constructed prototype in an anechoic chamber.

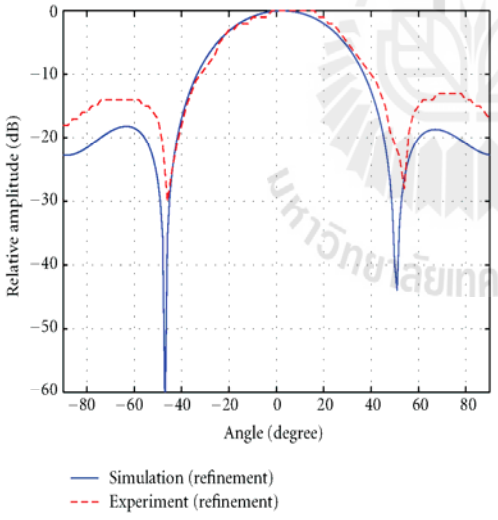

FIGURE 16: Simulated and measured radiation pattern using refinement method for frequency 2.15 GHz, when the main beam direction is 7°.

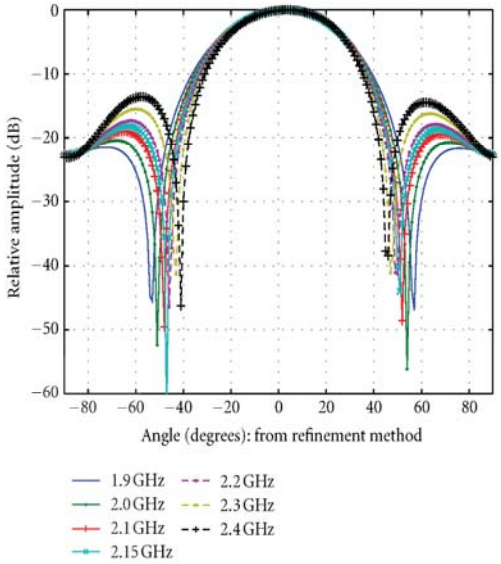

FIGURE 17: Simulated radiation pattern using refinement method for frequencies from 1.9 to 2.4 GHz, when the main beam direction is 7°.

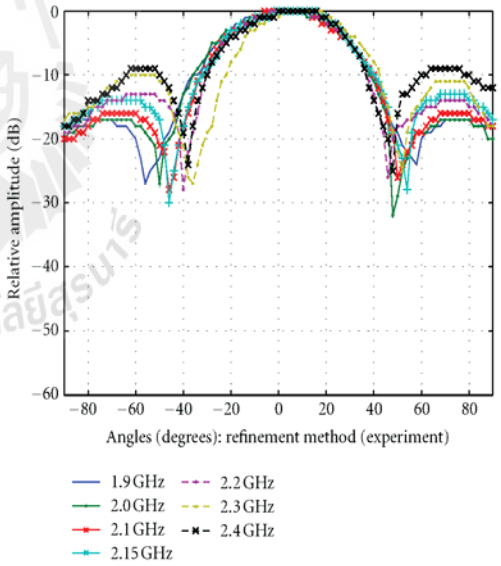

FIGURE 18: Measured radiation pattern using refinement method for frequencies from 1.9 to 2.4 GHz, when the main beam direction is 7°.

located at the 2nd shelf followed by the weighting network which is placed on the 3rd shelf as we can see in Figure 14. The top of the shelf is where we put the 4 × 4 antenna array as mentioned in last section. Also, the power combiners are placed on the top shelf and pass the output signal to the computer.

5. Experimental Results

5.1. Experimental Setup. The constructed prototype is tested in anechoic chamber as shown in Figure 15. The obtained results in terms of beamforming performance will be compared to the ones obtained from computer simulation. The measurement is taken place at single frequency from

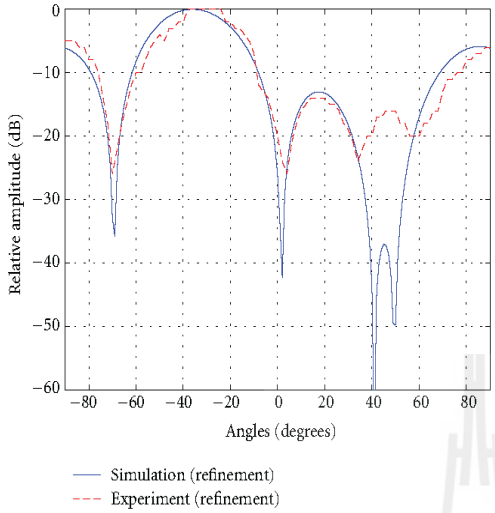

Figure 19: Simulated and measured radiation pattern using refinement method for frequency 2.15 GHz, when the main beam direction is 34°.

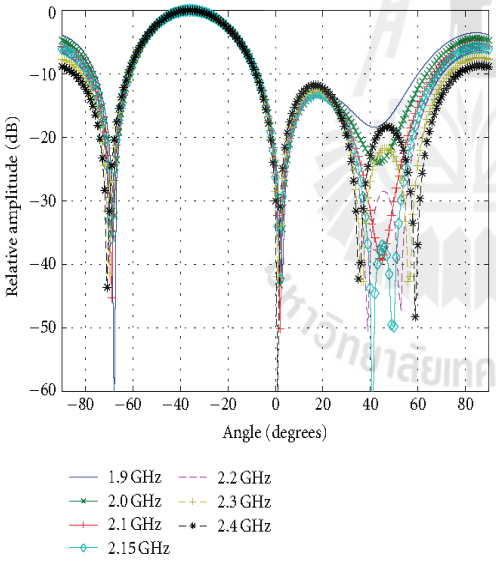

Figure 20: Simulated radiation pattern using refinement method for frequencies from 1.9 to 2.4 GHz, when the main beam direction is −34°.

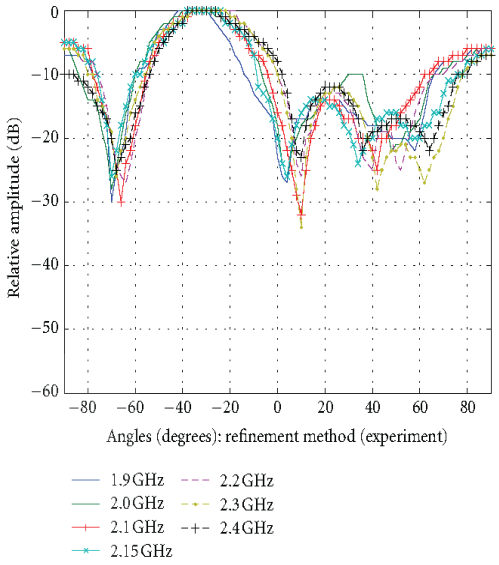

Figure 21: Measured radiation pattern using refinement method for frequencies from 1.9 to 2.4 GHz, when the main beam direction is −34°.

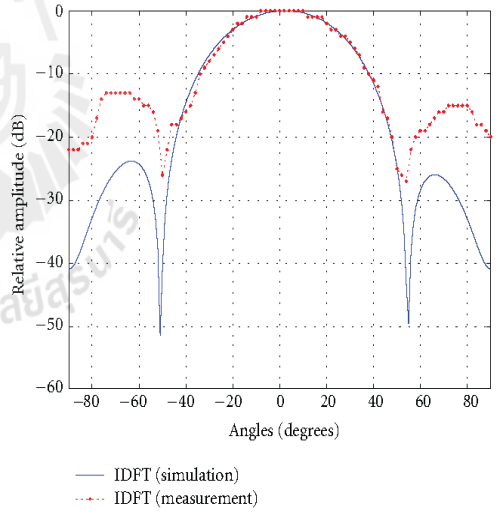

Figure 22: Simulated and measured radiation pattern using IDFT method at frequency 2.15 GHz, when the main beam direction is 2°.

1.9 to 2.4 GHz. All the process starting from giving desired mainbeam direction performs automatically. However to show some example, the desired directions to be chosen are 7 directions: 2°, 7°, −17°, ±34°, 57°, and 75°.

5.2. Experimental Results. In this section we validate the beamforming performance of the proposed refinement method through the prototype measurement described in last section. The performance is compared between employing IDFT method and proposed refinement method. There are 3 cases for this section as follows. Please note that the operating frequencies are assumed from 1.9 to 2.4 GHz.

Case A. the beamforming performance using the proposed refinement method is tested. In this case, the mainbeam direction is chosen at 7°. The parameters for this case are as $w_0 = 4$ dB, $\Delta\phi = 5°$, $\Delta\text{MLL} = -11$ dB, and $\Delta\delta = 0°$. After

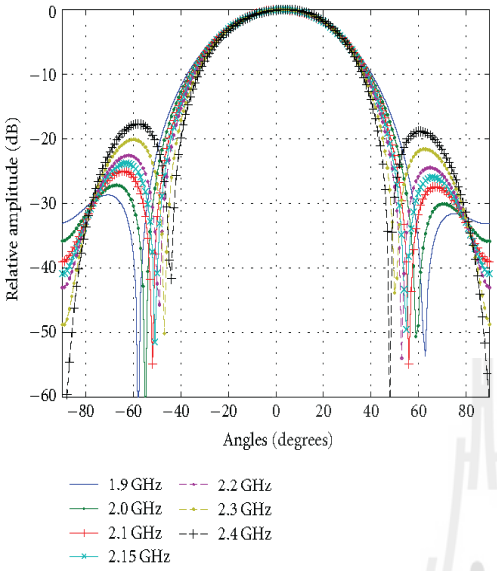

Figure 23: Simulated radiation pattern using IDFT method for frequencies from 1.9 to 2.4 GHz, when the main beam direction is 2°.

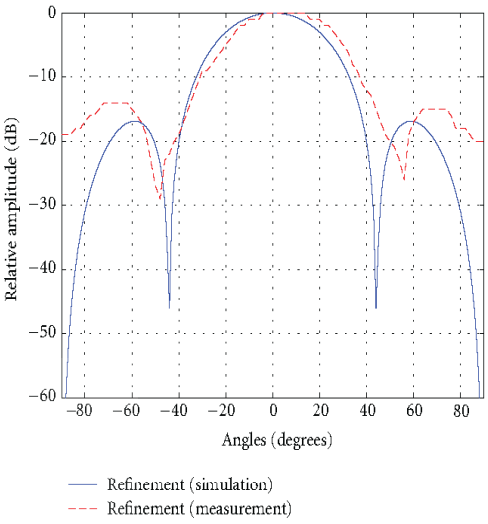

Figure 25: Simulated and measured radiation pattern using refinement method at frequency 2.15 GHz, when the main beam direction is 2°.

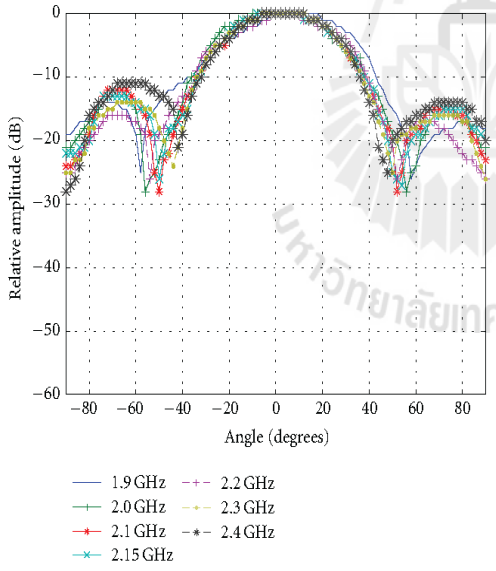

Figure 24: Measured radiation pattern using IDFT method for frequencies from 1.9 to 2.4 GHz, when the main beam direction is 2°.

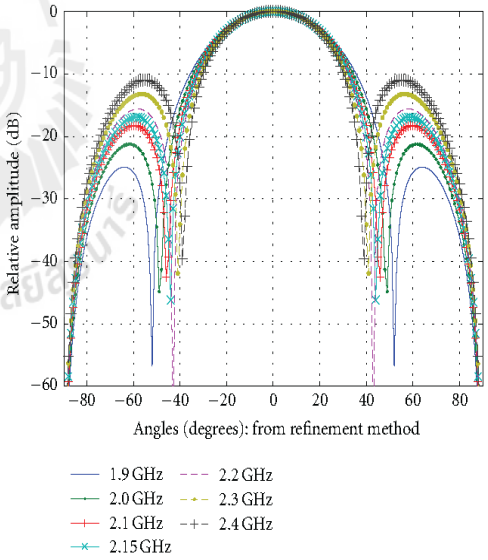

Figure 26: Simulated radiation pattern using refinement method for frequencies from 1.9 to 2.4 GHz, when the main beam direction is 2°.

the refinement process is done, we have found that the range of attenuation or amplification for weighting coefficients can be reduced from 16 to 4 dB.

The beamforming performance in terms of radiation pattern at frequency 2.15 GHz when using proposed refinement method according to condition for *Case A* is shown in Figure 16. In the figure, comparison between the result obtained from computer simulation and experiment is shown. As we can see, both results have a good agreement to each other. Figure 17 shows the beamforming obtained from simulation for *Case A* throughout the designated band. We can see that the mainbeam direction does not deviate from the given direction (7° for this case).

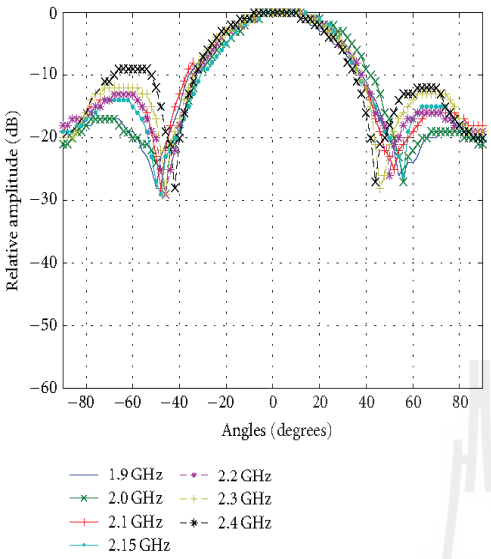

FIGURE 27: Measured radiation pattern using refinement method for frequencies from 1.9 to 2.4 GHz, when the main beam direction is 2°.

Case B. For this case, the mainbeam is supposed to be pointed to −34°. Also the parameters for refinement are as follows: $w_0 = 4$ dB, $\Delta\phi = 2°$, ΔMLL = −15 dB, and $\Delta\delta = 0°$. After the refinement process is done, we have found that the range of attenuation or amplification can be reduced from 30 dB to 4 dB. This is considerable practical.

Figure 19 shows the beamforming performance obtained from simulation and measurement for *Case B* at frequency 2.15 GHz. As we can see, after refinement method is done, the error in mainbeam direction is 2°, and the error in minor lobe level is within −15 dB. Also, there is no error in beamwidth. This error occurred because we allow some error in the refinement method. Comparing with the results obtained from *Case A*, we can obtain higher range reduction of weighting coefficients while expecting some error in mainbeam direction, minor-lobe level and beamwidth.

Figures 20 and 21 reveal the beamforming performance for *Case B* throughout the designated band, both from simulation and measurement, respectively. We can observe more error in mainbeam direction, average minor-lobe level and beamwidth compared with the ones presented in Figures 17 and 18. As expected, the ones obtained from measurement are likely to have higher minor-lobe level.

Case C. For this case, the beamforming performance using proposed refinement method comparative with IDFT method is pointed out. The parameters for *Case C* are as follows: $w_0 = 4$ dB, $\Delta\phi = 2°$, ΔMLL = −11 dB, and $\Delta\delta = 0°$. Please note that the mainbeam direction for this case is changed to 2°. As a result, this case allows us to reduce the range of weighting coefficients from 8 dB to 4 dB.

Figure 22 shows the beamforming performance at 2.15 GHz using IDFT method for both simulation and measurement. Figures 23 and 24 show radiation pattern throughout the designated band, 1.9 to 2.4 GHz, obtained from simulation and measurement, respectively. As we can see, its beamforming behavior looks stable throughout the band. However, the ones obtained from measurement have slightly higher minor lobe level.

Figures 25 to 27 show the performance similar to the ones from Figures 22 to 24 but the proposed refinement method is taken place after we obtain the weighting coefficients from IDFT method. Its beamforming at 2.15 GHz is shown in Figure 25 while Figures 26 and 27 show it performance throughout the designated band via simulation and measurement, respectively. As we can see, the beamforming behavior looks similar to the cases using IDFT method with narrower range of weighting coefficients.

6. Conclusion

This paper has presented the method to reduce the range of weighting coefficients for fully spatial beamformer, so-called refinement method. This is considerably useful as the weighting coefficients for this kind of beamformer are real valued; therefore, narrower range of weighting coefficients is advantage. As a result, the choice of attenuators or amplifiers becomes practical. This refinement method is taken place after weighting coefficients are calculated using IDFT method. This proposed method can be succeeded in every mainbeam direction when error in some parameters is allowed. Those parameters are mainbeam direction, average minor lobe level, and beamwidth. The more errors are allowed, the more success cases can be achieved. A full prototype of fully spatial beamformer was constructed to test the validation of the proposed refinement method. The results in terms of radiation pattern obtained from simulation and measurement are compared. The obtained results reveal that we can reduce the range of attenuation or amplification using the proposed refinement method while some significant radiation behaviors are remained.

Acknowledgment

This work was supported by Suranaree University of Technology (SUT) and by the Office of the Higher Education Commission under NRU project of Thailand.

References

[1] I. Hamburg, A. Hamburg, M. Gavota, and M. Lazea, "Integrating wireless technology in e-learning for disabled," in *Proceedings of the International Conference on Information and Communication Technologies: From Theory to Applications (ICTTA '04)*, pp. 123–124, April 2004.

[2] M. Ghavami, "An adaptive wideband array using a single real multiplier for each antenna element," in *Proceedings of the 13th IEEE International Symposium on Personal, Indoor and Mobile Radio Communications (PIMRC '02)*, vol. 4, pp. 1805–1809, September 2002.

[3] S. C. Rani, P. V. Subbaiah, and K. C. Reddy, "Smart antenna algorithm for WCDMA mobile communication system,"

International Journal of Computer Science and Network Security, vol. 8, no. 7, 2008.

[4] M. Uthansakul and M. E. Bialkowski, "Impact of wideband signals on smart antenna system," in *Proceedings of the 15th International Conference on Microwaves, Radar and Wireless Communications (MIKON '04)*, vol. 2, pp. 501–504, May 2004.

[5] M. Uthansakul and M. E. Bialkowski, "Frequency-angle dependence compensation of non-uniform components for wideband smart antenna," in *Proceedings of the IEEE MITT-S International Microwave Symposium Digest*, vol. 2, pp. 1253–1256, June 2004.

[6] M. Uthansakul and M. E. Bialkowski, "An investigation into smart antenna configurations for wideband communication," in *Proceedings of the 15th International Conference on Microwaves, Radar and Wireless Communications (MIKON '04)*, vol. 2, pp. 505–508, May 2004.

[7] L. Rui, G. Yuchun, Z. Xin, and S. Xiaowei, "An investigation into broadband smart antenna systems for wireless communication," in *Proceedings of the International Conference on Microwave and Millimeter Wave Technology (ICMMT '07)*, pp. 1–4, April 2007.

[8] S. S. Jeon, Y. Wang, Y. Qian, and T. Itoh, "A novel smart antenna system implementation for broad-band wireless communications," *IEEE Transactions on Antennas and Propagation*, vol. 50, no. 5, pp. 600–606, 2002.

[9] M. Hefnawi and G. Y. Delisle, "Performance analysis of wideband smart antenna systems using different frequency compensation techniques," in *Proceedings of the 6th IEEE Symposium on Computers Communications (ISCC '01)*, pp. 237–243, July 2001.

[10] M. Hefnawi and G. Y. Delisle, "Adaptive array performance with focussing technique," in *Proceedings of the IEEE Antennas and Propagation Society International Symposium*, vol. 2, pp. 1016–1019, July 1997.

[11] M. Uthansakul and M. E. Bialkowski, "Wideband smart antenna using non-uniform components," in *Proceedings of the 15th International Conference on Microwaves, Radar and Wireless Communications (MIKON '04)*, vol. 3, pp. 1542–1545, May 2004.

[12] M. Ghavami, "Wideband smart antenna theory using rectangular array structures," *IEEE Transactions on Signal Processing*, vol. 50, no. 9, pp. 2143–2151, 2002.

[13] M. E. Bialkowski and M. Uthansakul, "A wideband array antenna with beam-steering capability using real valued weights," *Microwave and Optical Technology Letters*, vol. 48, no. 2, pp. 287–291, 2006.

[14] M. Uthansakul and M. E. Bialkowski, "Investigations into a wideband spatial beamformer employing a rectangular array of planar monopoles," *IEEE Antennas and Propagation Magazine*, vol. 47, no. 5, pp. 91–99, 2005.

[15] M. Uthansakul and M. E. Bialkowski, "Fully spatial wide-band beamforming using rectangular array of planar monopoles," *IEEE Transaction on Antenna and Propagation*, vol. 54, no. 2, 2006.

[16] M. Uthansakul and M. E. Bialkowski, "A wideband spatial beamformer employing a rectangular array of planar monopoles," in *Proceedings of the IEEE Antennas and Propagation Society International Symposium and USNC/URSI Meeting*, pp. 303–306, July 2005.

[17] M. Uthansakul and M. E. Bialkowski, "Designing a wideband spatial beamformer for low sidelobe radiation pattern performance," in *Proceedings of the Asia-Pacific Microwave Conference (APMC '05)*, December 2005.

[18] C. Bunsanit, P. Uthansakul, R. Wongsan, and M. Uthansakul, "Low profile multi-beam former operating in wide frequency band," in *Proceedings of the International conference on Electrical Engineering/Electrical, Computer, Telecommunication and Information Technology*, pp. 774–777, May 2009.

WIDEBAND MULTIBEAM FORMATION USING FULLY SPATIAL SIGNAL PROCESSING FOR INDOOR COMMUNICATIONS

Monthippa Uthansakul, Kitti Attakitmongkol, Chayanit Bunsanit, and Peerapong Uthansakul
School of Telecommunication Engineering, Suranaree University of Technology Muang, Nakhon Ratchasima 30000, Thailand;
Corresponding author: uthansakul@sut.ac.th

Received 9 February 2010

ABSTRACT: *Recently, an outstanding wideband beamformer utilizing only space domain, not time or frequency domain, has been proposed, so-called wideband spatial beamformer. The advantage of this beamformer is that it requires only attenuators or amplifiers to perform beam formation in wide frequency band as its weighting coefficients become real values. As a result, tapped delay lines, frequency filters, or phase shifters are avoidable. This article presents an extension work for the mentioned wideband spatial beamformer. The beamforming algorithm is modified to produce multibeam patterns with one set of real-valued weights for the purpose of energy saving. The proposed concept is tested through simulated and measured results to confirm beamforming capability.* © 2010 Wiley Periodicals, Inc. Microwave Opt Technol Lett 52:2423–2427, 2010; View this article online at wileyonlinelibrary.com. DOI 10.1002/mop.25506

Key words: *antenna arrays; beamforming; multiple beams; wideband operations*

1. INTRODUCTION

The growth of wireless communications has gone with unprecedented rate over the last two decades as it can be seen through an exponential increase in number of user year-over-year. This is because wireless technologies help people's daily lives much faster and easier. As a result, lots of wireless technologies have emerged mainly for today's personal communications, e.g., WiMAX, WiFi, 3G, Bluetooth, and broadband WLAN. Those technologies operate in different frequency bands and also provide different advantages [1]. For example, 3G is suitable for long distance communication with reduced bandwidth whereas WiFi can be used to communicate at a short distance providing higher data transmission rate. On the other hand, WiMAX covers larger area, which overcomes disadvantages of WiFi. To consume maximum efficiency for all kind of wireless access, we have to carry many mobile terminals, which is considerably not practical. According to this, integration of those technologies into one gadget device, e.g., personal digital assistant is envisaged in foreseen future. From this point of view, the antenna systems capable of operating in wide frequency band have gained lots of attention from researchers nowadays. In addition, multiple antenna systems, e.g., smart antenna systems [2] are currently on focus as they have the potential of achieving high data rate access and increased capacity of wireless communication systems. The key factor of the mentioned systems is their beamforming capability.

From literatures, the beamformer that is able to control its radiation pattern through a wide frequency band, so-called wideband beamformer, can be classified into three categories. The first category is a space-time beamformer [3] that utilizes an antenna array for spatial filtering and tapped delay lines for temporal filtering. This has a drawback as a large number of tapped delay lines is required to be able to give stability in beam steering through a wide frequency band. For the second category, it is called space-frequency beamformer [3]. This is an alternative approach to perform wideband beam formation without the use of tapped delay lines. Instead, frequency filters are utilized to decompose the received wideband signals from the antenna elements into nonoverlapping narrowband signals. Then, narrowband beamforming algorithm or conventional algorithm can take place within a decomposed sub-band. However, this still has some shortcomings as follows. As the utilized algorithm works well for the signals having a few percent of fractional bandwidth, the frequency response of the filters needs to be very narrow resulting in requirement of a larger number of filters when the operational bandwidth is extended. In addition, the response of filters has to be sharp enough so that the overlapping of frequency in each sub-band does not exist. For the last category, involving only space domain has been recently proposed, namely fully spatial beamformer [4]. The work presented in Ref. 4 indicates the advantages of this type of beamformer as follows. The wideband beam formation in one particular direction requires only one set of real-valued weights, not complex weighting coefficients, which can be realized by amplifiers or attenuators. Then, the use of tapped delay lines, frequency filters, or phase shifters can be avoidable. The practical realization of this beamformer has been presented in Ref. 5. However, this may introduce an energy loss in unused areas when utilizing for indoor purposes as it provides one broad main beam. For instance, in the hospital, we loss energy in some unused areas, e.g., housekeeping laundry. Moreover, the generated wireless signal becomes interferers in some restricted areas, e.g., ECG room, pathology room, or operating rooms, which are prohibited areas and all equipment in those rooms needs a very accurate operation. However, those impairments can be eliminated using a system capable of producing multiple beams. Then, energy can be efficiently used. Also, we can avoid interference signals in some particular areas. Nonetheless, these antenna systems must be low of cost and simple. To support incoming integrated service mentioned before, the system has to be able to operate in wide frequency band. This is a motivation of this article. Therefore, this article presents a wideband beamformer capable of forming multiple beams to any given directions. The idea of producing beams from the work presented in Ref. 5 is adopted. Therefore, we can have the antenna systems operating wide frequency band in which the beam directions can be simply given by adjusting attenuators or amplifiers.

This article is organized as follows. After brief introduction indicating motivation and contribution of this article, a brief background of fully spatial beamformer presented in Ref. 6 is given in Section 2. In this section, the concept of multibeam formation is also introduced. Afterward, the received signals captured from the constructed array sensors are digitally weighted to confirm the capability of beam formation in Section 3. The results and discussion obtained from Section 3 are given in Section 4. Finally, this article is concluded in Section 5.

2. WIDEBAND MULTIBEAM FORMATION

The concept of wideband beam formation presented in Ref. 5 as shown in Figure 1 is adopted in this article. A rectangular antenna array, in which the array elements are spaced by half wavelength of highest frequency, is utilized. To steer its main beam to any given direction, weighting coefficients can be calculated by taking inverse discrete Fourier transform (IDFT) to a symmetry function defining a required radiation pattern, so-called objective function, $H(u_1, u_2)$. Note that further detail of beamforming algorithm can be pursued in Ref. 5. The obtained weighting coefficients of this beamformer are real values. This

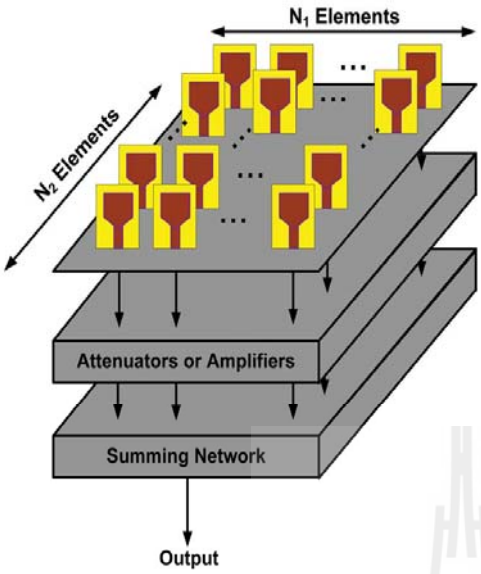

Figure 1 Wideband spatial beamformer constituted by rectangular array, attenuator or amplifier, and summing network. [Color figure can be viewed in the online issue, which is available at wileyonlinelibrary.com]

is considered to be the advantage for this beamformer over other types of beamformer as attenuators or amplifiers can be used without the use of phase shifters, tapped delay lines, or frequency filters. This results in simplicity of the system.

In the beamformer, objective function is a key design representing a predefined radiation pattern giving maximum gain at a desired direction. This function also keeps stability over a designated wide frequency band. As a result, the beamformer becomes frequency invariant. As presented in Ref. 5, the objective function is produced using Sinc function [6]. As a result, only one main beam is achieved and the sidelobe levels are relatively high. In this article, the objective function is created using Chebyshev function [7] as shown in (1). The reason is that lower sidelobe levels can be expected.

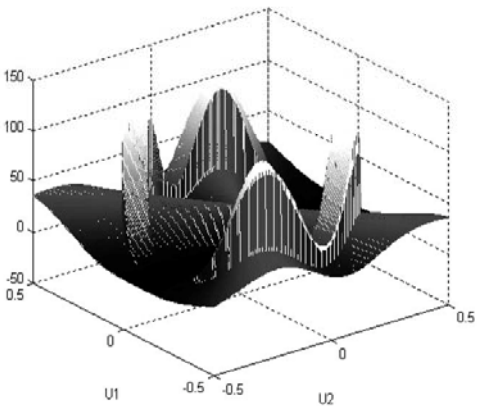

Figure 2 Plot of $H(u_1, u_2)$ when desire beam angle are $-50°$ and $65°$

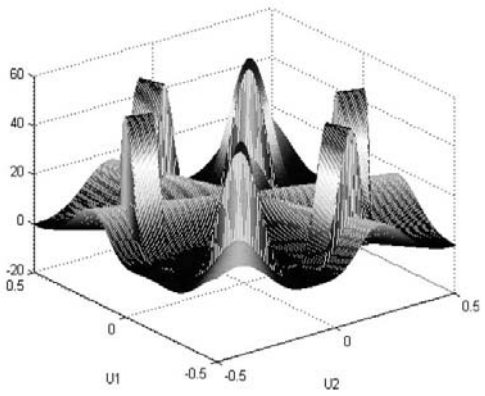

Figure 3 Plot of $H(u_1, u_2)$ when desire beam angle are $-70°$, $-20°$, and $50°$

$$H(u_1,u_2)=\begin{cases} X & \text{desired frequency band} \\ 1/\sqrt{10} & \text{otherwise} \end{cases} \tag{1}$$

where

$$X=\begin{cases} (-1)^N \cosh(n \operatorname{arccosh}|x|) & x<-1 \\ \cos(n \arccos x) & |x|\le 1 \\ \cosh(N \operatorname{arccosh} x) & x\ge 1 \end{cases}$$

$$x = x_0 \cos\{\pi \sin[\tan^{-1}\left(\frac{u_1}{u_2}-\phi\right)]/2\}$$

$$x_0 = \cosh(\cosh^{-1} \mathrm{SLL}_{\mathrm{dB}}/N-1)$$

$$N = N_1 = N_2$$

and ϕ stands for direction or angle at which the main beam is to be directed to and $\mathrm{SLL}_{\mathrm{dB}}$ is the desired sidelobe level in decibel.

For energy saving, the concept of multibeam formation is implemented as follows. The new objective function is created by merging multiple objective functions as written in (2).

$$H(u_1,u_2)=H_{\phi_1}(u_1,u_2)+H_{\phi_2}(u_1,u_2) \tag{2}$$

where $H_{\phi_1}(u_1,u_2)$ and $H_{\phi_2}(u_1,u_2)$ stand for objective functions in which the main bean is directed to ϕ_1 and ϕ_2, respectively.

The plots of objective function obtained from (2) are demonstrated in Figures 2 and 3 when two and three directions of main beam are required, respectively. Note that a number of main beam directions presented in those figures is double as the symmetry of the objective function on u_1–u_2 plane [5]. The objective function presented in Figure 2 is produced when having two main beam directions directed to $-50°$ and $65°$ off boresight direction and 4×4 array of omnidirectional antennas is used. Figure 3 presents the objective function created from combination of three Chebyshev functions having maximum gain at $-70°$, $-20°$, and $50°$ off

TABLE 1 Weighting Coefficient for 4 × 4 Beamformer Having Two Main Beams at −50° and 65° Operating for Frequency From 1.9 to 2.4 GHz

Number of Antenna Elements	Attenuation Factor (dB)
6, 8, 9, 11	0
5, 7, 10, 12	4
1, 16	8
2, 15	12
4, 13	16
3, 14	32

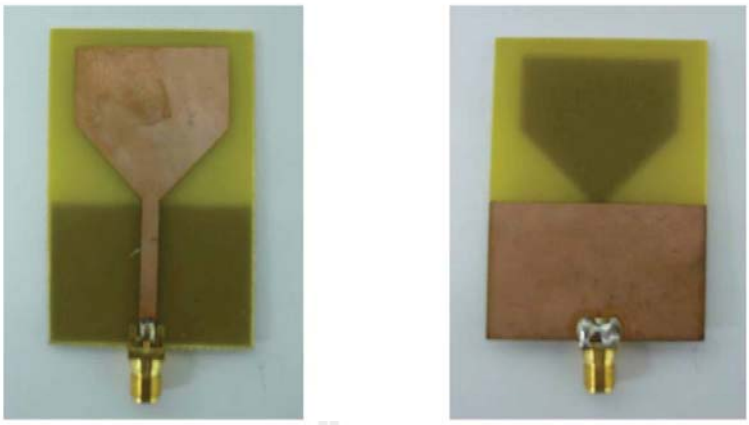

(a) (b)

Figure 4 Photograph of PCB antenna fabricated on FR4 having thickness of 1.6 mm. [Color figure can be viewed in the online issue, which is available at wileyonlinelibrary.com]

boresight direction and 8 × 8 array of omnidirectional antennas is used. Note that the operating frequency band starts from 1.9 to 2.4 GHz.

An example of weighting coefficients utilized for directing two main beams at −50° and 65° is shown in Table 1 when 4 × 4 array of omnidirectional antenna is used. These weighting coefficients are calculated by taking IDFT to the objective function presented in Figure 2. According to this, practical realization of beamforming network is very simple, both for analog and digital domains.

3. MEASUREMENT

Here, we present the design and development of a 4 × 4 array which is capable of beam steering in the azimuth direction over an increased operational bandwidth, which would be difficult to achieve by applying conventional narrowband beam steering technique. The design focuses on the frequency band from 1.9 to 2.4 GHz. This band covers on two communication standards, WCDMA and Bluetooth. The printed circuit board (PCB) antenna presented in Ref. 8 is adopted in this work as it is able to operate in wide frequency and also its

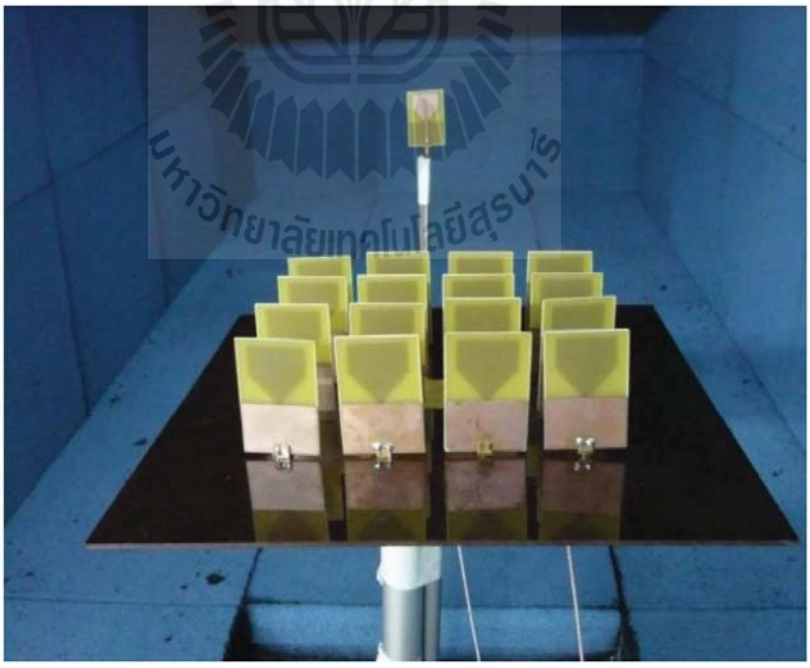

Figure 5 Photograph of measurement setup in anechoic chamber. [Color figure can be viewed in the online issue, which is available at wileyonlinelibrary.com]

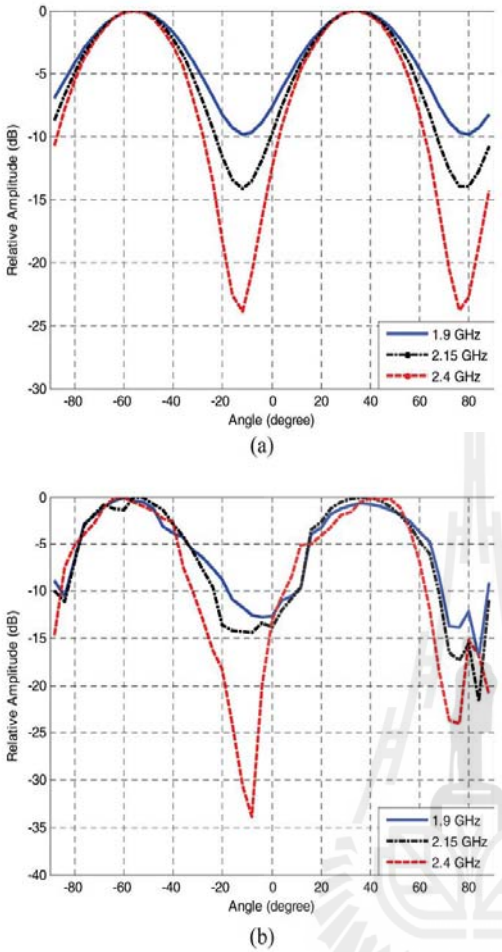

Figure 6 Radiation pattern of 4×4 beamformer for desired directions of $-60°$ and $30°$ plotted for frequencies 1.9, 2.15, and 2.4 GHz from (a) simulation (b) measurement. [Color figure can be viewed in the online issue, which is available at wileyonlinelibrary.com]

manufacturing is not complicated. However, the size and dimension has been originally adjusted to cover the operational frequency band from 1.9 to 2.4 GHz. The photograph of modifying fabricated PCB antenna is presented in Figure 4, which is constructed on FR4-based board having the thickness of 1.6 mm. The measured of fabricated antenna provides a return loss (S_{11}) better than 10 dB covering the desired operational band from 1.9 to 2.4 GHz. In addition, the measured radiation patterns confirm that the antenna provides nearly radiation pattern of monopole antenna. Having completed the design of single antenna element, the next step concerns the design and construction of an array comprising of 4×4 elements of PCB antenna. The photograph of constructed antenna array is presented in Figure 5 when the antenna elements are spaced by half wavelength at 3 GHz (50 mm), which is higher than the upper frequency of the assumed band (2.4 GHz). The use of this higher frequency (3 GHz) is required in the beamforming algorithm to avoid the edge effect when finding the weighting coefficients.

The measurement is taken place in an anechoic chamber at the Suranaree University of Technology. One single PCB antenna is used as the transmit antenna. The received signals are recorded when the incoming signal is coming from 0° to 360° in azimuth around the array. Afterward, the recorded signals are digitally weighted offline. The obtained results compared with simulation results are shown in the next section.

4. RESULTS AND DISCUSSION

In this article, the beamforming capability of the proposed concept is tested through computer simulation. Here, the radiation pattern is used to indicate the beamforming capability. The chosen operational frequencies are 1.9, 2.15, and 2.4 GHz. The main focus is paid to its capability of multiple beam forming in wideband operation. The desired directions for the main beam to be directed to are separated into three cases: $-60°$:30°, $-50°$:65°, and $-40°$:40°. The results for those three cases are shown in Figures 6–8, respectively.

The results indicate that we have a good agreement between simulated and measured results. The main beam directions are relatively stable throughout the designated frequencies. We also notice that null's locations obtained from measurement are

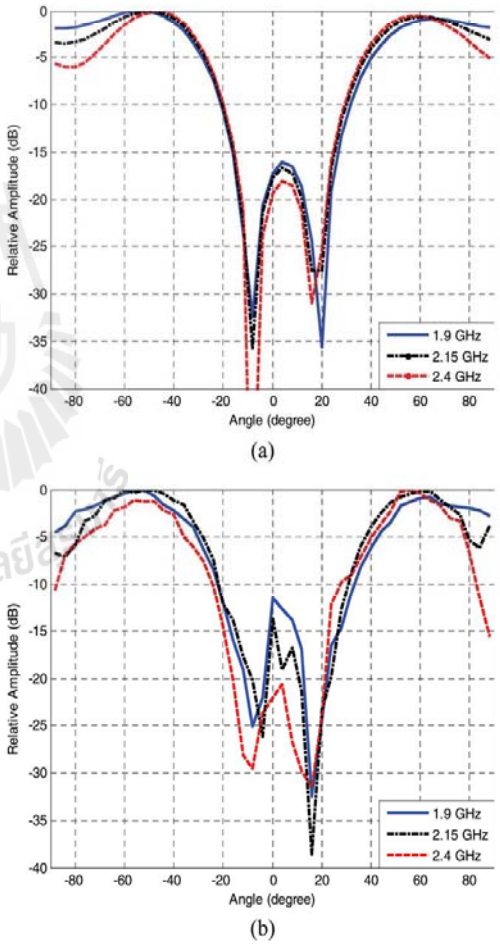

Figure 7 Radiation pattern of 4×4 beamformer for desired directions of $-50°$ and 65° plotted for frequencies 1.9, 2.15, and 2.4 GHz from (a) simulation (b) measurement. [Color figure can be viewed in the online issue, which is available at wileyonlinelibrary.com]

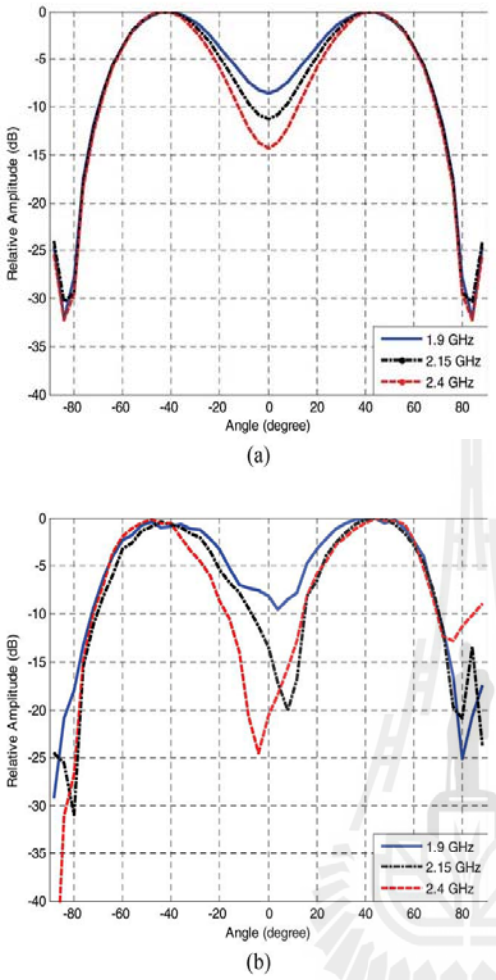

Figure 8 Radiation pattern of 4 × 4 beamformer for desired directions of −40° and 40° plotted for frequencies 1.9, 2.15, and 2.4 GHz from (a) simulation (b) measurement. [Color figure can be viewed in the online issue, which is available at wileyonlinelibrary.com]

deviated from ones obtained from simulation. This may be caused from phase error from the received signal. However, controlling of null's locations is out of scope for this article. From the obtained results, we can say that this low-profile system is suitable being an antenna system for indoor usage in next generation of wireless communications. The reasons are that it is able to operate in wide frequency band and this beamformer requires low expense for implementation both for analog and digital domains.

5. CONCLUSIONS

This article presents an extension work of the spatial wideband beamformer proposed in literatures. The beamformer requires attenuators or amplifiers to adjust the amplitude of received signals from a rectangular antenna array as the calculated weighting coefficients become real values. The extension has been made for producing wideband multiple beams using only one set of weights. This can be accomplished through the modification of an objective function representing the required radiation. In this article, it can be produced using Chebyshev function when its maximum gain is given at the desired direction. To obtain multiple beams, combination of objective functions at different desired directions is desirable. The performance of the proposed concept is tested through computer simulation and measurement. It has revealed that the beamformer performs very well in forming multiple beams in designated directions over the assumed frequency band. This is considerably suitable for next generation of wideband indoor wireless communications.

ACKNOWLEDGMENTS

This work is supported by Research Grant from Thailand Research Fund (TRF-MRG5180202) and Suranaree University of Technology, Thailand.

REFERENCES

1. H. Ileana, H. Adrian, G. Mihai, and M. Lazea, Integrating wireless technology in e-learning for disabled, In: Information and Communication Technologies: From Theory to Applications, 2004, pp. 123–124.
2. M. Uthansakul and E.B. Marek, Impact of signals on smart antenna system, In: Proceedings of the MIKON, 2, 2004, pp. 501–504.
3. M. Uthansakul and E.B. Marek, An investigation into smart configurations for wideband communication, In: Proceedings of the XV International Conference Microwave, Radar and Wireless Communications, 2, 2004, pp. 505–508.
4. M. Uthansakul and E.B. Marek, A wideband spatial beamformer employing a rectangular array of planar monopoles, In: IEEE Digest on Antenna and Propagation Symposium, Washington, DC, 2005.
5. M. Uthansakul and E.B. Marek, Fully spatial wideband beam forming using a rectangular array of planar monopoles, IEEE Trans Antenna Propag 54 (2006), 527–533.
6. M. Ghavami, Wideband smart antenna theory using rectangular array structures, IEEE Trans Signal Proc 50 (2002), 21143–2151.
7. M. Uthansakul and E.B. Marek, Designing a wideband spatial beamformer for low sidelobe radiation pattern performance, In: Microwave Conference Proceeding, 2005.
8. M.A. Husseini, A.E. Haji, and K.Y. Kabalan, A 1.9–13.5 GHz low-cost microstrip antenna, In: Proceedings of the Wireless Communications and Mobile Computing Conference, 2008, pp. 1023–1025.
9. G.L. Stuber, Principles of mobile communication, Kluwer Academic Publishers, Boston, MA, 2002.
10. R.C. Hansen, Phased array antennas, Wiley, New York, 1998.

A 4.9-dB NF 53.5- to 62-GHz MICROMACHINED CMOS WIDEBAND LNA WITH SMALL GROUP-DELAY-VARIATION

Chi-Chen Chen,[1] Yo-Sheng Lin,[1] Pen-Li Huang,[2] and Shey-Shi Lu[2]
[1] Department of Electrical Engineering, National Chi Nan University, Puli, Taiwan, Republic of China; Corresponding author: stephenlin@ncnu.edu.tw
[2] Department of Electrical Engineering, Graduate Institute of Electronics Engineering, National Taiwan University, 106 Taipei, Taiwan, Republic of China

Received 22 February 2010

ABSTRACT: *A 53.5- to 62-GHz wideband low-noise amplifier (LNA) with excellent phase linearity property using standard 0.13 μm CMOS technology is reported. To achieve sufficient gain, the LNA is composed of six cascade common-source stages. Current-sharing technique is adopted to reduce power dissipation. The LNA (STD LNA) consumed 29.1 mW and achieved input return loss (S_{11}) of −10.3 to −19.5 dB, output return loss (S_{22}) of −13.8 to −27.8 dB, forward gain (S_{21}) of 8.1 to 11.1 dB, and reverse*

Low Profile Multi-Beam Former Operating in Wide Frequency Band

C. Bunsanit, P. Uthansakul, R. Wongsan and M. Uthansakul
E-mail: d5140022@g.sut.ac.th, {uthansakul,rangsan,mtp}@sut.ac.th

Abstract- **Recently, an outstanding wideband beamformer utilizing only space domain, not time or frequency domain, has been proposed, so called wideband spatial beamformer. The advantage of this beamformer is that it requires only attenuators or amplifiers to perform beam formation in wide frequency band as its weighting coefficients become real values. As a result tapped-delay lines, frequency filters or phase shifters are avoidable. This paper presents an extended work for the mentioned wideband spatial beamformer. The beamforming algorithm is modified in order to produce multi-beam patterns with one set of real-valued weights with the purpose of energy saving. The proposed concept is tested through simulation results to confirm beamforming capability.**

I. Introduction

The growth of wireless communication has gone with unprecedented rate over the last two decades as it can be seen through an exponential increase in number of user year-over-year. This is because wireless technologies help people's daily lives much faster and easier. As a result, lots of wireless technologies have emerged mainly for today's personal communications e.g., WI-MAX, WiFi, 3G, Bluetooth and broadband WLAN. Those technologies operate in different frequency bands and also provide different advantages [1]. For example, 3G is suitable for long distance communication with reduced bandwidth whereas WiFi can be used to communicate at a short distance providing higher data transmission rate. On the other hand, WIMAX covers larger area which overcomes disadvantages of WiFi. To consume maximum efficiency for all kind of wireless access, we have to carry many mobile terminals, which is considerably not practical. According to this, integration of those technologies into one gadget device e.g., Personal Digital Assistant (PDA) is envisaged in foreseen future. From this point of view, the antenna systems capable of operating in wide frequency band have gained lots of attention from researchers nowadays. In addition, multiple antenna systems e.g., smart antenna systems [2] are currently on focus as they have potential of achieving high datarate access and increased capacity of wireless communication systems. The key factor of the mentioned systems is their beamforming capability.

From literatures, the beamformer which is able to control its radiation pattern through a wide frequency band, so called wideband beamformer, can be classified into three categories. The first category is a space-time beamformer [3] which utilizes an antenna array for spatial filtering and tapped-delay lines for temporal filtering. This has a drawback as a large number of tapped-delay lines is required to be able to give stability in beam steering through a wideband frequency band. For the second category, it is called space-frequency beamformer [3]. This is an alternative approach to perform wideband beam formation without the use of tapped-delay lines. Instead, frequency filters are utilized to decompose the received wideband signals from the antenna elements into non-overlapping narrowband signals. Then, narrowband beamforming algorithm or conventional algorithm can take place within a decomposed sub-band. However, this still has some shortcomings as follows. As the utilized algorithm works well for the signals having a few percent of fractional bandwidth, the frequency response of the filters needs to be very narrow resulting in requirement of a larger number of filters when the operational bandwidth is extended. In addition, the response of filters has to be sharp enough so that the overlapping of frequency in each sub-band does not exist. For the last category, involving only space domain has been recently proposed, namely fully spatial beamformer [4]. The work presented in [4] indicates the advantages of this type of beamformer as follows. The wideband beam formation in one particular direction requires only one set of real-valued weights, not complex weighting coefficients, which can be realized by amplifiers or attenuators. Then, the use of tapped-delay lines, frequency filters or phase shifters is avoidable. The practical realization of this beamformer has been presented in [5]. However, this may introduce an energy loss in unused areas when utilizing for indoor purposes as it provides one broad main beam. Therefore, the idea to develop the work presented in [5] is to produce multiple beams operating in wide range of frequency. In addition, those beams must be also adjustable, not fixed multiple beams. This can draw lots of attention from researchers and companies as we can produce adjustable wideband multi-beams with low profile systems employing only an antenna array and attenuators or amplifiers.

This paper is organized as follows. After brief introduction indicating motivation and contribution of this paper, the benefits of wideband multiple-beam former is discussed in Section II. Section III gives a background of fully spatial beamformer presented in [5]. In this section, the concept of multi-beam formation is also introduced. Afterwards, the performance of the proposed concept in term of beamforming capability is tested through computer simulation in Section IV. Finally, this paper is concluded in Section V.

978-1-4244-3388-9/09/$25.00 ©2009 IEEE

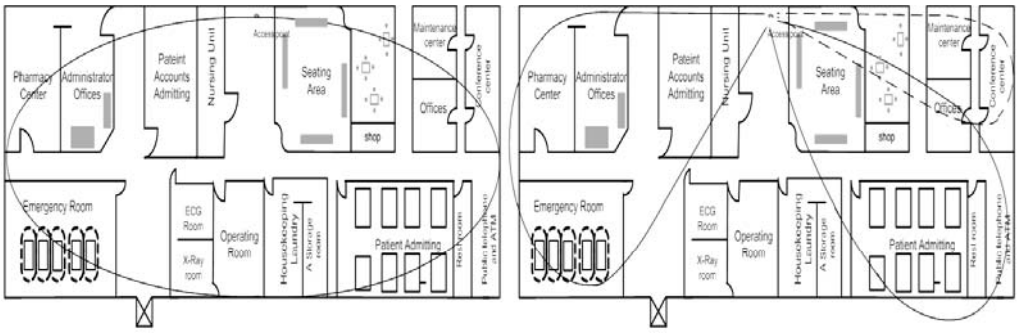

(a) (b)

Figure 1. Wireless access scenarios in a hospital when (a) one omni-directional and (b) multiple beams are produced.

II. Benefits of Multiple Beams for Indoor Communications

Fig.1a presents an example of an existing wireless access in an indoor building which usually radiates in omni-direction. As we can see in a hospital layout, we loss energy in some unused areas e.g., housekeeping laundry. Moreover, the generated wireless signal becomes interferers in some areas e.g., ECG room, pathology room, or operating rooms, which are prohibited areas and all equipment in these rooms needs a very accurate operation.

However, those impairments can be eliminated using a system capable of producing multiple beams as shown in Fig. 1b. As a result, energy can be efficiently used. Also, we can avoid interference signals in some particular areas. Nonetheless, this antenna system must be low of cost and simple. To support incoming integrated services mentioned before, the system has to be able to operate in wide frequency band. This is a motivation of this paper. Therefore, this paper presents a wideband beamformer capable of forming main beams to any given directions. The simplicity of this system is that directions of its main beam directions can be selected with simply adjusting attenuators or amplifiers. The detail of the mentioned beamformer is as follows.

III. Wideband Multi- Beam Formation

The concept of wideband beam formation presented in [5] is adopted in this paper. A rectangular antenna array, in which the array elements are spaced by half-wavelength of highest frequency, is utilized. To steer its main beam to any given direction, weighting coefficients can be calculated by taking Inverse Discrete Fourier Transform (IDFT) to a symmetry function defining a required radiation pattern, so called objective function. Note that further detail of beamforming algorithm can be pursued in [5]. The obtained weighting coefficients of this beamformer are real values. This is considered to be advantage for this beamformer over other types of beamformer as attenuators or amplifiers can be employed without the use of phase shifters, tapped-delay lines, or frequency filters. This results in simplicity of the system.

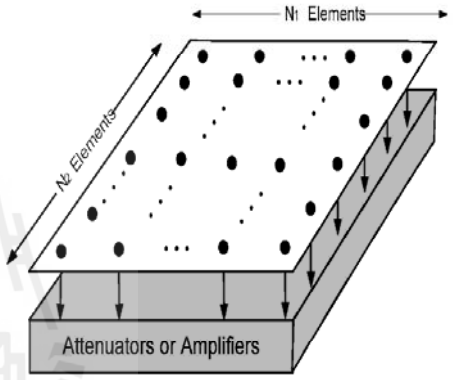

Figure 2. Configuration of wideband spatial beamformer.

In the beamformer, objective function, $H(u_1,u_2)$, is a key design representing a predefined radiation pattern giving maximum gain at a desired direction. This function also keeps stability over a designated wide frequency band. As a result, the beamformer becomes frequency-invariant. As presented in [5], the objective function is produced using Sinc function. From the obtained results, only one main beam is achieved and the sidelobe levels are relatively high. In this paper, the objective function is created using Chebyshev function as shown in (1) as lower sidelobe levels can be expected.

$$H(u_1,u_2)=\begin{cases} x & desired\ frequency\ band \\ 1/\sqrt{10} & otherwise \end{cases} \quad (1)$$

$$x = x_0 \cos\{\pi \sin[\tan^{-1}(\frac{u_1}{u_2}-\phi)]/2\}$$

where $x_0 = \cosh(\cosh^{-1} SLL_{dB}/N - 1)$

$N = N_1 = N_2$

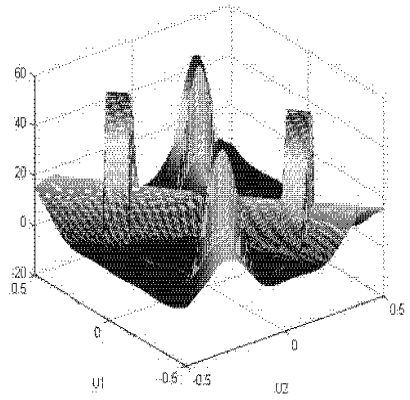

Figure. 3 Plot of H(u1,u2) when desire beam angle are -50° and 60°

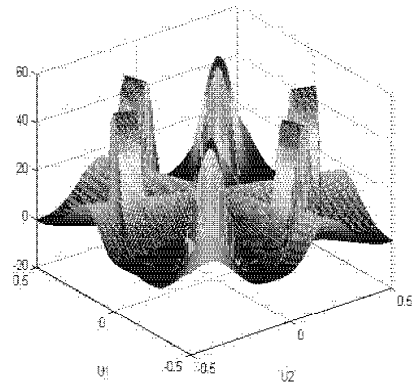

Figure. 4 Plot of H(u1,u2) when desire beam angle are -70°,-20° and 50°

and ϕ stands for direction or angle at which the main beam is to be directed to and SIL_{dB} is the desired sidelobe level in decibel.

For energy saving, the concept of multi-beam formation is implemented as follows. The new objective function is created by merging multiple objective functions, each for single direction as written in (2).

$$H(u_1,u_2) = H_{\phi_1}(u_1,u_2) + H_{\phi_2}(u_1,u_2) \qquad (2)$$

Where $H_{\phi_1}(u_1,u_2)$ and $H_{\phi_2}(u_1,u_2)$ stand for objective functions in which the main bean is directed to ϕ_1 and ϕ_2, respectively

Plots of objective function obtained from (2) are demonstrated in Figs. 3 and 4 when two and three directions of main beam are required, respectively. Note that a number of main beam direction presented in these figures is double as the symmetry of the objective function on u_1-u_2 plane [5]. The objective function presented in Fig. 3 is produced when having two main beam directions directed to -50° and 60° off boresight direction. Fig. 4 presents the objective function created from combination of three Chebyshev functions having maximum gain at -70°,-20° and 50° off boresight direction.

Also, an example of weighting coefficients utilized for directing two main beams at -50° and 60° is shown in Table I. These coefficients are calculated by taking IDFT to the objective function presented in Fig. 3. As we can see in this table, only three different values of attenuators, 6 12 and 16.5 dB, are required to produce two main beams directed to -50° and 60° for frequency from 1.9 to 2.5 GHz. According to this, practical realization of beamforming network is very simple, both for analog and digital domains.

Next section shows how the change of objective function affects the beamforming performance.

TABLE I

WEIGHTING COEFFICIENT FOR 8×8-BEAMFORMER HAVING TWO MAIN BEAMS AT -50° AND 60° OPERATING FOR FREQUENCY FROM 1.9 TO 2.5 GHZ.

Number of Antenna Elements	Attenuation Factor (dB)
6,9,10,11,12,14,16,19,20,22,23,27,28,29,30,35,36,37,38, 42,43,44,46,47,49,51,54,55,56,59	0
1,13,15,17,18,31,32,33,34,48,50,52,53,64	6
24,25,40,41	12
2,3,4,5,7,8,21,26,39,45,57,58,60,61,62,63	16.5

IV. SIMULATION AND RESULTS

In this paper, the beamforming performance of the proposed concept is tested through computer simulation in term of radiation pattern. The frequency range is chosen from 1.9 to 2.5 GHz. The array spacing is chosen as a half wave-length at 3 GHz to avoid the edge effect when performing IDFT to the objective function, thus d = 0.05 m. The utilized objective function is created from (1) and (2). The 8×8 planar monopole antennas are assumed. This is because it is able to operate in wide frequency band and small of size.

Figs. 5 and 6 reveal the radiation pattern of the beamformer when the objective function is created from (1) and (2). For these two cases, the main beam is assigned to be directed to -30°and 20°, and -65°and 65° respectively. As we can see, the obtained radiation patterns provide a stable main beam in the assigned direction throughout the designated frequency band, from 1.9 to 2.5 GHz. In addition, its sidelobe levels are relatively low.

The further investigation is paid to producing three beams in different directions as shown in Figs. 7 and 8. As expected, the beamformer performs very well in pointing its main beam to three given directions throughout the designated wide frequency band.

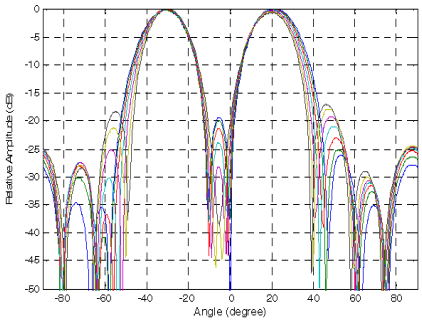

Figure. 5 Radiation pattern of 8×8 beamformer for desired directions of -30°and 20° plotted for frequencies from 1.9 to 2.5 GHz.

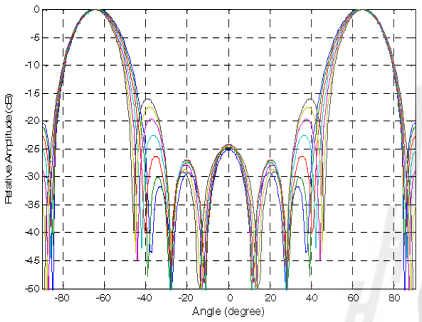

Figure. 6 Radiation pattern of 8×8 beamformer for desired directions of -65°and 65° plotted for frequencies from 1.9 to 2.5 GHz.

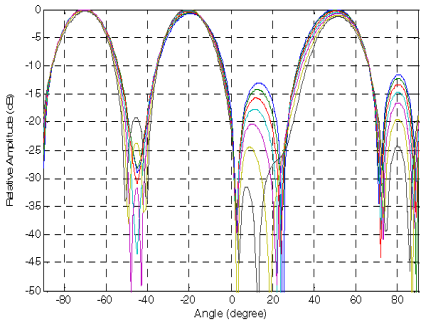

Figure. 7 Radiation pattern of 8×8 beamformer for desired directions of -70°, -20°and 50° plotted for frequencies from 1.9 to 2.5 GHz.

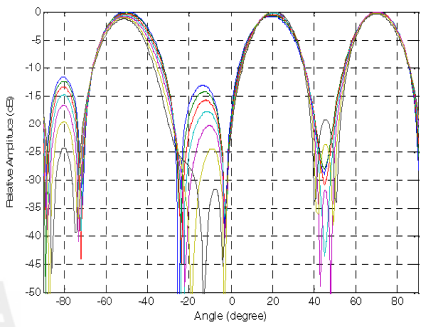

Figure. 8 Radiation pattern of 8×8 beamformer for desired directions of -50°, 20°and 70° plotted for frequencies from 1.9 to 2.5 GHz.

From the obtained results, we can say that this low profile system is suitable being an antenna system for indoor usage in next generation of wireless communications. The reasons are that it is able to operate in wide frequency band and this beamformer requires low expense for implementation both for analog and digital domains.

V. CONCLUSION

This paper presents an extended work for the spatial wideband beamformer proposed in literature. The beamformer requires attenuators or amplifiers to adjust the amplitude of received signals from a rectangular antenna array as the calculated weighting coefficients are real values. The extension has been made for producing wideband multiple beams using only one set of weights. This can be accomplished through the modification of an objective function representing the required radiation. In this paper, it can be produced using Chebyshev function when its maximum gain is given at the desired direction. To obtain multiple beams, combination of objective functions at different desired directions is desirable. The performance of the proposed concept is tested through computer simulation. It has revealed that the beamformer performs very well in forming multiple beams in designated directions. This is considerably suitable for next generation of indoor wideband wireless network.

ACKNOWLEDGMENT

The authors acknowledge the financial support from Thailand Research Fund (TRF) and Suranaree University of Technology, Thailand.

REFERENCES

[1] I. Hamburg, A. Hamburg, M. Gavota and M. Lazea, "Integrating wireless technology in e-learning for disabled," *Information and Communication Technologies: From Theory to Applications*, pp.123-124, 19-23 April 2004.

[2] M. Uthansakul and M. E. Biakowski, "Impact of wideband signals on smart antenna system," *Proc. MIKON 2004,* vol. 2, pp. 501-504, May, 2004.

[3] M. Uthansakul and M. E. Biakowski, "An Investigation into smart antenna configurations for wideband communication." in *Proc. XV Inter. Conf. Microwave, Radar and Wireless Comn.*, vol.2, Poland, pp. 505-508, May 2004.

[4] M. Uthansakul and M. E. Biakowski, "A wideband spatial beamformer employing a rectangular array of planar monopoles," *Proc. 2005 IEEE Int. Ant. and Prop. Symp.*, Washington 3-8 July, 2005.

[5] M. Uthansakul and M. E. Biakowski, "Fully spatial wideband beam forming using a rectangular array of planar monopoles," *IEEE Trans. Ant. and Prop.*, vol.54, pp. 527-533, Feb. 2006.

[6] M. Uthansakul and M. E. Biakowski, "Designing a wideband spatial beamformer for low sidelobe radiation pattern performance," *Microwave Conference Proceeding.*, vol.3, 4-7 Dec, 2005.

[7] M Ghavami, "Wideband smart antenna theory using rectangular array structures," *IEEE Trans. On Signal Proc.*vol.50, no.9, pp.21143-2151, Sept.2002.

[8] G. L. Stuber, Principles of Mobile Communication. Kluwer Academic Publishers, 2002, ch1.

[9] R. C. Hansen, Phased Array Antennas. John Wiley & Sons, Inc, 1998, ch3.

BIOGRAPHY

Miss Chayanit Bunsanit was born in Yala, Thailand, in 1976. She graduated with the Bachelor Degree of Engineering in Telecommunication Engineering in 1999 from Suranaree University of Technology, Nakorn Ratchasima, Thailand. After that, she attended King Mongkut's University of Technology North Bangkok, Bangkok Thailand and received a Master of Science in Technical Education (Electrical Technology) in 2003. She worked at Valaya Alongkorn Rajabhat University Under the Royal Patronage for two years. Then she is currently pursuing her Ph.D program in Telecommunication Engineering, School of Telecommunication Engineering, Suranaree University of Technology. Her research interests are antenna engineering and its application.